STATE OF CALIFORNIA • DEPARTMENT OF TRANSPORTATION

TECHNICAL REPORT DOCUMENTATION PAGE

TR0003 (REV 10/98)

ADA Notice

For individuals with sensory disabilities, this document is available in alternate formats. For information call (916) 654-6410 or TDD (916) 654-3880 or write Records and Forms Management, 1120 N Street, MS-89, Sacramento, CA 95814.

1. REPORT NUMBER	2. GOVERNMENT ASSOCIATION NUMBER	3. RECIPIENT'S CATALOG NUMBER
CA14-2175		

4. TITLE AND SUBTITLE	5. REPORT DATE
Concrete Confinement Model Synthesis Study A Critical Review of Column Confinement Reinforcement Used in Current Seismic Bridge Design Practice	August 2014
	6. PERFORMING ORGANIZATION CODE
7. AUTHOR Aaron Shelman and Sri Sritharan	8. PERFORMING ORGANIZATION REPORT NO.
9. PERFORMING ORGANIZATION NAME AND ADDRESS Department of Civil, Construction and Environmental Engineering	10. WORK UNIT NUMBER
	11. CONTRACT OR GRANT NUMBER 65A0389
12. SPONSORING AGENCY AND ADDRESS California Department of Transportation Division of Engineering Services 1801 30th Street, MS #9-2/5i Sacramento, CA 95816	13. TYPE OF REPORT AND PERIOD COVERED Final Report April, 2011 – June 2013
	14. SPONSORING AGENCY CODE

15. SUPPLEMENTARY NOTES

Prepared in cooperation with the State of California Department of Transportation

16. ABSTRACT

This study focuses on critically evaluating confinement requirements suggested for plastic hinge regions of bridge columns suggested by California Department of Transportation (Caltrans). In addition to section analyses, a series of pushover and earthquake dynamic analyses were conducted on several bridge columns to formulate appropriate recommendations to improve the confinement requirements. It is shown that the plastic hinge length, ultimate compression strain and ductility demand should be revised to improve the seismic performance of bridge columns. In addition, the impact of unexpectedly high inelastic demands that some earthquake can impose on bridge columns should be adequately addressed.

17. KEY WORDS	18. DISTRIBUTION STATEMENT
Seismic; bridge; concrete; column; design; confinement; analysis; model; fiber-section	No restriction. This document is available to the public through the National Technical Information Service, Springfield, Virginia 22161

19. SECURITY CLASSIFICATION *(of this report)*	20. NUMBER OF PAGES	21. COST OF REPORT CHARGED
Unclassified	116	

Reproduction of completed page authorized.

A. Shelman, S. Sritharan

A Critical Review of Column Confinement Reinforcement Used in Current Seismic Bridge Design Practice

Submitted to the
California Department of Transportation
Caltrans Project Contract: 65A0389

JUNE 2013
(Updated AUGUST 2014)

Final

REPORT

IOWA STATE UNIVERSITY
OF SCIENCE AND TECHNOLOGY

Department of Civil, Construction and Environmental Engineering

A Critical Review of Column Confinement Reinforcement Used in Current Seismic Bridge Design Practice

by

Aaron Shelman
Graduate Research Assistant, Iowa State University

Sri Sritharan
Wilson Engineering Professor, Iowa State University

Caltrans Project Contract: 65A0389

A Final Report to the California Department of Transportation

Department of Civil, Construction and Environmental Engineering
Iowa State University
Ames, IA 50011

June 2013

(Updated August 2014)

DISCLAIMER

This document is disseminated in the interest of information exchange. The contents of this report reflect the views of the authors who are responsible for the facts and accuracy of the data presented herein. The contents do not necessarily reflect the official views or policies of the State of California or the Federal Highway Administration. This publication does not constitute a standard, specification or regulation. This report does not constitute an endorsement by the Department of any product described herein.

For individuals with sensory disabilities, this document is available in Braille, large print, audiocassette, or compact disk. To obtain a copy of this document in one of these alternate formats, please contact: Division of Research and Innovation, MS-83, California Department of Transportation, P.O. Box 942873, Sacramento, CA 94273-0001.

ABSTRACT

Modern seismic design of concrete bridges relies generally on forming plastic hinges at the columns ends, thereby developing ductile response for the structures when subjected to moderate to large earthquake. Attaining this ductile bridge behavior requires the establishment of adequate amounts of transverse confinement reinforcement (i.e., ρ_s) in the column critical regions. Numerous design authorities have specified different approaches for estimating ρ_s. While some of these requirements are comparable, others have been found to vary significantly by a factor as much as two to three. One obvious reason for such a large difference in the confinement requirement is that a demand parameter such as a target curvature ductility factor is not used in developing the design equation. Instead of a more prescriptive requirement, Seismic Design Criteria of the California Department of Transportation (Caltrans) only specifies a minimum confinement requirement and anticipates the designer to ensure adequate ductility for the bridge based on a push over analysis.

This report demonstrates the differences in a few of the drastically different confinement reinforcement requirements and how parameters such as the axial load ratio and longitudinal steel reinforcement ratio influence these requirements. To further understand the impact of different confinement approaches and investigate the confinement reinforcement design method adopted by Caltrans, a series of pushover (i.e., static) and dynamic analyses were conducted on bridge columns with different aspect ratios, and the curvature and displacement ductility demands experienced by the columns were evaluated.

Through the different levels of analysis, it was found that a confinement requirement that utilizes variables such as a target curvature demand, column geometry, axial load ratio, longitudinal reinforcement content, and column aspect ratio may provide a more realistic estimate for ρ_s. When the confinement reinforcement was based on that producing one of the highest ρ_s value, it satisfied the intended design procedure of seismic design criteria, which calls for a minimum column displacement ductility of 3, and the expected displacement ductility level of 5. However, the displacement ductility demand above 5 was experienced by columns with aspect ratios between 3 and 4 when they were subjected to records from previous California earthquakes. Other issues emerged from the study are that the conferment reinforcement

requirement is dictated by the ultimate strain capacity of the confined concrete. This strain capacity is influenced by multiple parameters and should be more clearly defined before developing a more rational design method to define the confinement reinforcement in bridge columns. Another parameter that needs attention is the plastic hinge length. Though the plastic hinge length has been typically taken as a function of only the column clear height for idealizing the plastic region along the column, this term has been found to be dependent on the concrete compressive strength, longitudinal reinforcement ratio, horizontal reinforcement ratio and other factors. Based on the findings of the investigation, a road map for improving the Caltrans design requirements is presented.

ACKNOWLEDGMENTS

The research team thanks the following individuals for their support and assistance in the completion of the research presented in this report. Without their help, support and advice, much of this research would not have been possible:

- Caltrans for sponsoring this research project and Charlie Sikorsky for serving as the project manager; and
- Michael Keever, Tom Ostrom and members of the Caltrans Project Advisory Panel for their advice and assistance.

TABLE OF CONTENTS

Technical Report Documentation Page i

Title Page ii

Disclaimer iii

Abstract iv

Acknowledgments vi

Table of Contents vii

List of Figures x

List of Tables xiv

Chapter 1: Introduction 1

1.1 Confinement Reinforcement 2

1.2 Design Approaches 4

1.2.1 Force-Based Design (FBD) 4

1.2.2 Direct Displacement-Based Design (DDBD) 5

1.2.3 Performance-Based Design 6

1.3 Scope of Report 7

1.4 Report Layout 8

Chapter 2: Literature Review of Current Confinement Requirements 9

2.1 Transverse volumetric reinforcement ratio for circular columns 9

2.1.1 Bridge Manual of Transit New Zealand (1994) 10

2.1.2 Watson et al. (1994) 11

2.1.3 ATC-32 (1996) 12

2.1.4 Alaska DOT&PF, MODOT and NCDOT 13

2.1.5 Caltrans Bridge Design Specifications Manual (2003) 13

2.1.6 South Carolina DOT Seismic Design Specifications for Highway Bridges (2008) 15
2.1.7 ACI 318-08 15
2.1.8 Bridge Manual of Transit New Zealand (2005) and NZS 3101 (2008) 16
2.1.9 AASHTO Guide Specifications for LRFD Seismic Bridge Design (2010) 19
2.1.10 Caltrans Seismic Design Criteria (2010) 19
2.1.11 AASHTO LRFD Bridge Design Specifications (2012) 20
2.2 Transverse Reinforcement Area Based Equations 21
2.2.1 Watson et al. (1994) 23
2.2.2 Priestley et al. (1996) 24
2.2.3 ATC-32 (1996) and Caltrans (2003) 25
2.2.4 ACI 318-08 25
2.2.5 NZS 3101 (2008) 27
2.2.6 Japan Society of Civil Engineers (2010) 30
2.2.7 AASHTO LRFD Bridge Design Specifications (2012) 30
2.3 Summary 32
Chapter 3: Review of Confinement Reinforcement and Material Model Equations 35
3.1 Comparison of Available Confinement Equations 35
3.1.1 Concrete Compressive Strength 35
3.1.2 Axial Load Ratio 38
3.1.3 Column Diameter and Ratio of Core and Gross Concrete Cross-Sectional Area ... 40
3.1.4 Longitudinal Reinforcement 43
3.1.5 Summary 44
3.2 Experimental Testing 45
3.2.1 Size Effects 48
3.2.2 Confined Concrete Strength 51

3.2.3 Strain at Peak Confining Stress 54
3.2.4 Ultimate Strain Capacity 57
3.3 Impact of ρ_s on Design 61
3.3.1 Section Curvature Capacity 65
3.3.2 OpenSEES vs Equation Based Displacement Ductility 68
3.4 Summary 75
Chapter 4: OpenSEES Dynamic Analyses 78
4.1 Earthquake Records 79
4.1.1 Imperial Valley Earthquake Record 79
4.1.2 Northridge Earthquake Record 80
4.1.3 Loma Prieta Earthquake Record 81
4.2 Typical Dynamic Analysis Results 83
4.3 Earthquake Demand 85
4.3.1 Displacement Ductility 86
4.3.2 Curvature Ductility 88
4.4 Needed Improvements 91
Chapter 5: Conclusions and Recommendations 93
5.1 Conclusions 93
5.2 Recommendations 94
5.3 Road Map 96
Chapter 6: References 98

LIST OF FIGURES

Figure 1-1: Confinement damage to reinforced concrete columns 1
Figure 1-2: Examples of confinement reinforcement in high seismic regions 3
Figure 3-1: Impact of unconfined concrete compressive strength on horizontal confinement reinforcement ratio [Note: PH = within the plastic hinge region] 37
Figure 3-2: Impact of axial load ratio on horizontal confinement reinforcement ratio [Note: PH = within the plastic hinge region]..... 39
Figure 3-3: Impact of column diameter on the horizontal confinement reinforcement ratio [Note: PH = within the plastic hinge region] 42
Figure 3-4: Impact of the amount of longitudinal reinforcement on the horizontal confinement reinforcement ratio [Note: PH = within the plastic hinge region] 44
Figure 3-5: Testing and setup for additional concrete specimens at Iowa State University..... 47
Figure 3-6: Typical idealized stress-strain for the stress-strain behavior of concrete 48
Figure 3-7: Effect of cylinder diameter on both the confined and unconfined concrete compressive strength..... 49
Figure 3-8: Effect of cylinder diameter on both the confined and unconfined strain at peak strength..... 50
Figure 3-9: Effect of cylinder diameter on both the confined and unconfined strain at 50% of peak strength on the descending branch 50
Figure 3-10: Comparison of theoretical and experimental confined compressive stregnth for 3 in. diameter specimens (fc'= 4000 psi) 52
Figure 3-11: Comparison of theoretical and experimental confined compressive stregnth for 4 in. diameter specimens (fc' = 3500 psi) 52
Figure 3-12: Comparison of theoretical and experimental confined compressive stregnth for 4 in. diameter specimens (fc' = 5400 psi) 53
Figure 3-13: Comparison of theoretical and experimental confined compressive stregnth for 6 in. diameter specimens (fc' = 5000 psi) 53
Figure 3-14: Comparison of theoretical and experimental data for the strain at peak confining stress for 3 in. diameter specimens (fc' = 4000 psi)..... 55

Figure 3-15: Comparison of theoretical and experimental data for the strain at peak confining stress for 4 in. diameter specimens (fc' = 3500 psi) 55
Figure 3-16: Comparison of theoretical and experimental data for the strain at peak confining stress for 4 in. diameter specimens (fc' = 5400 psi) 56
Figure 3-17: Comparison of theoretical and experimental data for the strain at peak confining stress for 6 in. diameter specimens (fc' = 5000 psi) 56
Figure 3-18: Comparison of ultimate concrete strain for 3 in. diameter cylinder specimens (fc' = 4000 psi) 58
Figure 3-19: Comparison of ultimate concrete strain for 4 in. diameter cylinder specimens (fc' = 3500 psi) 59
Figure 3-20: Comparison of ultimate concrete strain for 4 in. diameter cylinder specimens (fc' = 5400 psi) 59
Figure 3-21: Comparison of ultimate concrete strain for 6 in. diameter cylinder specimens (fc' = 5000 psi) 60
Figure 3-22: Moment-curvature analysis details in OpenSees (2010) 63
Figure 3-23: Comparison of OpenSEES moment-curvature results to XTRACT and VSAT for a 96 in. diameter column 64
Figure 3-24 : Comparison of moment-curvature analyses based on number of bars in a 24 in. diameter collumn 64
Figure 3-25: Curvature ductility of circular cross-sections assuming confinement according to Eq. (2-2) [ATC-32 1996] 65
Figure 3-26: Data for a 48 in. column using Eq. (2-2) [ATC-32 1996] for confinement reinforcement 66
Figure 3-27: Curvature ductility of circular cross-sections assuming confinement according to Eq. (2-16) [AASHTO 2012] 67
Figure 3-28: Curvature ductility of circular cross-sections assuming confinement according to Eq. (2-17) [Caltrans 2003, AASHTO 2012 and ACI 2008 Minimum] 68
Figure 3-29 : Double integration versus pushover analysis at the ultimate condition for a 48 in. diameter column with an aspect ratio of 10 70
Figure 3-30: Moment-curvature comparison of idealized with full nonlinear analysis 70

Figure 3-31: Comparison of equation based and OpenSees pushover computations for a 48 in. diameter column with an aspect ratio of 3 and 10 72
Figure 3-32: Influence of design parameters on the alpha coefficient for determining the analytical plastic hinge length used in Eq. (3-2) for a 48 in. diameter column 73
Figure 3-33: Comparison of idealized force-displacement based response with modified coefficients for a 48 in. diameter column with an aspect ratio of 3 and 10 73
Figure 3-34: Comparison of displacement ductility using a 48 in. diameter column and two approaches one equation based and one computer based 75
Figure 4-1: Acceleration time history of the 1940 Imperial Valley Earthquake record at the El Centro site for the N-S component 80
Figure 4-2: Acceleration time history of the 1994 Northridge Earthquake record at the Tarzana Cedar Hill Nursery site 81
Figure 4-3: Acceleration time history of the 1989 Loma Prieta Earthquake record at the Coralitos – Eureka Canyon Road site 82
Figure 4-4: Comparison of 5% damped spectral accelerations for selected earthquake ground motion records with the SDC (2010) ARS curves 82
Figure 4-5: Typical nonlinear force – displacement response of a SDOF column with a natural period of 1.5 seconds subjected to selected earthquake ground motion records 83
Figure 4-6: Displacement time history for the force-displacement response of a SDOF column with a 1.5 sec period subjected the selected Northridge Earthquake Record 84
Figure 4-7: Results for a column with an aspect ratio of 9 and a natural period of 0.5 seconds when subjected to the selected Loma Prieta Earthquake record 85
Figure 4-8: Comparison of displacement ductility capacity and demand obtained from dynamic analyses of bridge columns subjected to the Imperial Valley Earthquake record 86
Figure 4-9: Comparison of the displacement ductility capacity and demand obtained from dynamic analyses of bridge columns subjected to the Loma Prieta Earthquake record ... 87
Figure 4-10: Comparison of the displacement ductility capacity and demand obtained from dynamic analyses of bridge columns subjected to the Northridge Earthquake record 87
Figure 4-11: Comparison of the curvature ductility capacity and demand obtained from dynamic analyses of bridge columns subjected to the Imperial Valley Earthquake record 89

Figure 4-12: Comparison of the curvature ductility capacity and demand obtained from dynamic analyses of bridge columns subjected to the Loma Prieta Earthquake record..... 90
Figure 4-13: Comparison of the curvature ductility capacity and demand obtained from dynamic analyses of bridge columns subjected to the Northridge Earthquake record..... 90

LIST OF TABLES

Table 2-1: A summary of variables used for determining spiral confinement reinforcement..... 33

Table 2-2: A summary of variables used for volumetric equations based on the specification of required area..... 34

Table 2-3: A summary of variables used in anti-buckling equations for determining ρ_s 34

Table 3-1: Experimental testing additional test specimens..... 46

Table 3-2: Previous experimental testing specimens at 20 °C (68 °F) with no longitudinal reinforcement in confined specimens 46

Table 3-3: Idealized moment-curvature results for a 48 in. diameter column section 69

Table 3-4: Pushover comparison for a 48 in. diameter column using OpenSEES and the modified coefficients in Eq. (3-2) 74

Table 4-1: Dynamic properties for computer simulations (units of kips, seconds and inches).... 79

CHAPTER 1: INTRODUCTION

Recent great earthquakes such as the Chilean earthquake of 2010 (M_w = 8.8) and the Tohoku Japan earthquake of 2011 (M_w = 9.0) have served as yet another reminder that seismic activity can effect highly populated regions of the world. In these regions, a significant amount of infrastructure exists and their survival and functionality is critical in the post-earthquake response of emergency vehicles and personnel as well as economic impact to the daily life. This report focuses on the design of concrete bridge columns in high seismic regions through a critical review of confinement reinforcement. The current trend in the design of infrastructure in most of these regions is to ensure that the structure can withstand such a large event without experiencing collapse, but they may not be functional following the earthquake. A key part in achieving this type of design in concrete structures is to better understand the impact of confinement reinforcement in the critical regions of a structure so that resulting poor confinement as shown in Figure 1-1 does not take place.

Upper Left: Hanshin Expressway during the 1995 Kobe Earthquake

Lower Left: Nakasone Viaduct during the 2011 Great East Japan Eartquake (Kawashima et. al 2011)

Right: 1994 Northridge Earthquake (NOAA/NGDC 2013)

Figure 1-1: Confinement damage to reinforced concrete columns

The type of concrete failure depicted in Figure 1-1 is typically prevented through the use of adequate confinement reinforcement. The amount of confinement reinforcement needed in a given design, depends not only on the design approach, but also on other variables such as axial load ratio, concrete compressive strength, area of longitudinal steel, size of confining reinforcement and many others. However, not all of these variables are typically included in the equations used in the establishment of the confining reinforcement. At this time, however, it is appropriate to state that a set consensus does not exist as to the appropriate amount of horizontal steel needed to adequately confine concrete in bridge columns. This is because the typical confinement reinforcement requirements do not use curvature or displacement demands expected in the system as a requirement, which would better define the amount of confinement reinforcement. Rather, implicit approaches based on experimental tests are commonly used that rely on the material properties and column geometry, but not any variable that represents the demand.

1.1 Confinement Reinforcement

The design and construction of structural concrete elements in the field of seismic engineering typically employs the use of confinement reinforcement to ensure a ductile response of critical regions in a bridge column when subjected to a design level or greater earthquake. Confinement reinforcement is usually included in the form of closed loop ties, welded hoops or continuous spirals (e.g., Figure 1-2), so that as lateral load is applied to the structural system the horizontal reinforcement resists the lateral expansion of the concrete by providing lateral resistance, thus increasing the capacity and ductility of the concrete section. This approach is very important in capacity design methods, in which designers ensure an adequate ductile response of bridge column critical regions while preventing development of undesirable failure mechanisms throughout the structure. Different guidelines and specifications suggest different methods of computing the appropriate amount of transverse reinforcement for confinement purposes [e.g., AASHTO (2011), Caltrans (2011) and Priestley (1996)], and each one uses some common and uncommon parameters about the concrete, steel reinforcement and cross-section details. These different approaches provide amounts of horizontal reinforcement that vary by as much as two to three times the smaller value. A main reason for the large disparity in the approaches, as previously noted, is due to not targeting a demand parameter such as curvature,

ϕ_{demand}, which is a factor of the earthquake being considered for design purposes. Thus, it is important to define an adequate approach for the establishment of confinement reinforcement so that the desired sectional and global response of the structural system is attained in a high seismic region.

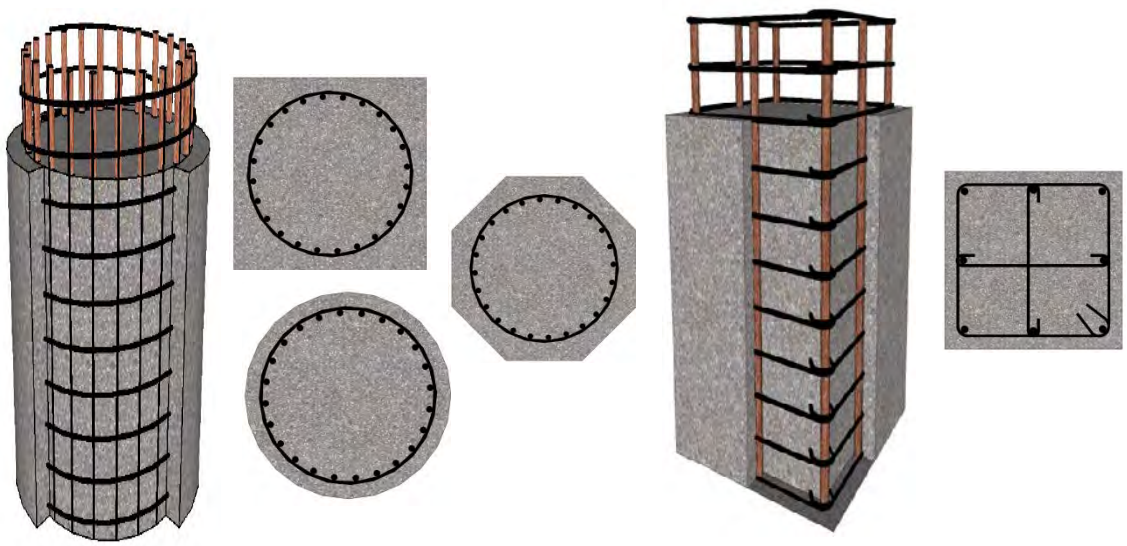

(a) Spiral Reinforcement (b) Tie/Hoop Reinforcement

Figure 1-2: Examples of confinement reinforcement in high seismic regions

The amount of confinement or transverse reinforcement within a given column cross-section is generally defined through the use of three requirements. The first is a minimum or maximum value of reinforcement that is specifically stated to be a required horizontal reinforcement volumetric ratio and satisfies the confinement requirements. The second approach used in high seismic regions is to define a minimum amount of reinforcement needed to ensure that the longitudinal reinforcing bar does not prematurely buckle under applied loading. The third method defines the amount of horizontal reinforcement need to ensure that a given column can resist the shear demands. The first two are the requirements investigated within this report as these particular methods generally control the design of the system except in very short columns. The anti-buckling requirements were included within this report as this value will control the design in certain high seismic regions across the world at low axial load ratios. The amount of reinforcement required based on expected shear demands in a system were not included within this report as the approaches are highly variable depending on the guidelines used for the design.

Additionally, the shear reinforcement is highly dependent on the applied shear to the system and does not always control the design in critical regions with ductile design being the primary goal.

1.2 Design Approaches

In regions that have recently experienced major seismic events, many changes to the design approach used for reinforced concrete structures have occurred. However, two main approaches to the lateral design of a structure subjected to a design level or greater earthquake are in existence. These approaches consist of defining objectives based on forces or lateral displacements. The trend in the U.S. design approaches has begun to recognize the importance of the direct displacement-based approach instead of the traditional force-based approach. A third method to design lateral force resisting members has arisen in current practice based on the desired performance of a structure or system with multiple objectives. This method in particular can be done using either a force-based or displacement-based approach.

1.2.1 Force-Based Design (FBD)

Force-based design has been around for nearly a century as Hardy Cross determined moment-distribution in the early 1920s (Leet et al. 2011). This method of analysis and other approaches (e.g., the flexibility and stiffness methods) developed later on allowed for relatively simple means of computing forces applied to a structural member. Members are then designed such that they will not fail under the applied load. In seismic situations, an equivalent static method is commonly used to determine the lateral forces and associated member forces that a design level earthquake would apply to a given structure. These forces, however, may not always control the sizing of a member because effects from dead load, live load, wind load, serviceability conditions and other design criteria influence the overall size of members. Furthermore, the lateral forces computed in this method are generally based on the natural period of the structure in the first mode only, which must be determined using known geometry from other loading cases or an approximation based on height of the structure. This process, however, does not typically take into account many factors including the fact that strength and stiffness are dependent on one another. Displacement has been generally only checked within the recent past decades using a pushover analysis, ignoring inertial effects, to ensure that any displacement requirements were satisfied once a design was finalized. Should additional displacement be needed the design would be redone and most likely result in the use of additional confinement

reinforcement. The volumetric ratio of transverse reinforcement, ρ_s, would then be increased implicitly for improvement as this would improve the ductility.

Following the 1971 San Fernando Earthquake and the extensive damage caused to structures designed using the force-based procedures, a shift in design philosophy began to take place, albeit at a slow pace. The damage throughout many structures indicated that the fundamental concepts of structures being designed to remain elastic under loading must be modified to ensure an adequate behavior. To attain the desired response, researchers began to focus on ways to increase the ductility of a system to prevent collapse. Out of this came the capacity design philosophy which focused on carefully selecting plastic hinge regions while ensuring no collapse under design-level and greater earthquakes (Priestley et al. 1996 and Priestley et al. 2007). Insufficient ductility and/or drift in a design was handled by implicitly increasing the transverse confinement reinforcement until a satisfactory result was attained.

1.2.2 Direct Displacement-Based Design (DDBD)

FBD demonstrated further weaknesses in the damage noted during the 1989 Loma Prieta and 1995 Kobe earthquakes because of the lack of adequately defining the seismic forces applied to a system and the handling of stiffness for any given structure. Instead of focusing purely on the improvement of force predictions, research began to focus on the idea of reaching a target displacement without failure. This led to the development of the direct displacement-based design (DDBD) methodology, where researchers began to target drifts and/or displacements that a given structure should reach for a specific target hazard. The determination of an appropriate level of damping and ductility can then be used to determine an effective period for the structural member. This effective period can then be used to compute the effective stiffness of a member, which can then be related to a base shear force and distributed throughout to complete the design process. This method takes into account the fact that strength and stiffness are related to better improve the design process to prevent collapse under a design level or greater earthquake. In this approach, the amount of confinement reinforcement could be established based on the strain capacity of the confined concrete region. However, equations between the ultimate strain and desired curvature capacity seldom exist; thus, an iterative procedure is needed to define the confinement reinforcement needed for a system. For this purpose, an equation such as that recommended by Priestley et al. (1996), reproduced in Eq. (1-1), is used to link the amount of

horizontal reinforcement to the targeted curvature capacity of the bridge cross-section based on the work of Mander et al. (1988). Sritharan et al. (2001) found that this recommendation suggested for design resulted in a reserve capacity of the confined concrete section by as much as 50%.

$$\varepsilon_{cu} = 0.004 + \frac{1.4\rho_s f_{yh}\varepsilon_{su}}{f'_{cc}} \qquad \text{Eq. (1-1)}$$

where: ε_{cu} = ultimate concrete strain;

ρ_s = volumetric spiral reinforcement;

f_{yh} = yield strength of hoop steel;

ε_{su} = ultimate strain of steel reinforcement; and

f'_{cc} = confined concrete compressive strength.

1.2.3 Performance-Based Design

Performance-based design, although stated to have been around for quite a while by many sources, has emerged in the past couple of decades as the ideal design methodology for seismic situations. This method came to the forefront with the ATC-33 Project that attempted to create a standardized method for performance-based design and resulted in the publication of the *FEMA-273* (1997) and *FEMA-274* (1997) reports. In general, the performance-based methods for the seismic design of structures use multiple objectives with different criteria for each to define the desired response of a structure and can be completed using FBD or DDBD. The main sections suggested for performance-based design for seismic regions include (1) fully operational; (2) operational; (3) life safe, and (4) near collapse (Priestley 2000). These sections of the design approach rely on the designer having to meet requirements such as the structure withstanding a certain magnitude earthquake, attaining a certain displacement ductility or drift, and/or meeting a specific level of damage. In the American Association of State Highway and Transportation Officials (AASHTO) *Guide Specification for LRFD Seismic Bridge Design* (2010), it is stated that the bridge must meet the life safety objective for an event with a seven percent probability of exceedance in 75 years (~1000 year return period). Furthermore, individual ductility demands must be less than a certain value based on the type of column bent (i.e., single vs. multiple) and the orientation of pier walls. The California Department of Transportation (Caltrans) extends this approach in the *Seismic Design Criteria* by stating that the displacement ductility capacity of

a single member shall be greater than 3 while the demand should be established such that the displacement ductility demand shall be less than 4 (Caltrans 2010).

1.3 Scope of Report

The goal of the project was to examine various confinement equation requirements available today and understand the differences between them so that a more consensus approach for the definition of confinement reinforcement can be eventually developed. However, the difference between the available equations was significant and a critical examination of the development and use of transverse reinforcement equations in practice was subsequently undertaken. In attaining the goal of the project, the initial investigation into identifying and comparing approaches for confinement reinforcement suggested that equations differed by as much as two to three times the smaller value. Furthermore, variability existed in the common and uncommon parameters used per equation such that more than 15 different terms were prevalent in practice. Thus, to complete the project, a critical examination through the use of a detailed literature review was undertaken to identify transverse reinforcement equations from specifications, guidelines and reports found in the United States, New Zealand and Japan. These equations were then compared to identify differences and how they were affected by common variables used in the design process and current knowledge of confined concrete. Furthermore, analyses were undertaken by computer modeling and equation-based formulas to determine the impact of a few reinforcement ratios on the ductility of a cantilever column when subjected to a lateral force at the top of the column. These pushover analyses allowed for a baseline on the ductility capacity of a given cross-section and column aspect ratio. The resulting data set was then compared with a series of full earthquake records to determine whether or not current equations are adequately capturing the expected demand of failure prevention during a seismic event. Additionally, the hysteretic response of the bridge columns attained during the application of the earthquake records were used to identify the demand levels to be specified within a new equation for the establishment of an adequate level of confinement. The literature review combined with the analyses allowed for identification of critical parameters that should be included in any future confinement equation development.

1.4 Report Layout

Chapter one provides a brief introduction to the topic of confinement and its importance in design. Chapter two presents the results of the detailed literature review which examined research sources from journals and standards in the United States and around the world. Chapter three presents the portion of the investigation into the equation based approaches currently used in practice to define the behavior of bridge columns and how it compares to analytical modeling in the computer framework Open System for Earthquake Engineering Simulation (OpenSEES) (2010) with comparisons back to XTRACT (TRC Solutions and Chadwell 2007) and VSAT (Levings 2009). Chapter four examines the impact of actual time history records from three different major earthquakes and their impacts on the displacement ductility of the column. The responses are also compared with current ductility requirements to examine the applicability of the design values. Chapter five summarizes the results of the study, identify the areas needing improvements in SDC, and provide recommendations for future research into confinement of concrete cross-sections and curvature demand levels that are to be used for design purposes.

CHAPTER 2: LITERATURE REVIEW OF CURRENT CONFINEMENT REQUIREMENTS

As previously noted, transverse reinforcement is essential for seismic bridge column design, as it allows concrete columns to have a much greater degree of flexibility, thereby ensuring ductile bridge response. Specifically, by providing spiral or hoop reinforcement, the concrete used in bridge columns is made possible to respond plastically, which allows the sudden and violent ground movement to be handled by limiting the seismic force imparted to the structure, enabling the structure to deform without significant degradation or collapse. Various design authorities specify how much of this transverse reinforcement is needed based on the size of the column by either a ratio of the volume of horizontal steel to volume of concrete, ρ_s, or by requiring the closed loop hoop steel to have a certain area (A_{sh}) and spacing, s, within a given length along the concrete member. This chapter is dedicated to listing the authorities with specifications for each parameter, presenting the relevant equations, and summarizing the relationship between them. The requirements for the spirals and rectangular hoops are separated in this document based on the different requirements typically needed within the equations.

2.1 Transverse volumetric reinforcement ratio for circular columns

The wide discrepancy and disagreement between design standards and guidelines published by the different authorities in the United States and world can easily be seen by observing the current differences in transverse column reinforcement requirements. A comparison was made between various state departments of transportation, national and worldwide standards, research outcomes and guidelines for the design of concrete confinement reinforcement. The list below defines the resources used for establishing the comparison information provided in the rest of this section based on the equations used in the seismic design of bridge columns. The Alaska, Missouri and North Carolina Department of Transportations were listed on the list first as these locations have seismic requirements within their design guidelines in addition to federal requirements set forth by the Federal Highway Administration (FHWA), but the standards do not necessarily fit into a specific chronological order similar to the rest of the list. The guidelines list was extended to include the American Concrete Institute's – *Building Code Requirements for Structural Concrete (ACI 318-08) and Commentary (ACI 318R-08)* and the Standards New Zealand – *Design of Concrete Structures (NZS 3101)* as these two references adopt a similar

philosophy to seismic design as those of the bridge design guidelines. Furthermore, the New Zealand Transport Agency (formerly Transit New Zealand) states that the reinforced concrete design of bridges shall be performed in accordance with NZS 3101 (Transit New Zealand 2005).

- Alaska Department of Transportation and Public Facilities (Alaska DOT&PF), Missouri Department of Transportation (MODOT) and North Carolina Department of Transportation (NCDOT);
- Watson, S.; Zahn, F. A.; and Park, R., (1994);
- Standards New Zealand – *Design of Concrete Structures (NZS 3101: 1995);*
- Applied Technology Council (ATC) – *Improved Seismic Design Criteria for California Bridges: Provisional Recommendations (ATC-32)* (1996);
- Caltrans - *Bridge Design Specifications Manual* (2003);
- South Carolina Department of Transportation - *Seismic Design Specifications for Highway Bridges Version 2.0* (2008);
- American Concrete Institute (ACI) – *Building Code Requirements for Structural Concrete (ACI 318-08) and Commentary (ACI 318R-08);*
- Standards New Zealand – *Design of Concrete Structures (NZS 3101: 2008);*
- AASHTO - *Guide Specifications for LRFD Seismic Bridge Design 1st Edition with 2010 interim revisions* (2010);
- Caltrans - *Seismic Design Criteria Version 1.6* (2010); and
- AASHTO – *LRFD Bridge Design Specifications* (2012).

2.1.1 Bridge Manual of Transit New Zealand (1994)

In the 1994 issue of the *Bridge Manual of Transit New Zealand* a set of equations were provided to quantify the appropriate amount of transverse reinforcement for concrete confinement. The equation provided in the 1994 edition of the standards is provided herein as Eq. (2-1) and is based on the required curvature ductility, axial load ratio, strength reduction factor and ratio of gross concrete area to core concrete area. Terms such as the curvature ductility and strength reduction factor are taking into account the local section design and resistance factors common in load and resistance factored design (LRFD). The presence of the curvature ductility requirement highlights the importance of considering demand within the establishment of the horizontal confinement reinforcement. The requirements specified for the design in this particular methodology is based on a displacement ductility of six at the ultimate limit state which results in the curvature ductility design being a value of 10 for potential plastic hinge regions above the bottom story. For the bottom story, a curvature ductility of 20 is

required. It is important to note that the information input into this equation should be in megapascals and millimeters during computations.

$$\rho_s = \frac{\left(\frac{\phi_u}{\phi_y} - 33p_t m + 22\right)}{79} \frac{A_g}{A_c} \frac{f_c'}{f_{yt}} \frac{N^*}{\varphi f_c' A_g} - 0.0084 \qquad \text{Eq. (2-1)}$$

where: s = center to center spacing of transverse reinforcement;

h'' = dimension of core of column at right angles to direction of transverse bars under consideration;

A_g = gross area of column;

A_c = core area of column;

$\frac{\phi_u}{\phi_y}$ = curvature ductility factor required;

ϕ_u = ultimate curvature;

ϕ_y = curvature at first yield;

p_t = A_{st}/A_g;

A_{st} = total area of longitudinal column reinforcement;

m = $f_y/(0.85f_c')$;

f_y = lower characteristic yield strength of longitudinal steel;

f_{yt} = lower characteristic yield strength of transverse steel;

N^* = axial compressive load on column; and

φ = strength reduction factor = 0.85 for columns not protected by capacity design.

2.1.2 Watson et al. (1994)

These three researchers published a slightly different equation than the New Zealand equation in Section 2.1.1. The two equations differ by the value stated for use as the constant. In Watson et al. (1994) a value of 0.008 is published for use compared to the stated value of 0.0084 in the *Bridge Manual of Transit New Zealand* (1994). Although a slight difference is noted, there was no justification provided as to why there was a difference. Additionally, for low axial load ratios (ALR), $N/(f_c'A_g)$, in compression, the equation typically results in a negative number for the amount of confinement reinforcement within a cross-section. The same problem would occur for ALR that are in tension. Although this was the case, the researchers indicated

that the current code provided a minimum amount of reinforcement that was deemed adequate at small ALR ratios. When positive volumetric ratios are obtained, the values are essentially identical to those specified in the Eq. (2-1) and thus the equation was not reproduced here. The researchers further indicated that when a more detailed ductility calculation is not needed a curvature ductility of 20 was sufficient for a ductile design, and a curvature ductility of 10 was sufficient for a limited ductile design.

2.1.3 ATC-32 (1996)

The Applied Technology Council (ATC) did a study to improve the seismic behavior of California bridges. In their final recommendations, they provided an equation, Eq. (2-2), to find the horizontal volumetric reinforcement ratio for spirally reinforced columns inside and outside the plastic hinge region.

$$\rho_s = 0.16\frac{f'_{ce}}{f_{ye}}\left[0.5+\frac{1.25P}{f'_{ce}A_g}\right]+0.13\left[\rho_l-0.01\right] \qquad \text{Eq. (2-2)}$$

where: f'_{ce} = expected concrete strength;

f_{ye} = expected yield strength of the reinforcement;

P = column axial load;

A_g = gross column area; and

ρ_l = longitudinal reinforcement ratio.

This equation utilizes the geometric properties and material properties, but was expanded to take into account the effects of the column axial load and the longitudinal reinforcement ratio. The inclusion of these additional parameters, make this approach the most detailed recommendation proposed in the United States. Although the detailed approach is defined by ATC, an additional requirement within the plastic end regions of ductile columns is specified. This requirement states that the volumetric ratio shall not be less than the value obtained from the previous equation, nor less than, Eq. (2-3), which is an anti-buckling requirement for the longitudinal bars and is not specifically for confinement alone.

$$\rho_s = 0.0002n_b \qquad \text{Eq. (2-3)}$$

where: n_b = the number of longitudinal bars contained by the spiral or circular hoop

A second equation that accounts for the issue of anti-buckling within this text relates to the spacing needed between the spiral loops. This particular equation, Eq. (2-4), accounts for steel reinforcement that has an ultimate strength to yield strength ratio of less than 50%.

$$s \leq \left[3+6\left(\frac{f_u}{f_y}-1\right)\right] d_{bl} \qquad \text{Eq. (2-4)}$$

where: f_u = ultimate strength of the reinforcement;

f_y = yield strength of the reinforcement; and

d_{bl} = diameter of longitudinal reinforcement.

2.1.4 Alaska DOT&PF, MODOT and NCDOT

In the states of Alaska, Missouri and North Carolina, regions of high seismicity are present based on the past history of earthquakes and proximity to nearby known faults (USGS 2012). Although these sections of the United States are at risk for high ground motions, they do not maintain a specific set of standards or guidelines for use in the seismic design of bridges and structures (MODOT 2012, NCDOT 2012). Instead, they generally refer to the overall governing standards for the United States, typically considered to be the *AASHTO LRFD Bridge Design Specifications* (2012) and *AASHTO Guide Specifications for LRFD Seismic Bridge Design* (2010). For these specific states, it is important to note that this means the confinement reinforcement requirements described below in Sections 2.1.9 and 2.1.11 must be met.

2.1.5 Caltrans Bridge Design Specifications Manual (2003)

Prior to the Seismic Design Criteria (SDC) used in practice today, Caltrans had a bridge design manual that provided specific requirements about the design of columns for all conditions. This set of specifications state that ties are permitted only where it is not practical to use spiral or circular hoop reinforcement. Additionally, the 2003 manual by Caltrans provided three equations to specify a volumetric ratio for the transverse reinforcement. The first and second equations, Eq. (2-4) and Eq. (2-5), are very similar to ACI and AASHTO approaches, but take into consideration the impact of the column axial load as was the case in the ATC-32 specifications. Eq. (2-4) applies only when the column diameter is less than 3 ft (900 mm) in the plastic hinge region. Eq. (2-5) applies when the column diameter is greater than the limits applied to Eq. (2-4).

$$\rho_s = 0.45\left(\frac{A_g}{A_c} - 1\right)\frac{f_c'}{f_{yh}}\left(0.5 + 1.25\frac{P_e}{f_c' A_g}\right) \qquad \text{Eq. (2-4)}$$

where: f_c' = specified compressive strength of concrete;

f_{yh} = specified yield strength of transverse reinforcement not to exceed 100,000 psi;

A_g = gross area of a concrete section;

A_c = cross-sectional area of a structural member measured to the outside edges of transverse reinforcement; and

P_e = column axial load.

$$\rho_s = 0.12\frac{f_c'}{f_{yh}}\left(0.5 + 1.25\frac{P_e}{f_c' A_g}\right) \qquad \text{Eq. (2-5)}$$

where: f_c' = specified compressive strength of concrete;

f_{yh} = specified yield strength of transverse reinforcement not to exceed 100,000 psi;

A_g = gross area of a concrete section; and

P_e = column axial load.

The third equation presented within this document, Eq. (2-6), appears throughout many of the references from the United States. This particular equation was recommended by many organizations as the intention is to ensure that the core of the column can sustain the axial load after the exterior cover concrete has spalled off of the section (ACI 2008). The third equation was also intended to be a minimum amount of steel required within the plastic zone as this was the amount of steel needed to be provided outside the ductile region.

$$\rho_s = 0.45\left(\frac{A_g}{A_{ch}} - 1\right)\frac{f_c'}{f_{yt}} \qquad \text{Eq. (2-6)}$$

where: f_c' = specified compressive strength of concrete;

f_{yt} = specified yield strength of transverse reinforcement not to exceed 100,000 psi;

A_g = gross area of a concrete section; and

A_{ch} = cross-sectional area of a structural member measured to the outside edges of transverse reinforcement.

2.1.6 South Carolina DOT Seismic Design Specifications for Highway Bridges (2008)

The South Carolina Department of Transportation (SCDOT) provides a set of design specifications that must be followed for highway bridge design when subjected to seismic conditions (SCDOT 2008). The specifications state that spiral reinforcement is not allowed in a ductile design within the plastic hinge region of cast-in-place concrete, but rather the use of butt-welded hoops is required. Additionally, the design specifications state that the transverse reinforcement shall be sufficient to ensure adequate shear capacity and confinement with the inclusion that the quantity of reinforcement meets the requirements of Eq. (2-7). This equation, however, commonly appears as horizontal reinforcement requirements within joint regions between columns and beams (AASHTO 2010). Due to this being used as a joint requirement, the suggested equation was not included within later comparisons.

$$\rho_s \geq \frac{0.4A_{st}}{l_{ac}^2} \qquad \text{Eq. (2-7)}$$

where: ρ_s = volumetric ratio of transverse reinforcement;

A_{st} = total area of longitudinal reinforcement in the column/shaft; and

l_{ac} = anchorage length for longitudinal column reinforcement.

Besides the plastic hinge region, the SCDOT (2008) states that the transverse reinforcement outside of the plastic hinge region shall not be placed more than twice the spacing of the reinforcement in the plastic hinge region. Other information about the maximum spacing of transverse reinforcement meets the same requirements typically provided in AASHTO (2012) with those being the minimum of the following:

- Six inches inside the plastic hinge region;
- One-fifth the least dimension of the cross-section in columns or one-half the least cross-sectional dimension of piers;
- Six times the nominal diameter of the longitudinal reinforcement; and
- 12 inches outside the plastic hinge region.

2.1.7 ACI 318-08

The American Concrete Institute (ACI) *Building Code Requirements for Structural Concrete and Commentary* (ACI 2008) typically governs the concrete design of buildings and other structures. Although this is important to note, it is an appropriate source to examine for the

requirements of transverse reinforcement as it still deals with the design of columns subjected to lateral loading. In this set of requirements, two equations are provided to meet for the design of transverse reinforcement. The first one, Eq. (2-8), comes from Chapter 21 of *ACI 318-08* and states that the volumetric ratio of spiral or circular hoop reinforcement, ρ_s, shall not be less than this value. The commentary of this guidelines states that the value was specified to ensure adequate flexural curvature capacity in yielding regions (ACI 2008).

$$\rho_s = 0.12 \frac{f_c'}{f_{yt}} \qquad \text{Eq. (2-8)}$$

where: f_c' = specified compressive strength of concrete; and

f_{yt} = specified yield strength of transverse reinforcement not to exceed 100,000 psi.

The second equation, Eq. (2-9), previously stated in Section 2.1.5 of this report comes from Chapter 10 of *ACI 318-08* and specifies that the volumetric ratio shall not be less than this value, which ensures sufficient capacity after spalling of the cover concrete.

$$\rho_s = 0.45 \left(\frac{A_g}{A_{ch}} - 1\right) \frac{f_c'}{f_{yt}} \qquad \text{Eq. (2-9)}$$

where: f_c' = specified compressive strength of concrete;

f_{yt} = specified yield strength of transverse reinforcement not to exceed 100,000 psi;

A_g = gross area of a concrete section; and

A_{ch} = cross-sectional area of a structural member measured to the outside edges of transverse reinforcement.

Although these equations are used to specify the amount of reinforcement needed for buildings and other structures, both equations are identical to the equations presented in AASHTO (2012). This is because both organizations want the desired behavior of concrete to be similar and the values produced by these equation came from numerous axially load tests on concrete columns.

2.1.8 Bridge Manual of Transit New Zealand (2005) and NZS 3101 (2008)

Since 1994, the *Bridge Manual of Transit New Zealand* has undergone revisions with one of the latest being from 2005. In this set of guidelines, the design process for concrete columns is

now referred to the *Design of Concrete Structures Standard* produced by the Standards New Zealand Council (2008). In this standard, the amount of transverse reinforcement is required to meet different levels depending on whether or not it falls within a potential ductile plastic hinge region. In either approach, the updated standard provides a new equation, Eq. (2-10) or Eq. (2-11), that has been simplified from the 1994 version. Eq. (2-10) is the requirement to be met for confinement in general while Eq. (2-11) applies in the ductile plastic hinge region. This is a similar approach to that of Caltrans (2003) in which equations were given for the ductile and non-ductile zones. As in the other New Zealand equation, the units to be used are megapascals and millimeters.

$$\rho_s = \frac{(1-p_t m)}{2.4}\frac{A_g}{A_c}\frac{f_c'}{f_{yt}}\frac{N^*}{\varphi f_c' A_g} - 0.0084 \qquad \text{Eq. (2-10)}$$

where: A_g = gross area of column;

A_c = core area of column measured to the centerline of the confinement reinforcement;

p_t = A_{st}/A_g;

A_{st} = total area of longitudinal column reinforcement;

m = $f_y/(0.85f_c')$;

f_y = lower characteristic yield strength of longitudinal steel;

f_{yt} = lower characteristic yield strength of transverse steel;

N^* = axial compressive load on column; and

φ = strength reduction factor = 0.85 for columns not protected by capacity design.

$$\rho_s = \frac{(1.3-p_t m)}{2.4}\frac{A_g}{A_c}\frac{f_c'}{f_{yt}}\frac{N^*}{\varphi f_c' A_g} - 0.0084 \qquad \text{Eq. (2-11)}$$

where: A_g = gross area of column;

A_c = core area of column;

p_t = A_{st}/A_g;

A_{st} = total area of longitudinal column reinforcement;

m = $f_y/(0.85f_c')$;

f_y = lower characteristic yield strength of longitudinal steel;

f_{yt} = lower characteristic yield strength of transverse steel;

N^* = axial compressive load on column; and

φ = strength reduction factor = 0.85 for columns not protected by capacity design.

The main difference between Eq. (2-1) and Eqs. (2-10) and (2-11) is that the curvature ductility term and a number of other constants were removed, thus simplifying the amount of input information required. Additionally, limits were placed on values within the equations. These limits include the following:

- A_g/A_c shall not be greater than 1.5 unless it can be shown that the design strength of the column core can resist the design actions;
- p_t*m shall not be greater than 0.4; and
- f_{yt} shall not exceed 800 MPa.

Besides the requirements specified above, *NZS 3101* states that the columns must be designed with an adequate amount of transverse reinforcement such that premature buckling does not occur. Again, the buckling equation is dependent on whether or not the design is taking place within a potential ductile plastic hinge region. Thus, Eq. (2-12) presented herein applies outside the ductile hinge region while Eq. (2-13) applies within the ductile hinge region.

$$\rho_s = \frac{A_{st}}{155d''}\frac{f_y}{f_{yt}}\frac{1}{d_b} \qquad \text{Eq. (2-12)}$$

where: A_{st} = total area of longitudinal column reinforcement;

f_y = lower characteristic yield strength of longitudinal steel;

f_{yt} = lower characteristic yield strength of transverse steel;

d'' = depth of concrete core of column measured from center to center of peripheral rectangular hoop, circular hoop or spiral; and

d_b = diameter of reinforcing bar.

$$\rho_s = \frac{A_{st}}{110d''}\frac{f_y}{f_{yt}}\frac{1}{d_b} \qquad \text{Eq. (2-13)}$$

where: A_{st} = total area of longitudinal column reinforcement;

f_y = lower characteristic yield strength of longitudinal steel;

f_{yt} = lower characteristic yield strength of transverse steel;

d'' = depth of concrete core of column measured from center to center of peripheral rectangular hoop, circular hoop or spiral; and

d_b = diameter of reinforcing bar.

2.1.9 AASHTO Guide Specifications for LRFD Seismic Bridge Design (2010)

The LRFD Bridge Design Specifications by AASHTO (2012) have been modified by a second set of guide specifications. This specification specifically addresses the seismic design of bridges (AASHTO 2010). In this set of guidelines, additional requirements on the amount of transverse reinforcement have been provided. These requirements for the volumetric ratio of transverse reinforcement in the core of the column do not take into account the column size or strength. The specifications, however, are based on the seismic design category for which they are designed. These values are provided in Eq. (2-14) and Eq. (2-15) and are minimum values for the design levels.

- For Seismic Design Category B:

$$\rho_s \geq 0.003 \qquad \text{Eq. (2-14)}$$

- For Seismic Design Categories C and D:

$$\rho_s \geq 0.005 \qquad \text{Eq. (2-15)}$$

The spacing requirements suggested in the AASHTO Seismic Bridge Design Specifications (2010) are the same as those provided in Section 2.1.2 for the SCDOT. For this reason they are not reproduced in this section.

2.1.10 Caltrans Seismic Design Criteria (2010)

Similar to the SCDOT, Caltrans has a specific set of seismic design criteria (SDC) (2010) that a design engineer must meet. The main idea presented in the design criteria is that enough confinement reinforcement must be provided such that the performance requirements as set by the Department of Transportation are adequately met in addition to the federal requirements of the FHWA. The performance requirements in the document are based on laboratory testing with fixed base cantilever columns. Additionally, the cantilever column and fixed-fixed column use the same detailing for geometry as well as horizontal and transverse reinforcement. This assumption and the laboratory testing resulted in the specifications such that a single member must have a minimum displacement ductility capacity of three. In addition to the capacity

requirements, the sections must be designed such that the global demand displacement ductility meets the following criteria:

- Single Column Bents supported on fixed foundation $\mu_D \leq 4$;
- Multi-Column Bents supported on fixed or pinned footings $\mu_D \leq 5$;
- Pier Walls (weak direction) supported on fixed or pinned footings $\mu_D \leq 5$; and
- Pier Walls (strong direction) supported on fixed or pinned footings $\mu_D \leq 1$.

2.1.11 AASHTO LRFD Bridge Design Specifications (2012)

The intention of the displacement ductility values prescribed within the SDC is that the designer shall perform an inelastic pushover analysis to ensure the prescribed global displacement ductility is met. In this process the designer is also expected to ensure that the minimum displacement ductility of three is met for each member of the system. From this analysis, the amount of confinement reinforcement is determined such that the displacement ductility performance requirements are met. Furthermore, to prevent reinforcement congestion and higher ductility demand for an earthquake, the general practice is to keep an aspect ratio of the column to four or above. Once the ductile region design has been completed, SDC (2010) specifies that the transverse reinforcement outside the ductile region need not be less than half the amount of confinement reinforcement within the plastic hinge region.

The LRFD bridge design specifications published by AASHTO (2012) have numerous requirements on the amount of transverse reinforcement needed in a circular column, but are the exact same as those provided by ACI in Section 2.1.7 of this report. The equations for the volumetric ratio within the plastic hinge region that must be satisfied are reproduced again as Eq. (2-16) and Eq. (2-17).

$$\rho_s \geq 0.12 \frac{f_c'}{f_y} \qquad \text{Eq. (2-16)}$$

where: ρ_s = volumetric ratio of transverse reinforcement;

f_c' = specified compressive strength of concrete at 28 days, unless another age is specified; and

f_y = yield strength of reinforcing bars.

$$\rho_s \geq 0.45 \left(\frac{A_g}{A_c} - 1\right) \frac{f_c'}{f_{yh}} \qquad \text{Eq. (2-17)}$$

where: ρ_s = volumetric ratio of transverse reinforcement;

A_g = gross area of concrete section;

A_c = area of core measured to the outside diameter of the spiral;

$f_c^{'}$ = specified compressive strength of concrete at 28 days, unless another age is specified; and

f_{yh} = specified yield strength of spiral reinforcement.

The amount of reinforcement required must also meet some additional spacing requirements similar to those specified by the *SCDOT* (2008) and *ACI 318-08* (2008). These details are listed below:

- Clear spacing of the bars not less than 1 in. or 1.33 times the maximum aggregate size;
- The center to center spacing not greater than six times the diameter of the longitudinal bars;
- Spacing less than 4.0 in. in the confined region and 6.0 in. in non-confined regions; and
- Spacing less than one-quarter the minimum member dimension in the confined regions.

In addition to the spacing requirements and values of volumetric ratio of transverse reinforcement, a minimum amount of transverse reinforcement is required for shear both inside and outside the plastic hinge region.

2.2 Transverse Reinforcement Area Based Equations

Even though many guidelines provide information in regards to the volumetric ratio of horizontal reinforcement, ρ_s, some specifications provide transverse reinforcement details in the form of a specified area. This approach accounts for systems in which it may be beneficial to know the amount of area required for reinforcement instead of a volumetric ratio. For example, the area of transverse reinforcement may be more beneficial when there are two directions of concern with a column or beam having dimensions of cross-sections that vary in the principal direction of applied loading. To better understand all the possible equations that may come into confinement reinforcement, the area specifications and guidelines were also examined to demonstrate the differences that arise. Once the area of steel reinforcement is known for a given design, a volumetric ratio can be calculated to compare with other approaches if assumptions are made about the geometric dimensions of the column. In this section, it was assumed when appropriate that there was a column with equal dimensions in the primary directions was used

along with a consistent area and number of reinforcement legs in either direction if a volumetric ratio is provided.

By assuming a column of this type with equal amounts of transverse reinforcement in either direction, the volumetric ratio of column can be computed using Eq. (2-18) and substituting the appropriate area equation in for A_{st}. The substituted area equation, however, must be divided by a factor of 2 as the reinforcement area computed will be used in a minimum of two legs within the column cross-section. It is noted that Eq. (2-18) is a summation of the total volumetric ratio within the cross-section (i.e., $\rho_s = \rho_{sx} + \rho_{sy}$)

$$\rho_s = \frac{4A_{st}}{D's} \qquad \text{Eq. (2-18)}$$

where: A_{st} = area of transverse reinforcement;

D' = dimension of core measured from center to center of transverse reinforcement;

s = center to center spacing of transverse reinforcement; and

ρ_s = total volumetric ratio of transverse reinforcement.

The list below defines the resources used for establishing the comparison information provided in the rest of Section 2.2 of this report based on the chronological history of the equations used in the seismic design of bridge columns. The resources were selected to match the documents chosen within Section 2.1 of this report where select references not related to bridge column design were included based on design philosophy. The list was extended to include the *Code for Design of Concrete Structures for Buildings* published by the Canadian Standards Association (1994) and the *Standard Specification for Concrete Structures 2007 "Design"* published by the Japan Society of Civil Engineers (2010). These particular resources were selected for inclusion to expand the number of resources from high seismic regions of the world that conduct additional research into confinement of reinforced concrete columns. Furthermore, they were included within this section as they did not directly provide equations for the volumetric ratio of transverse reinforcement.

- Canadian Standards Association - *Code for Design of Concrete Structures for Buildings (CAN3-A23.3-M94)* (1994);
- Watson, S.; Zahn, F. A.; and Park, R., (1994);
- Priestley, M. J.; Seible, F.; and Calvi, G. M. – *Seismic Design and Retrofit of Bridges* (1996);

- Applied Technology Council (ATC) – *Improved Seismic Design Criteria for California Bridges: Provisional Recommendations (ATC-32)* (1996);
- Caltrans - *Bridge Design Specifications Manual* (2003);
- American Concrete Institute (ACI) – *Building Code Requirements for Structural Concrete (ACI 318-08) and Commentary (ACI 318R-08);*
- Standards New Zealand – *Design of Concrete Structures (NZS 3101: 2008);*
- AASHTO - *Guide Specifications for LRFD Seismic Bridge Design 1st Edition with 2010 interim revisions* (2010) ;
- Japan Society of Civil Engineers – *Standard Specification for Concrete Structures 2007 "Design" (2010);*
- Caltrans – *Seismic Design Criteria Version 1.6* (2010); and
- AASHTO – *LRFD Bridge Design Specifications* (2012).

2.2.1 Watson et al. (1994)

The research provided in this reference is similar to the *NZS 3101* (2008) equations with some of the noted differences being that extra parameters are included and the anti-buckling requirements are not directly discussed with these volumetric equations. When the equation is converted from the area approach to volumetric ratio based on the column with equal reinforcement all around, Eq. (2-19) is attained. When extrapolating this equation out to the effective lateral confining stress assuming a curvature ductility of 20, a longitudinal steel ratio of two percent, a ratio of gross to core area of concrete of 1.22, material property ratio of 0.066 and an axial load ratio of 40% (to ensure positive numbers), the coefficient of effectiveness would end up being a value of 0.67 to match the effective lateral confining stress associated with the spiral reinforcement equation assuming a 0.95 coefficient of effectiveness. Priestley et al. (1996) suggests a coefficient of effectiveness of 0.95 for circular sections, 0.75 for rectangular and 0.6 for rectangular walls. Thus, the effectiveness of 0.67 seems to fall within a reasonable range.

$$\rho_s = 2*\left(\frac{\frac{\varphi_u}{\varphi_y} - 33p_t m + 22}{111}\frac{A_g}{A_c}\frac{f_c'}{f_{yh}}\frac{P}{\phi f_c' A_g} - 0.006\right) \qquad \text{Eq. (2-19)}$$

where: s = center to center spacing of transverse reinforcement;

h″ = dimension of core of column at right angles to direction of transverse bars under consideration;

A_g = gross area of column;

A_c = core area of column;

$\frac{\varphi_u}{\varphi_y}$ = curvature ductility factor required;

φ_u = ultimate curvature;

φ_y = curvature at first yield;

p_t = A_{st}/A_g;

A_{st} = total area of longitudinal column reinforcement;

m = $f_y/(0.85f_c^{'})$;

f_y = lower characteristic yield strength of longitudinal steel;

f_{yt} = lower characteristic yield strength of transverse steel;

N^* = axial compressive load on column; and

ϕ = strength reduction factor = 0.85 for columns not protected by capacity design.

2.2.2 Priestley et al. (1996)

In the *Seismic Design and Retrofit of Bridges* book by Priestley (1996), an area equation was provided. Instead of reproducing that equation here, the volumetric ratio form, once rearranged using the aforementioned process, is provided in this document. The resulting equation, Eq. (2-20) is very similar to the ATC-32 (1996) approach with the only difference being the assumption that rectangular hoops are not as efficient as circular hoops. Thus, the multipliers in Eq. (2-20) are 50% and 100% higher than the spiral equation. When this approach is extrapolated out to the effective lateral confining stress using a five percent ALR, a two percent longitudinal reinforcement ratio and a ratio of material properties of 0.066, a coefficient of 0.6 would be needed to match the spiral equation with a coefficient of effectiveness of 0.95.

$$\rho_s = 0.24\frac{f_{ce}^{'}}{f_{ye}}\left[0.5+\frac{1.25P}{f_{ce}^{'}A_g}\right]+0.26(\rho_l-0.01) \qquad \text{Eq. (2-20)}$$

where: $f_{ce}^{'}$ = expected concrete strength;

f_{ye} = expected yield strength of the reinforcement;

P = column axial load;

A_g = gross column area; and

ρ_l = longitudinal reinforcement ratio.

Anti-buckling requirements are specified by Priestley et al. (1996) in which a certain amount of horizontal reinforcement must be provided to ensure that the longitudinal bar does not buckle

prematurely. The two equations are the same as those presented within Section 2.1.3 of this report. These equations are based on the number of longitudinal bars present in the cross-section and diameter of the longitudinal bar.

2.2.3 ATC-32 (1996) and Caltrans (2003)

In these two different approaches from the bridge manual published by Caltrans and the ATC-32 final recommendations, the resulting equations are the same as those published by Priestley et al. (1996). This means that they produce the same equation as provided in Eq. (2-20) for the design of columns with rectangular tie reinforcement. Thus, the equation is not reproduced herein.

2.2.4 ACI 318-08

Just like the spiral reinforcement equations, ACI provides two equations to give minimum area values for rectangular hoop reinforcement for rectangular columns. These equations are presented here as Eq. (2-21) and Eq. (2-22).

$$A_{sh}=0.3\frac{sb_c f_c^{'}}{f_{yt}}\left[\left(\frac{A_g}{A_{ch}}\right)-1\right] \qquad \text{Eq. (2-21)}$$

where: A_{sh} = total area of hoop reinforcement;

$f_c^{'}$ = specified compressive strength of concrete;

f_{yt} = specified yield strength of transverse reinforcement not to exceed 100,000 psi;

A_g = gross area of a concrete section;

A_{ch} = cross-sectional area of a structural member measured to the outside edges of transverse reinforcement;

s = center to center spacing of transverse reinforcement; and

b_c = cross-sectional dimension of member core measured to the outside edges of the transverse reinforcement composing area A_{sh}.

$$A_{sh}=0.09\frac{sb_c f_c^{'}}{f_{yt}} \qquad \text{Eq. (2-22)}$$

where: A_{sh} = total area of hoop reinforcement;

$f_c^{'}$ = specified compressive strength of concrete;

f_{yt} = specified yield strength of transverse reinforcement not to exceed

100,000 psi;

A_g = gross area of a concrete section;

A_{ch} = cross-sectional area of a structural member measured to the outside edges of transverse reinforcement;

s = center to center spacing of transverse reinforcement; and

b_c = cross-sectional dimension of member core measured to the outside edges of the transverse reinforcement composing area A_{sh}.

Rearranging the above equations and solving for the volumetric ratio Eqs. (2-23) and (2-24) are produced.

$$\rho_s = 0.6\left(\frac{f_c'}{f_{yt}}\right)\left[\frac{A_g}{A_{ch}} - 1\right] \qquad \text{Eq. (2-23)}$$

where: f_c' = specified compressive strength of concrete;

f_{yt} = specified yield strength of transverse reinforcement not to exceed 100,000 psi;

A_g = gross area of a concrete section; and

A_{ch} = cross-sectional area of a structural member measured to the outside edges of transverse reinforcement.

$$\rho_s = 0.18\frac{f_c'}{f_{yt}} \qquad \text{Eq. (2-24)}$$

where: f_c' = specified compressive strength of concrete; and

f_{yt} = specified yield strength of transverse reinforcement not to exceed 100,000 psi.

The above two equations, when compared back to Eqs. (2-8) and (2-9) are very similar in that the only difference is the multiplier at the beginning of the equations. Upon closer inspection, Eqs. (2-8) and (2-9) are obtained when Eq. (2-23) is multiplied by 75% and Eq. (2-24) by 66.5%. Thus, the specifications are assuming that additional steel is required when using rectangular hoops when compared to circular hoops and spirals for the confinement reinforcement. Similar to the prior sections, when the data is extrapolated out to the effective lateral confining stress, a coefficient of effectives for Eq. (2-23) and Eq. (2-24) would be 0.71

and 0.63, respectively. These assumptions are once again similar to the recommendations of Priestley et al. (1996) for the assumption on the effectiveness of the reinforcement.

2.2.5 NZS 3101 (2008)

The New Zealand concrete structure code states that the cross sectional area of rectangular hoop or tie reinforcement shall not be less than that given by the greater of four different equations. Two of the equations are applicable to regions that are not expected to be ductile hinging regions and the other two are for regions with ductile hinging expected. In each set of equations the reinforcement must be greater than the two values produced. One of the equations is for anti-buckling and the other is just a set requirement that must be met. The equations for the ductile plastic hinge region are provided as Eq. (2-25) and Eq. (2-26) with the latter being for anti-buckling. These equations have the same form as the prior equations based on spiral reinforcement and must be in units of megapascals and millimeters.

$$A_{sh} = \frac{(1.3\text{-}p_t m) s_h h''}{3.3} \frac{A_g}{A_c} \frac{f_c'}{f_{yt}} \frac{N^*}{\phi f_c' A_g} - 0.006 s_h h'' \qquad \text{Eq. (2-25)}$$

where: A_g = gross area of column;

A_c = core area of column;

p_t = A_{st}/A_g;

A_{st} = total area of longitudinal column reinforcement;

m = $f_y/(0.85f_c')$;

f_y = lower characteristic yield strength of longitudinal steel;

f_{yt} = lower characteristic yield strength of transverse steel;

N^* = axial compressive load on column;

ϕ = strength reduction factor = 0.85 for columns not protected by capacity design;

s_h = center to center spacing of hoop sets;

h'' = dimension of core of column at right angles to direction of transverse bars under consideration; and

f_c' = specified compressive strength of concrete.

$$A_{te} = \frac{\Sigma A_b f_y s}{96 f_{yt} d_b} \qquad \text{Eq. (2-26)}$$

where: ΣA_b = sum of the area of the longitudinal bars reliant on the tie;

f_y = lower characteristic yield strength of longitudinal steel;

f_{yt} = lower characteristic yield strength of transverse steel;

s = center to center spacing of stirrup-ties along member; and

d_b = diameter of reinforcing bar.

When converted to an equation for spiral volumetric ratio using the process provided in the prior sections, Eq. (2-27) and Eq. (2-28) are produced. When adjusted to examine the impacts on the effective lateral confining stress, the first equation results in an effectiveness coefficient of 0.64 when matching the value of confining stress using a 0.95 coefficient of effectiveness. It is assumed that the anti-buckling equation would result in a similar comparison.

$$\rho_s = \frac{2(1.3\text{-}p_t m)}{3.3}\frac{A_g}{A_c}\frac{f_c^{'}}{f_{yt}}\frac{N^*}{\phi f_c^{'} A_g} - 0.012 \qquad \text{Eq. (2-27)}$$

where: A_g = gross area of column;

A_c = core area of column;

p_t = A_{st}/A_g;

A_{st} = total area of longitudinal column reinforcement;

m = $f_y/(0.85f_c^{'})$;

f_y = lower characteristic yield strength of longitudinal steel;

f_{yt} = lower characteristic yield strength of transverse steel;

N^* = axial compressive load on column;

ϕ = strength reduction factor = 0.85 for columns not protected by capacity design; and

$f_c^{'}$ = specified compressive strength of concrete.

$$\rho_s = \frac{2\Sigma A_b f_y}{96 f_{yt} d_b d''} \qquad \text{Eq. (2-28)}$$

where: ΣA_b = sum of the area of the longitudinal bars reliant on the tie;

f_y = lower characteristic yield strength of longitudinal steel;

f_{yt} = lower characteristic yield strength of transverse steel;

d_b = diameter of reinforcing bar; and

d'' = depth of concrete core of column measured from center to center

of peripheral rectangular hoop, circular hoop or spiral.

Outside the ductile hinge regions, *NZS 3101* provides a series of equations that are about the same as Eqs. (2-10) and (2-12). The main difference once again was that the governing agency determined that ties were less efficient than spiral reinforcement. This is seen when comparing the effective lateral confining stress and the associated coefficient of effectiveness. In this instance the coefficient of effectiveness was found to be 0.58 when compared to the spiral effectiveness with a coefficient of 0.95. A similar trend is expected for the anti-buckling equations of *NZS 3101*. The resulting volumetric ratio equations are provided herein as Eq. (2-29) and Eq. (2-30) with the latter being the anti-buckling requirements.

$$\rho_s = \frac{2(1-p_t m)}{3.3}\frac{A_g}{A_c}\frac{f_c'}{f_{yt}}\frac{N^*}{\phi f_c' A_g} - 0.013 \qquad \text{Eq. (2-29)}$$

where: A_g = gross area of column;

A_c = core area of column;

p_t = A_{st}/A_g;

A_{st} = total area of longitudinal column reinforcement;

m = $f_y/(0.85f_c')$;

f_y = lower characteristic yield strength of longitudinal steel;

f_{yt} = lower characteristic yield strength of transverse steel;

N^* = axial compressive load on column;

ϕ = strength reduction factor = 0.85 for columns not protected by capacity design; and

f_c' = specified compressive strength of concrete.

$$\rho_s = \frac{2\Sigma A_b f_y}{135 f_{yt} d_b d''} \qquad \text{Eq. (2-30)}$$

where: ΣA_b = sum of the area of the longitudinal bars reliant on the tie;

f_y = lower characteristic yield strength of longitudinal steel;

f_{yt} = lower characteristic yield strength of transverse steel;

d_b = diameter of reinforcing bar; and

d'' = depth of concrete core of column measured from center to center of peripheral rectangular hoop, circular hoop or spiral.

2.2.6 Japan Society of Civil Engineers (2010)

Although an equation for the spiral volumetric ratio or area of hoop reinforcement required for concrete columns was not provided, an area requirement was stated within the concrete design specifications for seismic considerations. Specifically, Eq. (2-31) was provided for columns that use spiral reinforcement and defines the converted cross-sectional area of spirals, A_{spe}, which reduces the spiral area based on the spacing within the column. This value must be less than 3% of the effective cross-section (i.e., the core section of the column).

$$A_{spe} = \frac{\pi d_{sp} A_{sp}}{s} \leq 0.03 A_c \qquad \text{Eq. (2-31)}$$

where: d_{sp} = diameter of the effective cross section of spiral reinforced column;

A_{sp} = cross sectional area of spiral reinforcement;

A_c = effective cross-section of the column; and

s = spacing of spiral reinforcement.

When rearranged and solved for the volumetric ratio, the following expression, Eq. (2-32), was found for the horizontal reinforcement needed when using spiral reinforcement in a column design.

$$\rho_s = \frac{4\pi A_{sp}}{s^2} \leq \frac{0.03\pi d_{sp}}{s} \qquad \text{Eq. (2-32)}$$

where: d_{sp} = diameter of the effective cross section of spiral reinforced column;

A_{sp} = cross sectional area of spiral reinforcement; and

s = spacing of spiral reinforcement.

2.2.7 AASHTO LRFD Bridge Design Specifications (2012)

According to the bridge design specifications published by AASHTO (2012) the reinforcement in a rectangular column with rectangular hoop reinforcement, the total gross sectional area, A_{sh}, shall satisfy either Eq. (2-33) or Eq. (2-34).

$$A_{sh} \geq 0.30\, sh_c \frac{f_c'}{f_y}\left[\frac{A_g}{A_c} - 1\right] \qquad \text{Eq. (2-33)}$$

where: A_{sh} = total cross-sectional area of tie reinforcement, including supplementary cross-ties having a spacing of s and crossing a section having a core dimension h_c;

h_c = core dimension of tied column in the direction under

consideration;

s = vertical center to center spacing of hoops, not exceeding 4.0 in.;

A_c = area of column core;

A_g = gross area of column;

$f_c^{'}$ = specified compressive strength of concrete; and

f_y = yield strength of tie or spiral reinforcement.

$$A_{sh} \geq 0.12\, s h_c \frac{f_c^{'}}{f_y} \qquad \text{Eq. (2-34)}$$

where: A_{sh} = total cross-sectional area of tie reinforcement, including supplementary cross-ties having a spacing of s and crossing a section having a core dimension h_c;

h_c = core dimension of tied column in the direction under consideration;

s = vertical center to center spacing of hoops, not exceeding 4.0 in.;

$f_c^{'}$ = specified compressive strength of concrete; and

f_y = yield strength of tie or spiral reinforcement.

Similar to ACI's requirements, AASHTO provided two equations based on different variables for the required area of transverse reinforcement. Note that the first equation provided by *ACI 318-08* (2008) as stated in Eq. (2-21) is identical to Eq. (2-33), and the second equation of *ACI 318-08* (2008), Eq. (2-22), differs from AASHTO within the coefficient by AASHTO's coefficient being 33% higher. Using the same process as in the ACI area computations, Eq. (2-34) was rearranged and solved for the volumetric ratio. The result was Eq. (2-35) where the ratio between the ACI and AASHTO approaches is still a 33% increase. Additionally, Eq. (2-35) results in a coefficient of effectiveness of 0.5 to match the effective lateral confining stress of a spiral section with a coefficient of effectiveness of 0.95 and a material ratio of 0.066.

$$\rho_s = 0.24 \frac{f_c'}{f_{yt}} \qquad \text{Eq. (2-35)}$$

where: $f_c^{'}$ = specified compressive strength of concrete; and

f_{yt} = specified yield strength of transverse reinforcement not to exceed 100,000 psi.

As a side note, Eq. (2-35) is identical to that of the 1994 Canadian Code (*CAN3-A23.3-M94*) for the design of concrete structures (Bayrak and Sheikh 2004).

2.3 Summary

Across the world, there are many different approaches for determining the amount of confinement as well as which parameters are important in the lateral design process. Some of the older approaches (e.g., New Zealand 1994) included the local design parameters based on the curvature limit states of the column cross-section while others in practice today do not account for such a demand parameter. The large variation in design parameters for determining the adequate amount of horizontal reinforcement are summarized in Tables 2-1 through Table 2-3.

Upon examination of the tables, it can be noted that there is a significant difference in complexity of equation and amount of parameters used in each approach. Although this was the case, there was no general consensus as to what is the best approach to determining an adequate amount of horizontal reinforcement when dealing with lateral loading. However, what is clear here is that most equations were developed empirically. Two prominent variables that influence the confinement reinforcement are axial load and concrete strength, which are included in almost all equations. These variables define the needed confinement to prevent failure of an axially loaded column following spalling of cover concrete. When this requirement was extended for flexural members, other variables have been added. Even then, the axial load plays a key role as flexural member ductilities are significantly affected by this variable. Other variables that has less influence are longitudinal steel reinforcement ratio as well as the ratio between the cross sectional area to area of the gross section. These variables have not always been included as they are considered to introduce unnecessary complexities. Another most significant parameter causing variation between confinement equations is the ductility demand. If this variable is introduced, it is expected that variations between the confinement requirements will be reduced.

The remainder of the report will be dedicated to identifying the confinement variations and how this impacts the lateral design process whether due to a seismic event or other lateral load concern with due consideration to the requirements of Caltrans. Furthermore, the report shall identify the need for the inclusion of curvature demand expected by the design level event to be included into the development of any future confinement equation.

Table 2-1: A summary of variables used for determining spiral confinement reinforcement

		Variables													
Source	**Eqn.**	f'_c	f_{yt}	f'_{ce}	D'	A_g	A_{core}	ALR	ρ_l	f_{yl}	ϕ_u/ϕ_y	s	l_{ac}	LRFD Resistance Factor (ϕ)	Constant
AKDOT, MODOT, NCDOT		See AASHTO Requirements													
SC DOT	(2-7)								X				X		
AASHTO Bridge ('12)-1	(2-16)	X	X												
AASHTO Bridge ('12)-2	(2-17)	X	X			X	X								
AASHTO Seismic	(2-14) (2-15)														X
ACI 318-08 – 1	(2-8)	X	X												
ACI 318-08 – 2	(2-9)	X	X			X	X								
ATC-32	(2-2)		X	X				X	X						
Caltrans 2003 (Dia. 3 ft. or less)	(2-4)	X	X			X	X	X							
Caltrans 2003 (Dia. > 3 ft.)	(2-5)	X	X					X							
New Zealand (1994)	(2-1)	X	X		X	X	X	X	X	X	X	X		X	
Watson et al. (1994)	(2-1)	X	X		X	X	X	X	X	X	X	X		X	
NZS 3101 (2008) - 1	(2-10)	X	X			X	X	X	X	X				X	
NZS 3101 (2008) - 2	(2-11)	X	X			X	X	X	X	X				X	

Note: X – indicates the use of term in specified equation

Table 2-2: A summary of variables used for volumetric equations based on the specification of required area

		Variables												
Source	**Eqn.**	f'_c	f_{yt}	f'_{ce}	D'	A_g	A_{core}	ALR	ρ_l	f_{yl}	ϕ_u/ϕ_y	s	LRFD Resistance Factor (ϕ)	Constant
ACI 318-08 – 1	(2-23)	X	X			X	X							
ACI 318-08 – 2	(2-24)	X	X											
AASHTO Bridge ('12)-1	(2-34)	X	X											
AASHTO Bridge ('12)-2	(2-33)	X	X			X	X							
AASHTO Seismic	(2-14) (2-15)													X
Priestley (1996)	(2-20)		X	X				X	X					
ATC-32 (1996) & Caltrans (2003)		See Priestley (1996)												
NZS 3101 (2008) - 1	(2-27)	X	X			X	X	X	X	X			X	
NZS 3101 (2008) - 2	(2-29)	X	X			X	X	X	X	X			X	
Watson et al. (1994)	(2-19)	X	X		X	X	X	X	X	X	X	X	X	
JSCE (JGC No. 15)	(2-32)				X							X		

Note: X – indicates the use of term in specified equation

Table 2-3: A summary of variables used in anti-buckling equations for determining ρ_s

		Variables						
Source	**Eqn.**	f_u	f_{yt}	ρ_l	A_{st}	f_y	d_b	d''
NZS 3101 (2008)–1	(2-12)		X		X	X	X	X
NZS 3101 (2008)–2	(2-13)		X		X	X	X	X
Priestley et al. (1996) and ATC-32 (1996)	(2-3)			X				
Priestley et al. (1996) and ATC-32 (1996)	(2-4)	X				X	X	

Note: X – indicates the use of term in specified equation

CHAPTER 3: REVIEW OF CONFINEMENT REINFORCEMENT AND MATERIAL MODEL EQUATIONS

To better understand the influence of the multiple approaches to computing the amount of confinement reinforcement in a given cross-section, a series of moment-curvature and pushover analyses were conducted on cantilever bridge columns. These analyses were conducted using available computer software and hand approaches based on equations developed from structural theory and experimental testing. The goals of the multiple analyses were to identify the impacts of the different equations presented in Chapter 2 on the curvature capacity of critical column sections and displacement ductility capacity of bridge columns. Limited experimental testing was also conducted as part of the project to complement existing data and further examine current material models used in the establishment of stress-strain behavior for confined and unconfined concrete.

3.1 Comparison of Available Confinement Equations

The initial comparisons included a direct look at the impact of unconfined concrete compressive strength, column diameter, axial load ratio and longitudinal reinforcement ratio on the amount of required horizontal column reinforcement based on the variables presented within Table 2-1 through Table 2-3. Once completed, the results were used to minimize the number of equations used to examine the impact of specific equations on the local section behavior and lateral behavior of columns subjected to earthquake loading to establish whether or not current equations are satisfying expected demands from earthquakes and demonstrate the need to include demand within any approach for defining confinement reinforcement. In all cases, the equations investigated were spiral or butt welded circular hoop reinforcement equations as the general consensus throughout the previous chapter was that rectangular ties and hoops were about 70% as effective as circular confinement. Therefore, the end result could be to provide additional reinforcement by this ratio if rectangular reinforcement was desired in the design process.

3.1.1 Concrete Compressive Strength

The first set of analyses examined the impact of the unconfined concrete compressive strength on the requirement for horizontal confinement reinforcement ratio. This was done by examining the equations provided in Chapter 2 and summarized in Table 2-1 and Table 2-3 with

duplicates removed. Upon closer inspection of the *NZS 3101* (2008) equation, the data set was not included in this process as it was found to result in a negative value until the axial load ratio exceeded approximately 15% - 20%. This was outside the scope of this report in which the axial load ratio on exterior bridge columns of multi-column bents was assumed to not exceed 15%. Furthermore, Park (1996) stated that this requirement shall not control over the anti-buckling requirements until about a 30% axial load ratio was attained. Thus, the *NZS 3101* (2008) equation for anti-buckling within the ductile plastic hinge region was included in the comparison as this would produce the most confinement reinforcement from the New Zealand Standard. The SCDOT value was not provided in the comparison as this was typical joint reinforcement requirements (Sritharan 2005), but was stated as a requirement to meet for the design of column confinement.

For comparison purposes, a 4 ft diameter column with a longitudinal reinforcement ratio of 2% and an axial load ratio of 5% was selected based on expected usage within high seismic regions. Additionally, it was assumed that both horizontal and longitudinal steel reinforcement would have a yield strength of 60 ksi. The cover to the main longitudinal bar was selected to be 3 in. as this would be a conservative approach based on the *AASHTO* (2012) requirements for a bridge in a coastal region and would produce a higher ratio of gross concrete area to core concrete area. The horizontal confinement bar would be a #5 bar (d_{bh} = 0.625 in., where d_{bh} is the diameter of the horizontal reinforcement) when needed in a given confinement equation. In the buckling equations specified by *ATC-32* (1996) and *NZS 3101* (2008), the number and size of the longitudinal bars within the column cross-section was needed to compute the horizontal volumetric ratio. In these equations, the bar size was specified as #8 bar (d_{bl} = 1.0 in., where d_{bl} = diameter of longitudinal bar), #11 bar (d_{bl} = 1.41 in., where d_{bl} = diameter of longitudinal bar) or #14 bar (d_{bl} = 2.25 in., where d_{bl} = diameter of longitudinal bar) to capture a range of values that may be experienced with a 2% longitudinal reinforcement ratio within a 4 ft diameter bridge column. Concrete compressive strength was varied in these equations from 4 ksi to 8 ksi as this range was typical when using normal strength concrete in a bridge column design.

The results of the comparison are provided in Figure 3-1. This figure demonstrates that when it comes to concrete compressive strength, a number of equations were not affected while others were highly influenced to the point where buckling equations might control the design of the transverse reinforcement as was the case between 4 and 4.5 ksi depending on the size of the

longitudinal bar. The equations that remained constant throughout the variation in the concrete compressive strength were related to the prevention of buckling in the longitudinal bar. These equations are independent of concrete compressive strength as they are based on the strength and quantity of longitudinal steel in the bridge column cross-section. Furthermore, the equations using #8 bar in the details required a higher level of confinement as the number of bars increased compared to the #11 bar and #14 bar detailing in order to maintain the 2% longitudinal reinforcement ratio. The remaining equations within the comparison have a linear increasing trend from 4 ksi to 8 ksi as all the equations include a term for the ratio between the unconfined concrete compressive strength and the steel yield strength. This ratio constantly increases as the steel yield strength remains constant throughout the comparisons.

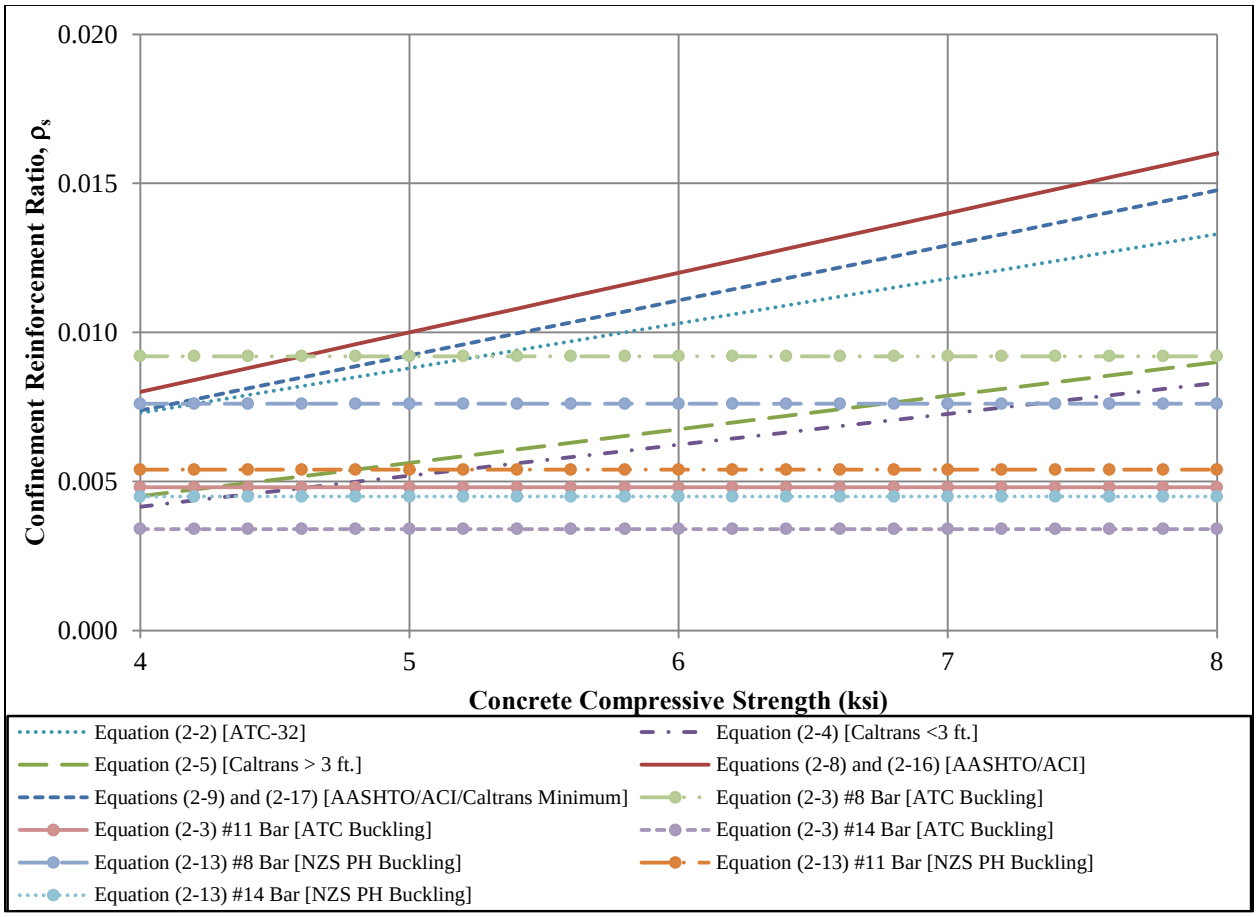

Figure 3-1: Impact of unconfined concrete compressive strength on horizontal confinement reinforcement ratio [Note: PH = within the plastic hinge region]

Examination of the transverse confinement equations presented in Figure 3-1 indicate that the highest level of reinforcement requirements as a function of concrete compressive strength

were specified within *AASHTO* (2012), *ACI* (2008), *Caltrans* (2003) and *ATC-32* (1996) when ignoring the impacts associated with premature buckling of the longitudinal reinforcement. With this assumption in mind, the highest value of the required volumetric horizontal ratio comes from Eq. (2-8) and Eq. (2-16) in which the requirements were specified to ensure an adequate flexural curvature capacity. This particular equation is purely a function of the concrete and steel reinforcing material properties within the system but resulted in a reinforcement ratio between 0.8% and 1.6%. The second highest term, ranging between 0.75% and 1.45%, was based on the minimum requirements specified within the *Caltrans* (2003), *AASHTO* (2012) and *ACI* (2008) documents that ensured the axial capacity of the core of the bridge column section without the cover concrete was the same as the gross concrete section. The recommended equation provided by *ATC-32*, Eq. (2-2), produced the next highest amount of reinforcement as the concrete compressive strength increased from 4 ksi to 8 ksi. The resulting amount of confinement reinforcement varied from 0.75% to 1.33%. This methodology was within 20% of the two aforementioned equations and took into account the highest number of variables during definition of the required transverse reinforcement; thus, the additional variables within this equation were investigated to determine the associated impact on the amount of required confinement reinforcement. The modified equations of *Caltrans* (2003) that take into account the importance of axial load ratio, Eq. (2-4) and Eq. (2-5), were approximately half the value of Eq. (2-8) and Eq. (2-9) which would have controlled the design of the cross-section.

Although ignored originally, the anti-buckling equations would have controlled the amount of transverse confinement steel at low concrete compressive strengths for the column and reinforcement setup used for the comparison, see Figure 3-1, if a #8 bar was used for the longitudinal reinforcement. However, if a #11 bar was used in the cross-section, the value could be exceeded by Eq. (2-8) by up to three times at a concrete compressive strength of 8 ksi. Furthermore, once the concrete compressive strength exceeded 4.6 ksi, Eq. (2-8) and Eq. (2-16) would control the amount of confinement steel in the system.

3.1.2 Axial Load Ratio

The next parameter investigated within the transverse confinement reinforcement equations was the axial load ratio. This parameter was selected for investigation as axial load influences the moment-curvature response of the section behavior; thus, the curvature ductility and

associated displacement ductility would be similarly affected. Similar to the concrete compressive strength a comparison was made with a 4 ft diameter column with a 2% longitudinal reinforcement ratio. The cover, horizontal bar and steel properties were maintained the same as the previous comparison. The main difference was that the design concrete strength would be 4 ksi as this is commonly specified in Caltrans' bridge design. The results of the comparison are provided in Figure 3-2.

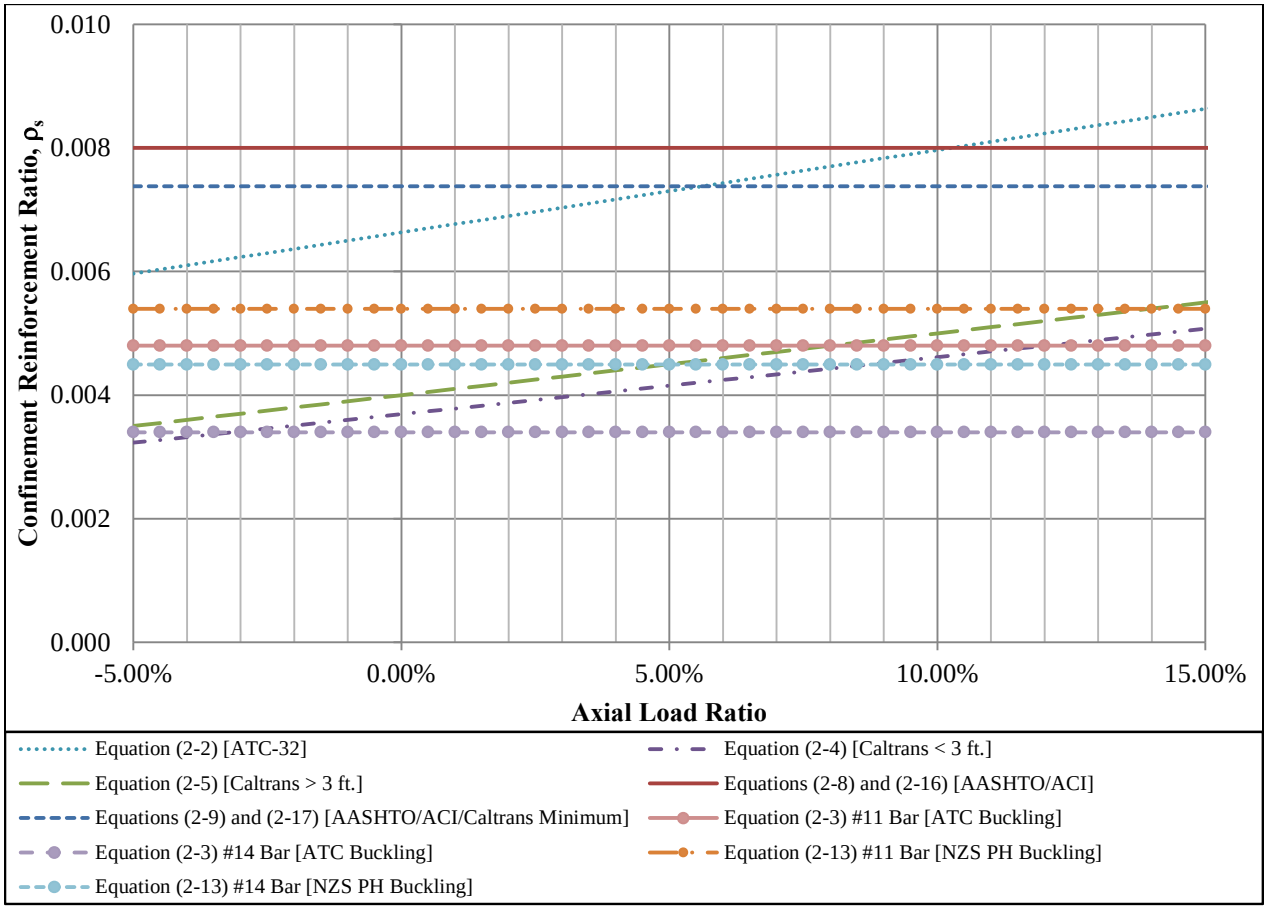

Figure 3-2: Impact of axial load ratio on horizontal confinement reinforcement ratio [Note: PH = within the plastic hinge region]

Figure 3-2 provides a series of curves in which linearly increasing and constant trends were present within the requirements for horizontal confinement reinforcement. The #8 bar buckling equations were investigated and resulted in higher requirements for the horizontal confinement reinforcement than any other equations; however, this diameter bar would result in the use of 36 bars for a 4 ft diameter cross-section and would not be practical in most designs. The constant trends within the data set were from both the buckling equations and the requirements of

AASHTO (2012) and *ACI* (2008). The use of a larger diameter longitudinal reinforcing bar resulted in the buckling equations not controlling the design of the concrete bridge column based on the applied axial load ratio. The elimination of the buckling equations resulted in Eq. (2-8) and Eq. (2-9) requiring the most amount of transverse confinement reinforcement within the cross-section examined up to an axial load ratio between 5% and 10%. Eq. (2-8), specified to ensure an adequate flexural curvature capacity in the cross-section, was consistently higher than Eq. (2-9) for the system examined as a function of axial load ratio. The approach suggested by *ATC-32* (1996) exceeded this value at an axial load ratio of 10%. However, the equation designed to maintain axial load capacity, Eq. (2-9) was exceeded at an axial load ratio of 5%. Since axial load ratios in excess of 10% are common in exterior columns of multi-column bents, the results of the analytical comparison demonstrate that the axial load ratio should be included into any future volumetric ratio equation.

To account for the impact of axial load ratio, modifications to Eq. (2-8) and Eq. (2-9) were specified in *Caltrans* (2003) that include axial load ratio as a variable, Eq. (2-4) and Eq. (2-5). Figure 3-2 indicates that these equations experienced a linearly increasing trend from -5% to 15%. However, the data resulting from these equations was generally one and a half to two times lower than the minimum requirements specified in *AASHTO* (2012) and *ACI* (2008) over the entire range examined. Furthermore, these equations were lower than the buckling equations specified by *ATC-32* (1996) and *NZS 3101* (2008) up to approximately a 5% ALR. The *NZS 3101* (2008) buckling equation utilizing a #11 bar longitudinally was higher than both of the *Caltrans* (2003) equations over the range examined within Figure 3-2. This reinforces the need to include multiple variables within any future proposed design equation for transverse confinement reinforcement.

3.1.3 Column Diameter and Ratio of Core and Gross Concrete Cross-Sectional Area

The column diameter, and thus the ratio of the gross to core cross-sectional area, of the section was investigated next as this term defines a key geometric property in any design. The diameters chosen for investigation ranged from 12 in. to 96 in., which are common throughout bridge designs. The concrete compressive strength was taken as 4 ksi, the steel yield strength was 60 ksi, a 5% axial load ratio was maintained and a longitudinal reinforcement ratio of 2% was selected as the average values for a concrete bridge column design. The cover for the main

steel was not changed and #11 and #14 bars were used in the buckling equations. It was concluded that the #8 bar should no longer be provided in the comparison based on the probability of use in a 4 ft. diameter bridge column with a 2% longitudinal reinforcement ratio.

Comparisons of results are provided in Figure 3-3, which shows evidence that the column diameter highly influences the amount of horizontal confinement reinforcement needed in a bridge column. This was noted based on the opposite trends within the results that indicate a polynomial decrease in the *Caltrans* (2003) minimum equation, Eq. (2-9), and a polynomial increase provided by the equations for anti-buckling, Eq. (2-3) and Eq. (2-13). The decreasing polynomial trend in the *Caltrans* (2003) minimum equation, Eq. (2-9), would control the design up to a column diameter of approximately 44 in. based on the need to ensure axial capacity without the presence of the cover concrete. At this point, a constant trend in the results based on the specification of transverse confinement such that a adequate flexural curvature capacity is attained, Eq. (2-8), controls until a 62 in. to 72 in. diameter column is reached. At this point, the anti-buckling equations, Eq. (2-3) and Eq. (2-13), control for the remainder of the diameters examined within this comparison. The exact controlling equation, however, depended on the diameter of the longitudinal bar being examined as it may not be practical to use #11 bars in a 96 in. diameter cross-section. The opposite trends in the results were somewhat expected as the decreasing polynomial trend contains a term based on the ratio between the gross-area of concrete and the core area of concrete in the bridge column. The increasing polynomial trend occurred as the anti-buckling equations rely on the number of bars present within the cross-section of a bridge column and must increase with column diameter to maintain the specified 2% longitudinal reinforcement ratio for the comparison.

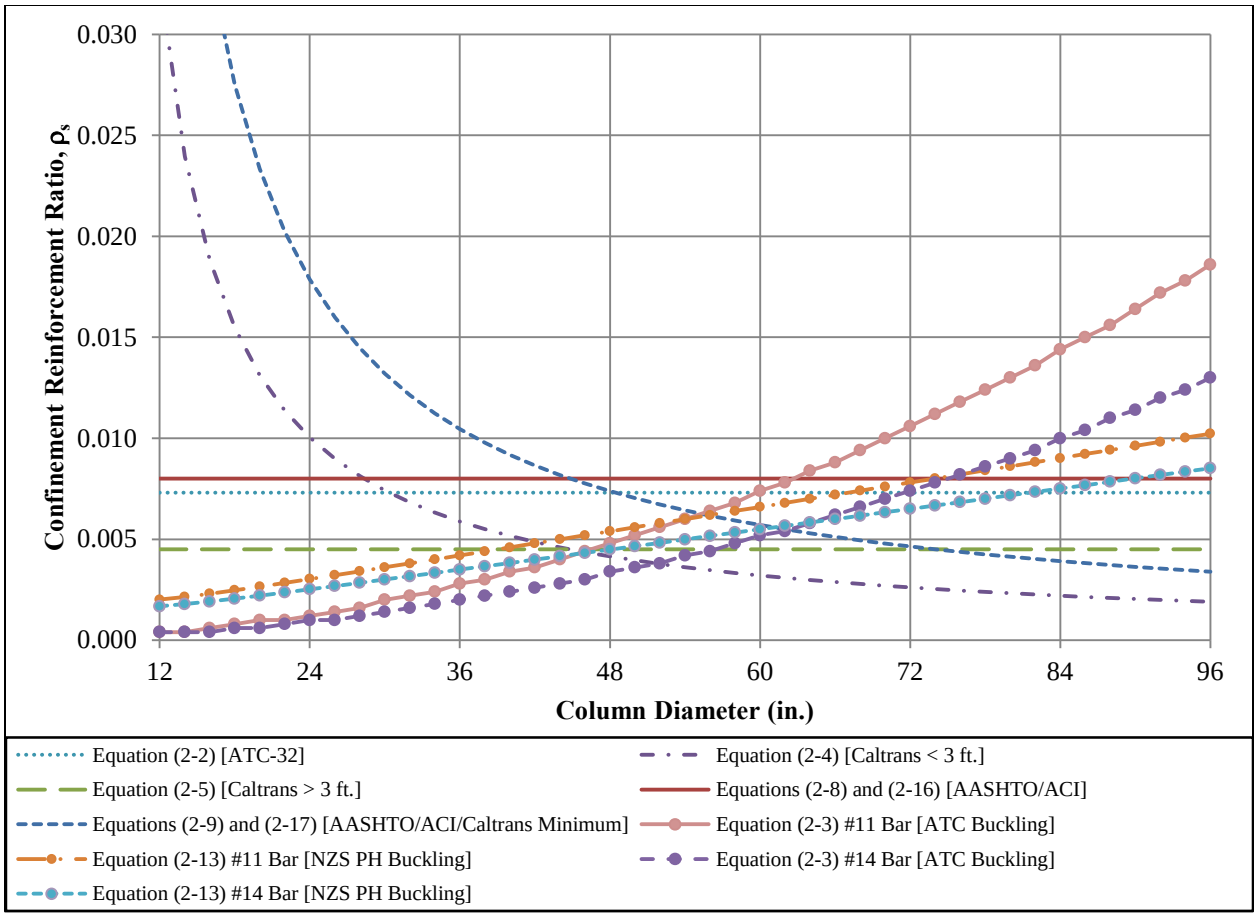

Figure 3-3: Impact of column diameter on the horizontal confinement reinforcement ratio [Note: PH = within the plastic hinge region]

Differences in requirements between a 24 in. diameter column and 72 in. diameter column were approximately a factor of 2 with the *Caltrans* (2003) minimum equation, Eq. (2-9), for the transverse confinement controlling the design at column diameters less than 48 in. This particular equation was expected to control the design within this range as many resources including *Caltrans* (2003) and *Priestley et al.* (1996) stated that this equation was for a bridge column with a diameter of less than 3 ft. The buckling equations used in Figure 3-3 may not always control the design for bridge columns in excess of 60 in. as an increased longitudinal bar diameter would result in a lower amount of required horizontal confinement reinforcement. Additionally, the equations presented in *Caltrans* (2003) that accounted for the influence of axial load ratio were once again two times lower than the controlling equations. The controlling equation in Figure 3-3 indicates that the ratio of the gross section area to the core section area is important in the overall design as noted by the polynomial behavior. Since the area of the core

and overall section take into account the column diameter, this means that a future developed design equation should take into account the column diameter or the ratio of the gross section to the core section.

3.1.4 Longitudinal Reinforcement

The final comparison made to examine the impact of variables on the design of horizontal confinement reinforcement was for the amount of longitudinal reinforcement in the bridge column. To make this comparison, a number of assumptions were made about the average concrete column design throughout California and the United States. This meant that a 4 ft. diameter column with a concrete compressive strength of 4 ksi and axial load ratio of 5% was again selected. Additionally, the steel had a yield strength of 60 ksi and the reinforcing bar was a #11 or #14 bar when the bar diameter was used as a variable in quantifying the transverse reinforcement. To make the comparison, the longitudinal reinforcement ratio was varied between 1% and 4% as these are typically the upper and lower limits that are used in a bridge column design.

The results of the comparison are shown in Figure 3-4,which contains both linear and constant trends as the longitudinal reinforcement ratio increases from 1% to 4%. The increasing trends in Figure 3-4 were from the anti-buckling and *ATC-32* (1996) equations as these equations included terms that account for the amount of steel within the bridge column cross-section. The constant trends within the comparison were based on the minimum equations presented in *AASHTO* (2012) and *ACI* (2008), which do not contain a term related to the amount of longitudinal reinforcement. These particular equations are a function of material and geometric properties of the bridge column design.

The *ATC-32* (1996) equation for confinement exceeded the requirements of *AASHTO* (2012) between a longitudinal reinforcement ratio of 2% and 2.5%. The minimum requirement specified by *AASHTO* (2012) and *Caltrans* (2003) was exceeded at approximately a 2% reinforcement ratio while the additional equation based on flexural curvature was exceeded at a 2.5% longitudinal reinforcement ratio. Once again, the equations presented in *Caltrans* (2003) based on the adjustment for axial load ratios were exceeded by a factor of two at a minimum. Furthermore, the buckling equations exceeded the requirements of *AASHTO* (2012) and *ACI* (2008) at the high end of the longitudinal reinforcement comparison when using a #11 bar within

the bridge column. Additionally, the *NZS 3101* (2008) buckling equation exceeded the required amount of confinement reinforcement using a #14 bar longitudinally. The *ATC-32* (1996) equation was exceeded at approximately a 3.4% longitudinal reinforcement ratio by the *NZS 3101* (2008) buckling equation using a #11 bar in the cross-section. However, it should be noted that a 3.4% longitudinal reinforcement ratio would contain 40 bars within a 4 ft. diameter cross-section and would not be realistic for a design.

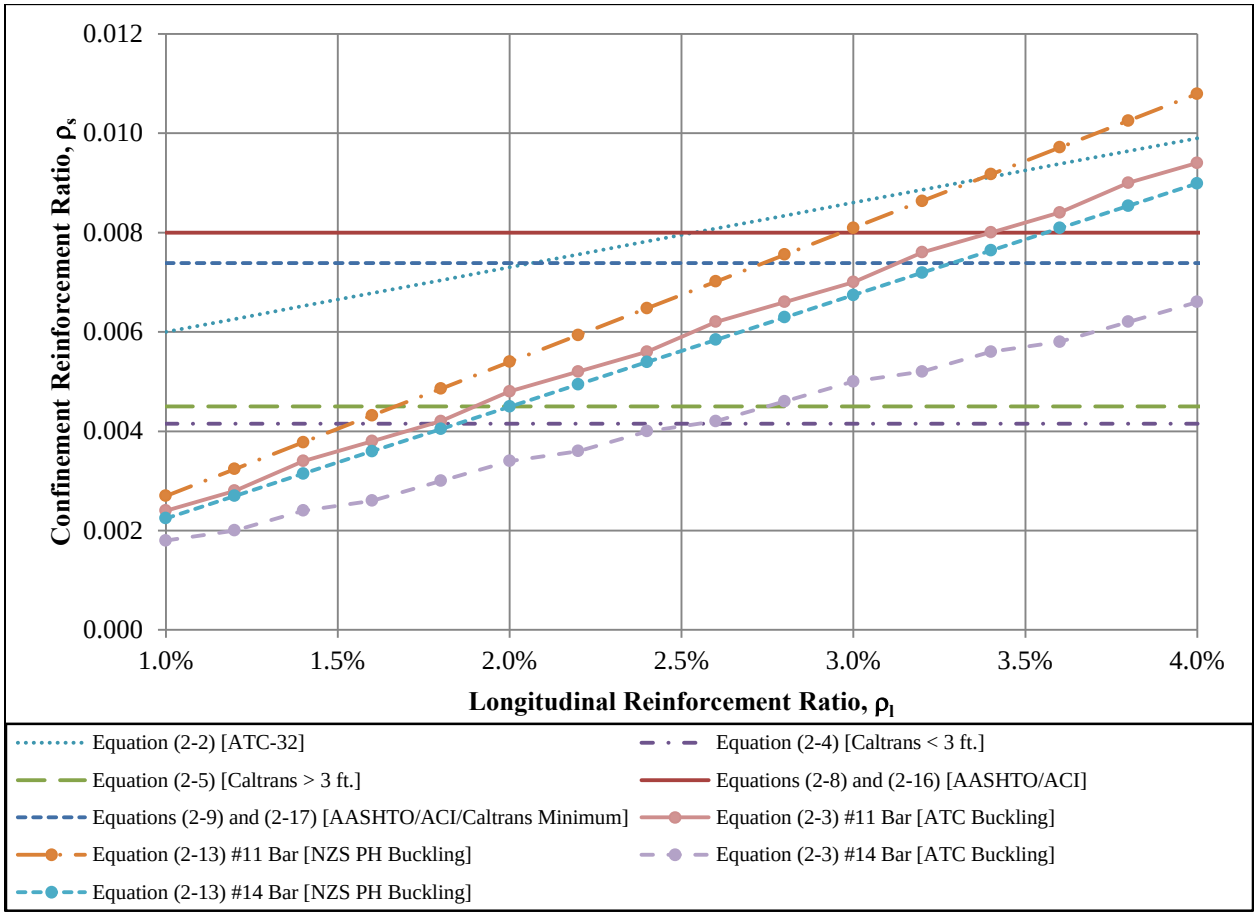

Figure 3-4: Impact of the amount of longitudinal reinforcement on the horizontal confinement reinforcement ratio [Note: PH = within the plastic hinge region]

3.1.5 Summary

Section 3.1 of this report undertook an analytical investigation into the available confinement equations within practice. The investigation examined the impact of unconfined compressive strength, column diameter, longitudinal reinforcement ratio and axial load ratio. It was found that buckling equations would periodically control the necessary amount of transverse reinforcement in the plastic hinge region of bridge columns, but this was highly dependent on the

geometry and amount of steel within the section. Minimum requirements within the axial load ratio comparison were exceeded by the linearly increasing trend of *ATC-32* (1996) between an axial load ratio of 5% and 10%. This would be crucial in a design process as exterior columns of a multi-column bent may experience an axial load ratio between -5% and 15%. Furthermore, material properties such as unconfined compressive strength were found to influence the amount of confinement reinforcement as this variable was commonly used in many of the equations examined. The minimum values specified by *Caltrans* (2003) were found to be exceeded by approaches suggested in *AASHTO* (2012) as well as *ATC-32* (1996) depending on the variable examined. The unconfined compressive strength variable was the one variable examined that did not have this trend occur within the resulting data set. The *Caltrans* (2003) equations that were modified to include the axial load ratio tended to be lower than the controlling confinement equations by a factor of 2. Based on the comparisons in Section 3.1, any equation development for the design of confinement reinforcement should take into account the unconfined compressive strength, longitudinal reinforcement ratio, axial load ratio, column geometry and other possible material properties such as yield strength of the transverse reinforcement.

3.2 Experimental Testing

As part of the overall study into the behavior of confinement reinforcement, a small exploratory study using controlled materials testing at Iowa State University was performed. This testing was a combination of available data from previous research and additional specimens that were constructed to take into account the influence of specimen size and the presence of unbounded longitudinal reinforcement. The multiple tests within the experimental study included different mix designs and the data was therefore not included all together on a single chart. This approach allows for the information to be expanded upon as needed during future studies. The experimental data was then compared with the confinement model proposed by Mander et al. (1988) and a methodology discussed in Priestley et al. (1996). This particular model was selected as it is commonly used in todays practice as stated in the SDC (Caltrans 2008). The model provides a way to predict the strength and ductility gain associated with transverse reinforcement based on the amount of longitudinal reinforcement, size of transverse reinforcement, spacing of transverse reinforcement and material properties associated with steel and unconfined concrete. Although a limited investigation, it provided insight as to the accuracy

of the equations and parameters that may be of significance when determining an adequate approach for designing the transverse reinforcement. The number of specimens used in the additional experimental testing and reasoning for each set of specimens is provided in Table 3-1 with the original test specimens taken from a previous testing cycle that investigated seasonal freezing effects on confined and unconfined concrete (Shelman et al. 2010) listed in Table 3-2.

Table 3-1: Experimental testing additional test specimens

Reinforcement Type	3″ x 6″ Cylinders	4″ x 8″ Cylinders	6″ x 12″ Cylinders	Reason
None	3	3	3	Investigate size effects on unconfined specimens and establishment of concrete strength
Confined at ρ_s = 1.22%	3	3	3	Investigate size effects on confined concrete specimens
Confined at ρ_s = 1.22% with unbonded longitudinal bars	--	3 (3 long. bar) 3 (6 long. bar)	--	Investigate the effect of longitudinal reinforcing on the behavior of confined concrete specimens
Confined at ρ_s = 0.61%	--	3	--	Establish baseline values for concrete mix with a loose confinement ratio
Confined at ρ_s = 0.61% with unbonded longitudinal bars	--	3 (6 long. bar)	--	Investigate the effect of longitudinal reinforcing on the behavior of confined concrete specimens
Total # of Specimens	**6**	**18**	**6**	

Table 3-2: Previous experimental testing specimens at 20 °C (68 °F) with no longitudinal reinforcement in confined specimens

Reinforcement Type	3″ x 6″ Cylinders	4″ x 8″ Cylinders	6″ x 12″ Cylinders	Reason
None		3		Establishment of concrete strength
Confined at ρ_s = 1.22%		3		Impact of varying levels of confinement reinforcement on concrete behavior
Confined at ρ_s = 0.9%		3		
Confined at ρ_s = 0.61%		3		
Total # of Specimens	**0**	**12**	**0**	

In the tests, cylinders were instrumented using a minimum of four gauges placed around the concrete cylinders to measure the change in displacement occurring throughout the test. The

overall test setup, basic gauge setup and a tested cylinder are shown in Figure 3-5. By combining this data with the axial load being applied at a rate of 0.5 mm/min (0.02 in./min), stress-strain curves could be produced and used to compare with the model suggested by Mander et al. (1988) and reproduced in Priestley et al. (1996) with an estimation for the ultimate strain for the confined concrete. The results of the experimental investigation are provided in the remainder of Section 3.2 of this report.

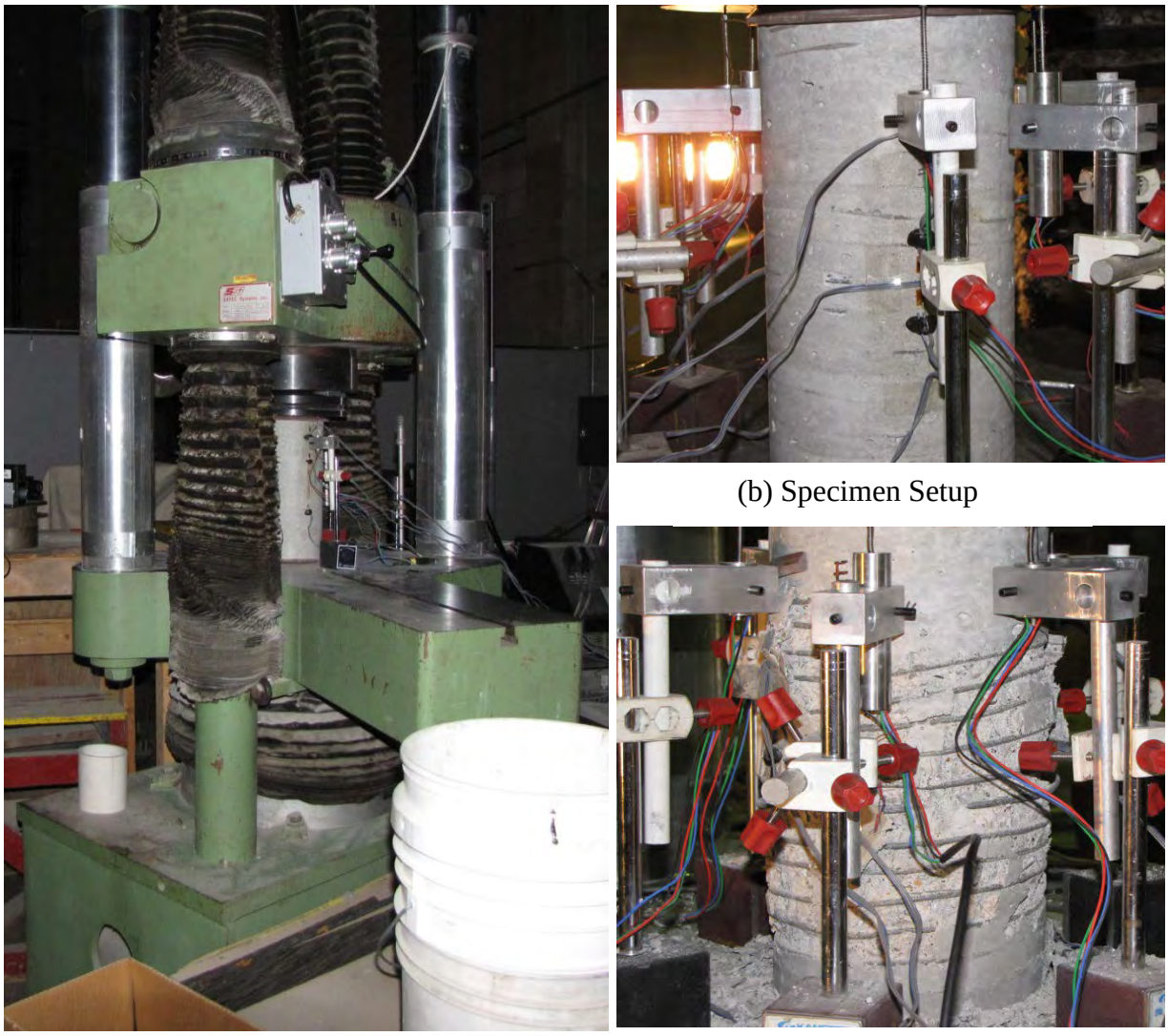

(a) Overall Testing Frame

(b) Specimen Setup

(c) Tested Specimen

Figure 3-5: Testing and setup for additional concrete specimens at Iowa State University

The idealized curves expected to arise from the testing of the multiple specimens within the experimental program take the form as shown in Figure 3-6. These curves describe the confined

and unconfined concrete behavior and its associated terminology. It can be seen that the influence of confinement reinforcement increases the compressive strength of the concrete while also causing a more ductile response until reaching the ultimate concrete compressive strain of the concrete.

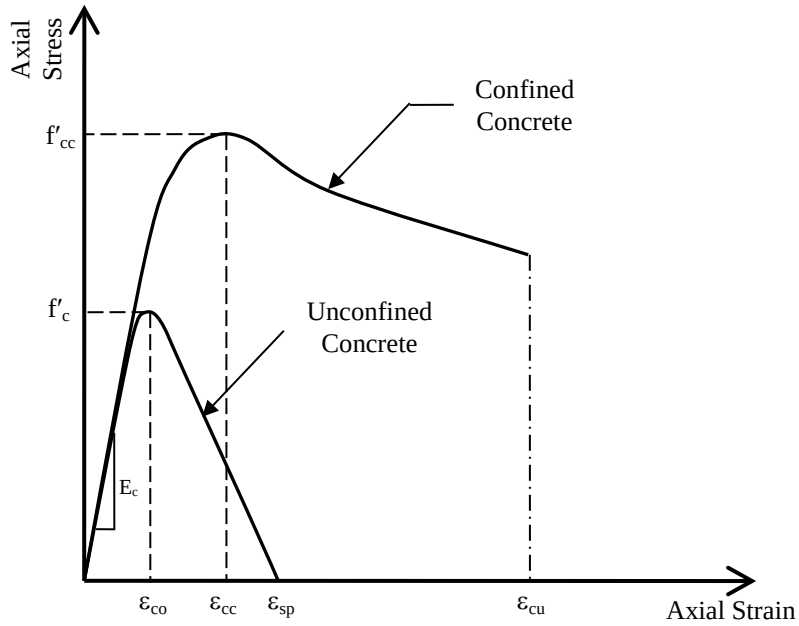

Terminology:
$f_c^{'}$ = peak unconfined compressive stress; E_c = concrete modulus of elasticity; ε_{co} = strain at peak unconfined concrete stress; ε_{co} = peak unconfined compressive strain; $f_{cc}^{'}$ = peak confined compressive stress; ε_{cc} = strain at peak confined concrete stress; and ε_{cu} = ultimate confined compressive strain;

Figure 3-6: Typical idealized stress-strain for the stress-strain behavior of concrete

3.2.1 Size Effects

The influence of cylinder size on the compressive strength of unconfined concrete has been investigated by numerous researchers as summarized and expanded upon in Vandegrift and Schindler (2006). This experimental portion of the report found that 4 in. x 8 in. cylinders experienced a compressive strength that was higher than a 6 in. x 12 in. cylinder at strengths less than 6000 psi, but also experienced a lower compressive strength than a 6 in. x 12 in. cylinder at compressive strengths greater than 6000 psi. Additional ratios described within the report by Vandegrift and Schindler (2006) maintained that the 4 in. x 8 in. cylinder experiences a compressive strength that was 0.85 to 1.15 times the strength of the 6 in. x 12 in. cylinder

depending on the strength range of the cylinders examined. Although an exploratory study with a small sample size, size effects were examined throughout the different variables to identify any possible variations. The testing at Iowa State University found that size effect was an area for further investigation based on the increasing and decreasing trends depicted in Figure 3-7 through Figure 3-9 where the diameter of the tested unconfined and confined cylinders were compared to the concrete compressive strength, strain at peak concrete compressive stress and strain at 50% of the peak concrete compressive stress. Although small, these variations are important when comparing with a constitutive model.

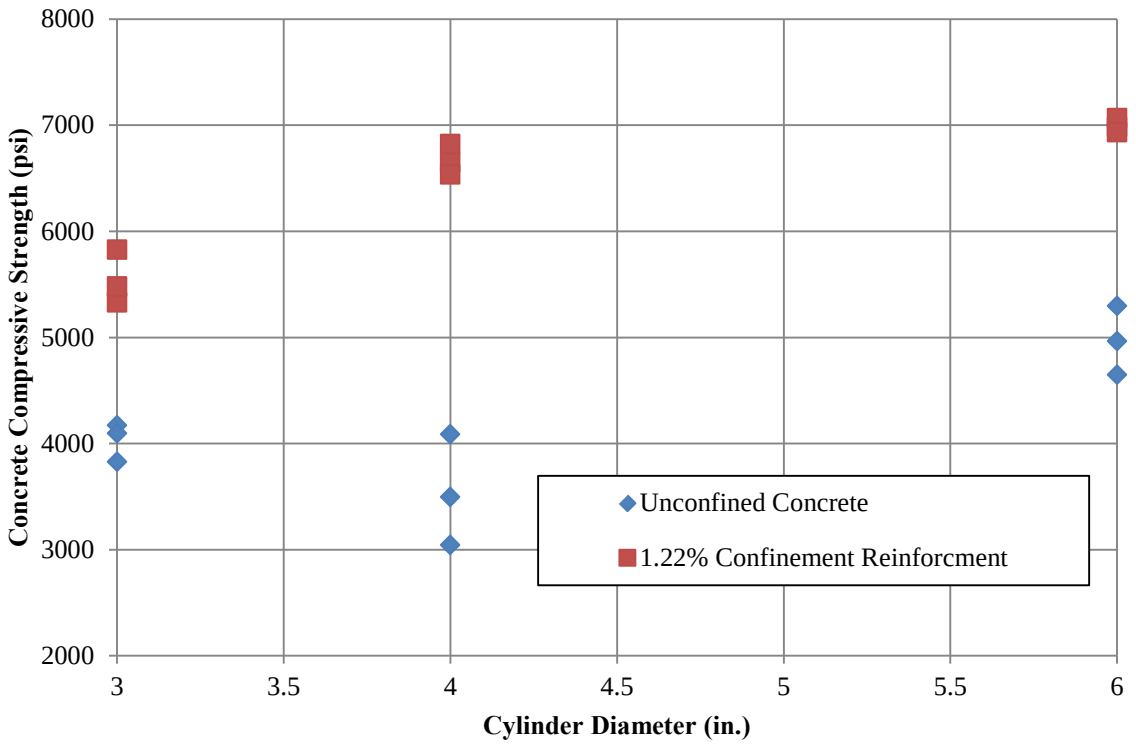

Figure 3-7: Effect of cylinder diameter on both the confined and unconfined concrete compressive strength

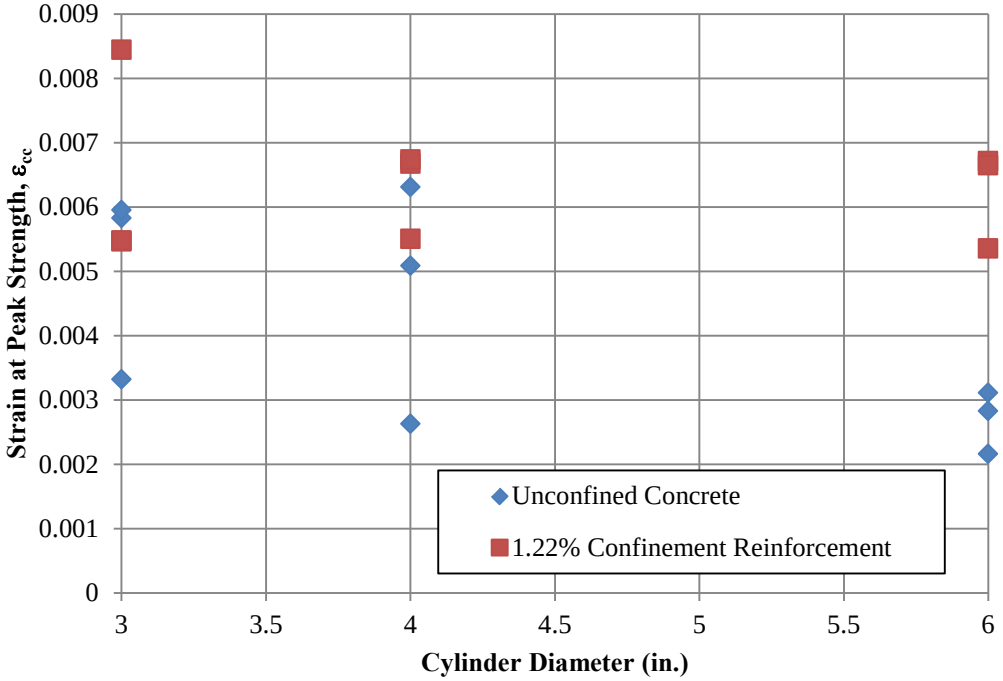

Figure 3-8: Effect of cylinder diameter on both the confined and unconfined strain at peak strength

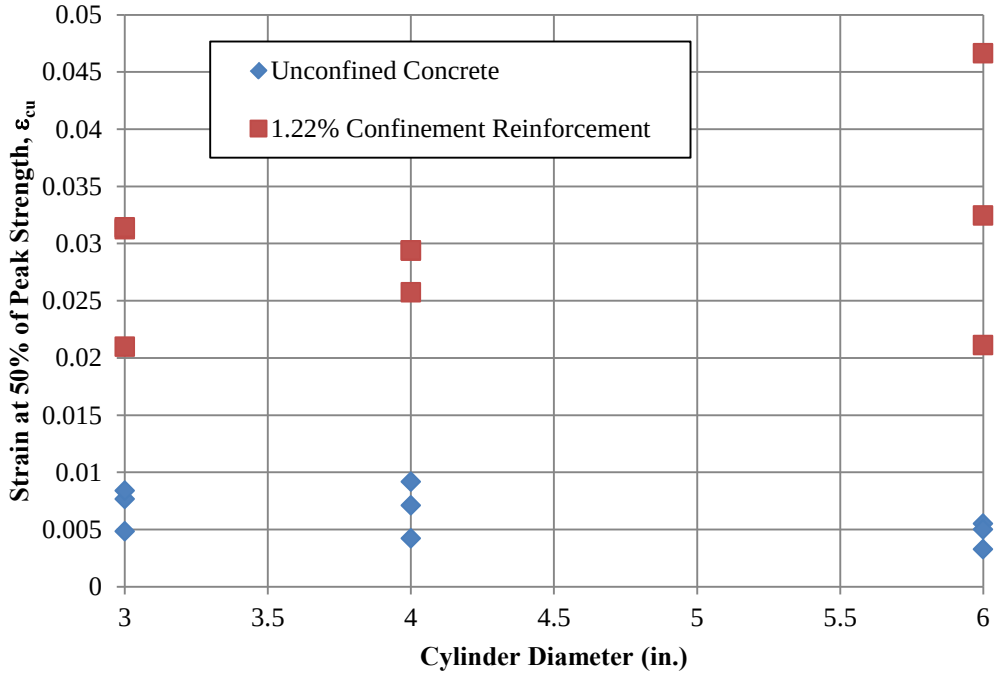

Figure 3-9: Effect of cylinder diameter on both the confined and unconfined strain at 50% of peak strength on the descending branch

3.2.2 Confined Concrete Strength

The first comparison made towards the adequacy of the common constitutive model was done for the confined concrete strength. This experimental strength was established as the peak confined stress attained during a given test as was described by the idealized curve in Figure 3-6. For comparison purposes, the theoretical model was constructed based on the strength attained during the testing of unreinforced concrete cylinders of similar size. For purposes of comparison the model was further established based on two methods of establishing the effectiveness of the confinement reinforcement. The first method was to compute the effectiveness as described in Mander et al. (1988) directly, which uses a ratio of the effective confined area to the area of concrete confined within the center line of the transverse reinforcement. The second approach for effectiveness was taken to be a constant value of 0.95 based on the recommendations of Priestley et al. (1996) for a spirally reinforced column section. The results of the comparison are provided in Figure 3-10 through Figure 3-13.

The figures indicate that the theoretical model suggested by Priestley et al. (1996), based on the work of Mander et al. (1988), and experimental testing were in adequate agreement as to the expected confined compressive strength for the different cylinder sizes tested. The experimental results of the 3 in. and 6 in. diameter cylinders lined up directly with the theoretical models. The 4 in. diameter cylinders experienced results that were higher and lower than the theory depending on the specimen set organized. This, however, could be a function of the unconfined compressive strength of the concrete used within the theoretical model. This was a possibility as the unconfined concrete compressive strength of the 4 in. diameter cylinders was lower than the average of the 3 in. diameter and 6 in. diameter cylinder tests. This would be counterintuitive to the expected trends based on the known behavior of concrete when considering the influence of cylinder size in the concrete testing.

The theoretical curves at the small diameter cylinders tended to have a reversal in the expected behavior based on the method of effectiveness. The assumption of a 95% effectiveness in Priestley et al. (1996) is a typical value for the ratio of the effective confined area to the core concrete, but was a non-conservative approach with the smaller specimen sizes. The ratio appears to begin to reach this typical value as the cylinder size increases as demonstrated in Figure 3-13, where the two curves are nearly identical with a 6 in. diameter cylinder. Thus, for

the current practice discussed in the SDC (2008) the suggested constitutive model adequately defines the concrete compressive strength in confined and unconfined concrete.

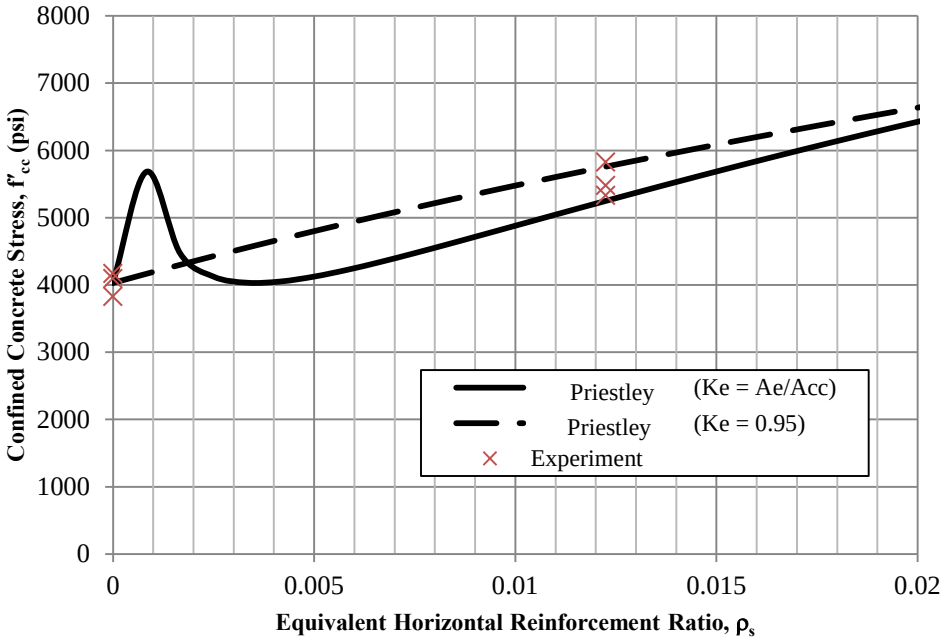

Figure 3-10: Comparison of theoretical and experimental confined compressive stregnth for 3 in. diameter specimens (f'_c= 4000 psi)

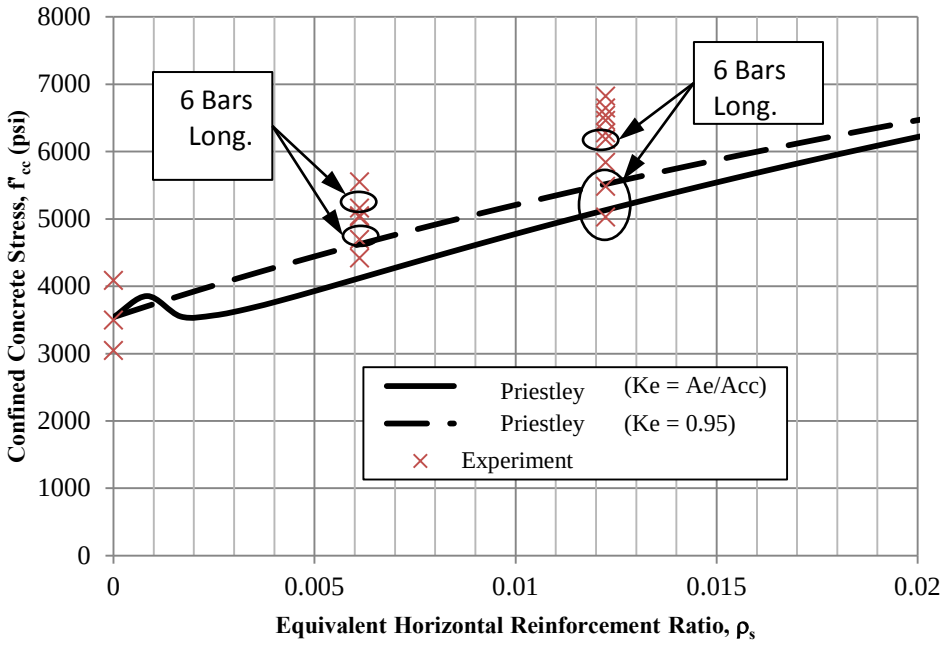

Figure 3-11: Comparison of theoretical and experimental confined compressive stregnth for 4 in. diameter specimens (f'_c = 3500 psi)

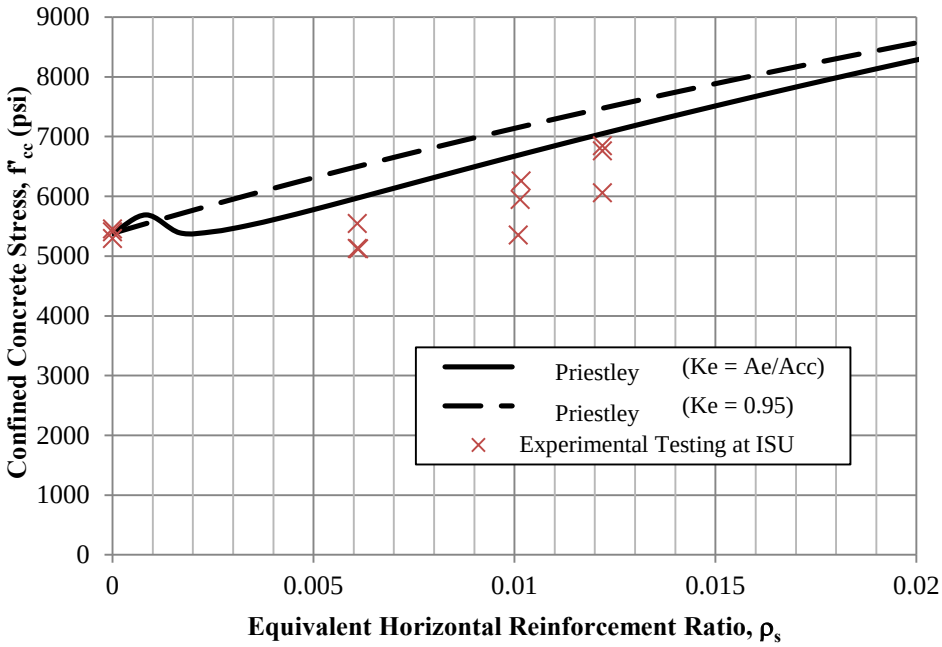

Figure 3-12: Comparison of theoretical and experimental confined compressive stregnth for 4 in. diameter specimens ($f_c^{'}$ = 5400 psi)

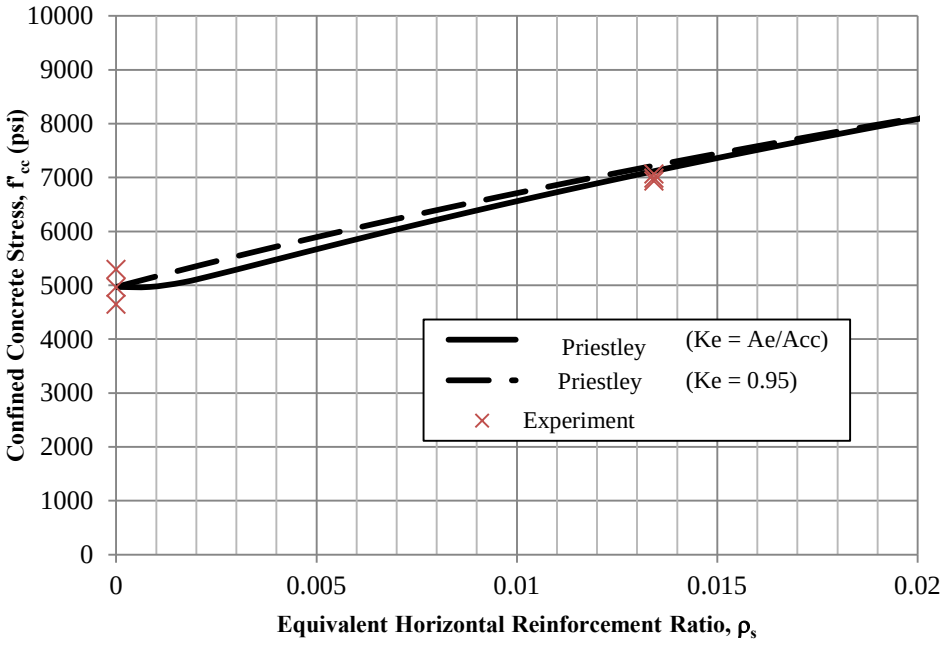

Figure 3-13: Comparison of theoretical and experimental confined compressive stregnth for 6 in. diameter specimens ($f_c^{'}$ = 5000 psi)

3.2.3 Strain at Peak Confining Stress

The second comparison of the experimental versus theoretical curves was the strain that occurs at the peak confining stress. This point establishes the location on the stress-strain curve at which the strength of the confined and unconfined concrete begins to soften. Furthermore, it indicates a point to which the elastic behavior of a concrete section could be extended in an adequately confined concrete section.

Experimental testing results are depicted in Figure 3-14 through Figure 3-17 and demonstrate that the strain at the peak confined stress can be adequately determined using the constitutive model suggested by Priestley et al. (1996). The value established using the theoretical means, however, may be a little more conservative as the experimental strain tended to be a little higher than the predicted curve. The difference in the experimental and constitutive model may be attributed to the strain assumed to occur at the peak unconfined compressive strength. The model presented in Priestley et al. (1996) and SDC (2008) suggest this point to maintain a strain value of 0.002 in/in. The experimental testing indicates that this value should be closer to 0.004 in/in. By increasing the strain at the peak unconfined compressive strength, the associated strain within the confined concrete model would further increase, thus shifting the data closer to the experimental testing. The increase in the unconfined concrete strain could increase the theoretical curve to the point that the experimental results would now be under predicted based on the level of confinement. Size effects do appear within this data set as the 6 in. diameter cylinders appeared to have an unconfined concrete strain closer to the specified strain of 0.002 in/in than the 3 in. diameter and 4 in. diameter cylinders. It may be appropriate to further increase this value in the SDC (2008) document or make it a regional value based on the concrete batched in a given region.

In addition to the strain term, the presence of longitudinal bar within the cross-section appeared to make a difference in the strain at the peak compressive strength as seen in Figure 3-15. This was partially dependent on the level of confinement and the number of bars within the cylinder as the 6 bars longitudinally influenced the response more than the 3 bars longitudinally. Additionally, the 1.22% horizontal confinement ratio was impacted more than the lower confinement ratio examined as part of this study. This is important in a future design as the current equations for the constitutive model do not take into account the presence of longitudinal

steel. It should also be noted that once again the constant effectiveness term used in the constitutive model was more appropriate for larger diameter specimens.

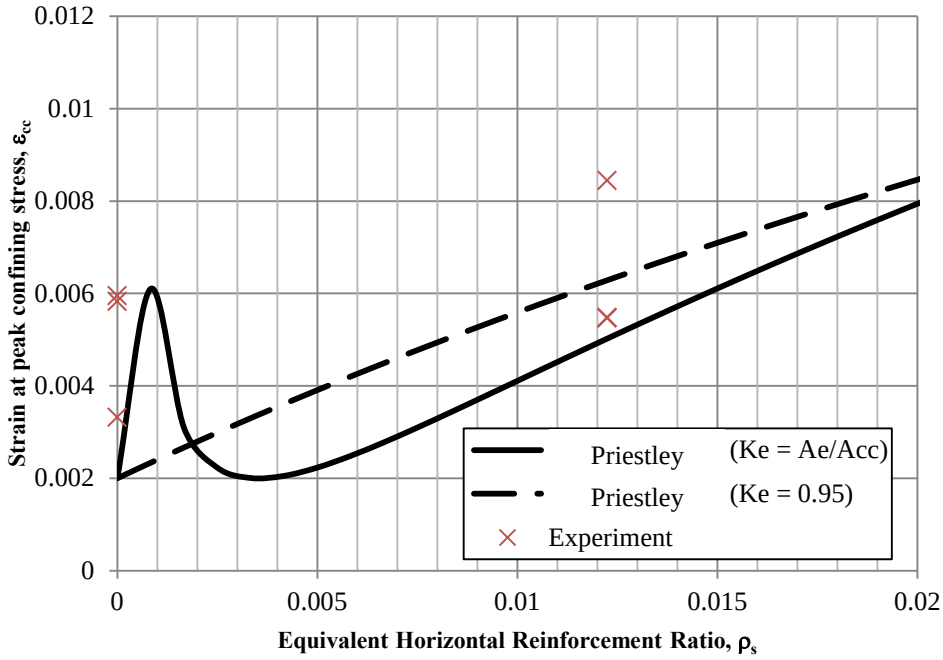

Figure 3-14: Comparison of theoretical and experimental data for the strain at peak confining stress for 3 in. diameter specimens ($f_c^{'}$ = 4000 psi)

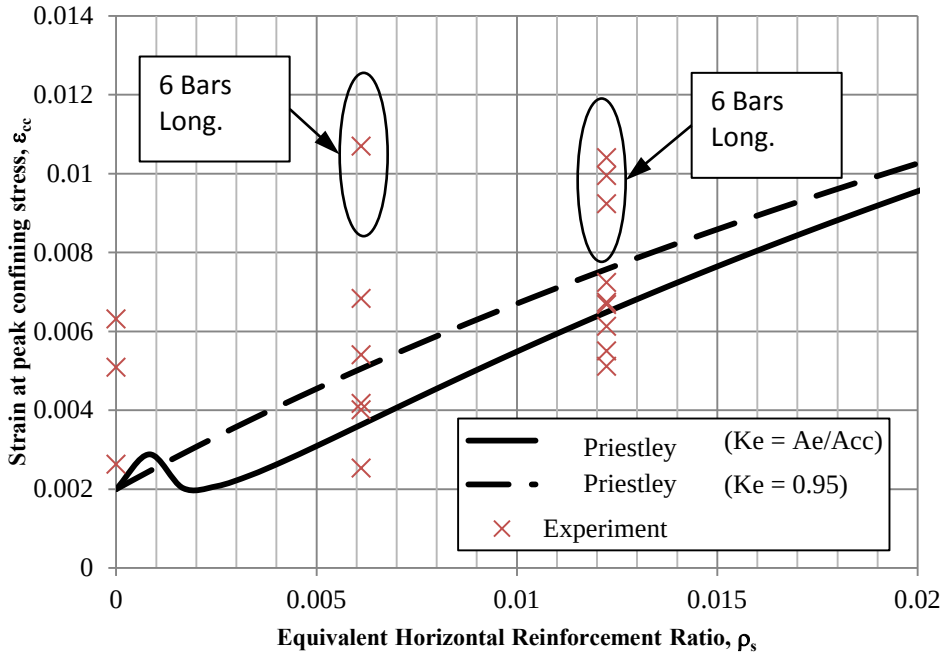

Figure 3-15: Comparison of theoretical and experimental data for the strain at peak confining stress for 4 in. diameter specimens ($f_c^{'}$ = 3500 psi)

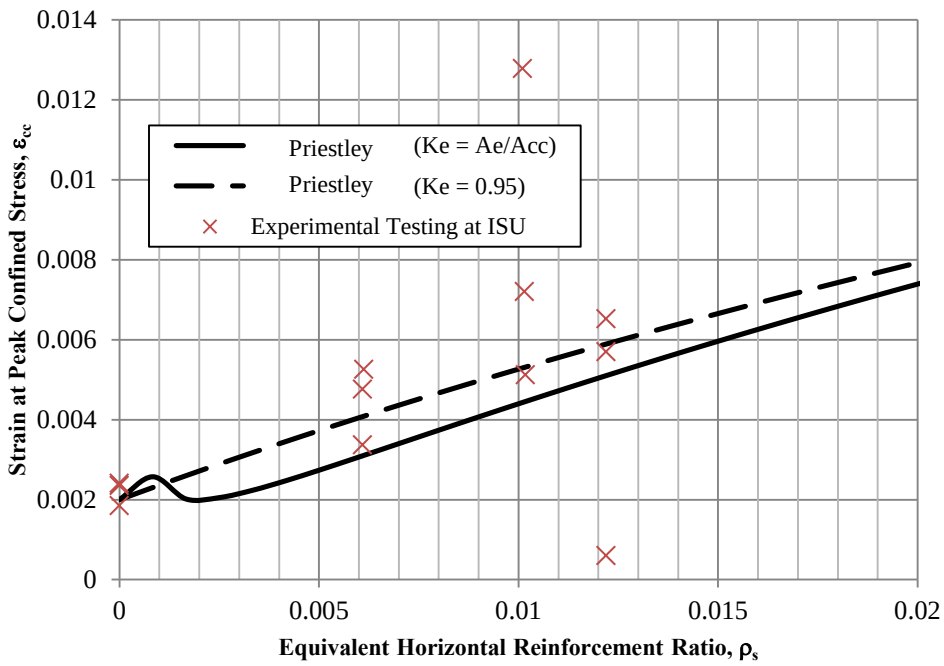

Figure 3-16: Comparison of theoretical and experimental data for the strain at peak confining stress for 4 in. diameter specimens ($f_c^{'}$ = 5400 psi)

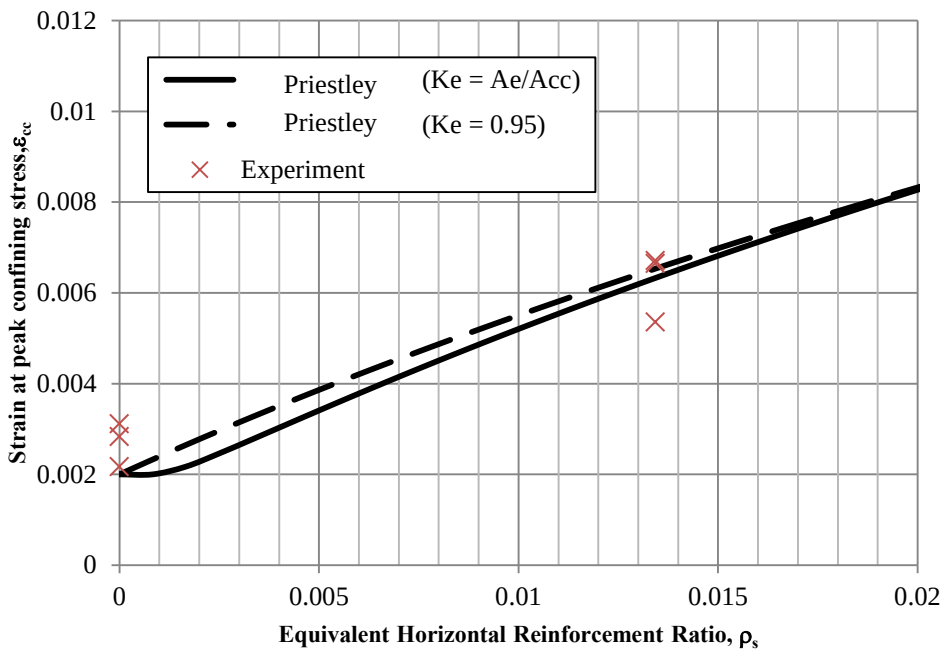

Figure 3-17: Comparison of theoretical and experimental data for the strain at peak confining stress for 6 in. diameter specimens ($f_c^{'}$ = 5000 psi)

3.2.4 Ultimate Strain Capacity

The ultimate strain capacity was the final variable examined as part of the experimental portion of this project. The ultimate strain of the column cross-section defines the capacity and the ductility that are key components in an extreme seismic event where ductile behavior is desired without failure. The ultimate strain capacity, however, is dependent on the amount of horizontal reinforcement surrounding the core of the concrete column. Establishment of this value at the first fracture of spiral reinforcement commonly follows the recommendations made by Mander et al. (1988) where the strain energy capacity of the confining reinforcement was related to the capacity of the concrete and steel energy of the remaining components. Priestley et al. (1996) used this idea and confined concrete sections under axial compression to determine a conservative approach for the establishment of the ultimate concrete strain. The final equation presented here as Eq. (3-1) tends to be a conservative approach by as much as 50%. Although a value can be attained from this equation for ultimate strain, the equation is a function of the horizontal reinforcement; thus, an iterative procedure must be used in order to get the desired ductile behavior of the bridge column.

$$\varepsilon_{cu}=0.004+\frac{1.4\rho_s f_{yh}\varepsilon_{su}}{f'_{cc}} \qquad \text{Eq. (3-1)}$$

where: ε_{cu} = ultimate concrete compression strain;

ρ_s = volumetric ratio of horizontal confinement;

ε_{su} = steel strain at maximum tensile stress;

f'_{cc} = confined compressive strength of concrete; and

f_{yh} = yield strength of tie or spiral reinforcement.

Providing a basis of comparison for this term was a critical part of the comparison for ultimate strain. For this project, Eq. (3-1) was used as the theoretical ultimate strain capacity of the concrete sections. The establishment of an appropriate comparison value for the experimental testing was done by comparing the amount of softening that took place between the peak confined concrete strength and the strength of the concrete at the ultimate strain capacity. This process indicated that a drop in the peak concrete strength of 20% to 80% would take place at the ultimate strain capacity. The most common range of softening within these theoretical constitutive models was found to be between 20% and 40%. Therefore, it was decided to compare the experimental results at a 20% and 50% drop in confined concrete strength to the

constitutive strain model suggested by Priestley et al. (1996) on the descending branch of the stress-strain curve. The 50% drop in peak stress was not able to be listed in the 4 in. diameter cylinders with an unconfined compressive strength of 5400 psi due to limitations of instrumentation at the time of testing.

The results of the experimental testing compared with theoretical constitutive model are provided in Figure 3-18 through Figure 3-21and show that the current approach to predicting an ultimate strain is dependent on specimen size as well as the location at which the ultimate condition is defined. In the 3 in. and 4 in. diameter specimens, the 20% drop in compressive stress data was 50% lower than the expected strain according to the constitutive model. However, the data based on a 50% drop in compressive stress typically met or exceeded the ultimate concrete strain suggested by Priestley et al. (1996). The 50% drop in concrete compressive strength may be a significant drop during the design of a bridge column in a high seismic region where the prevention of collapse would be desired under extreme events.

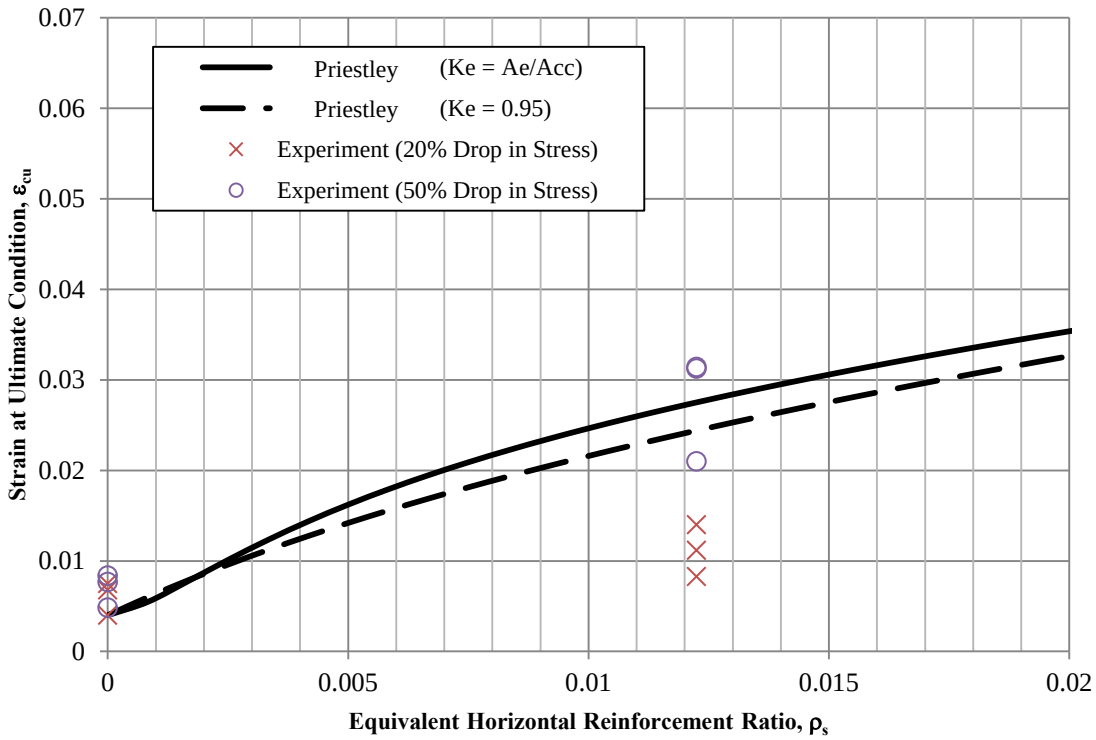

Figure 3-18: Comparison of ultimate concrete strain for 3 in. diameter cylinder specimens ($f_c^{'}$ = 4000 psi)

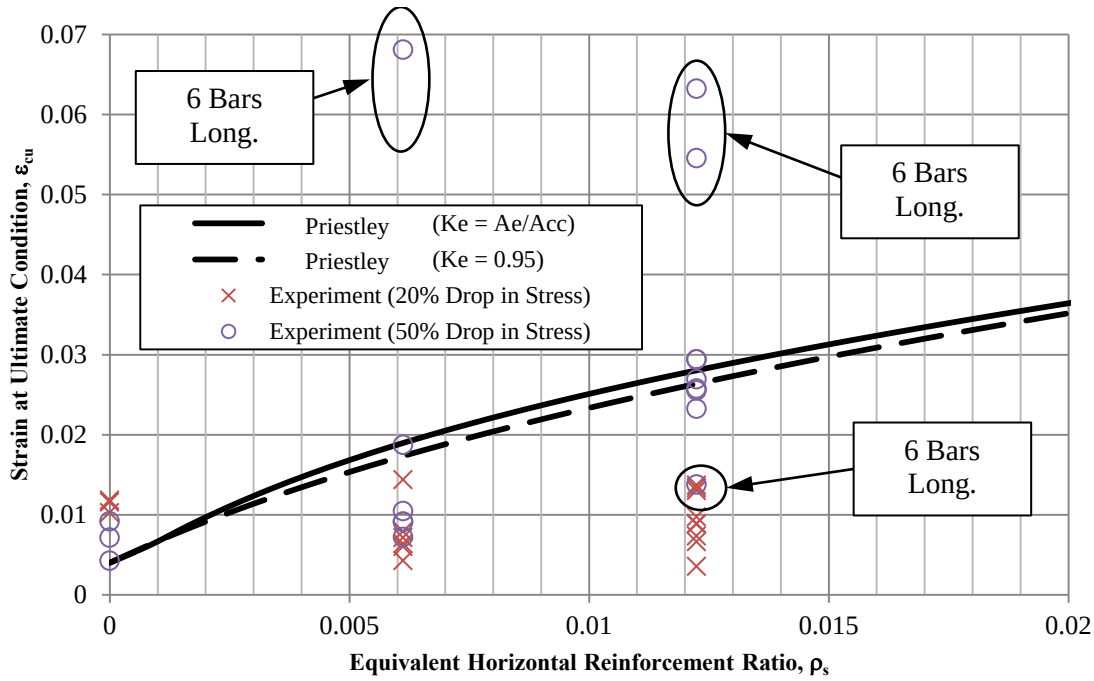

Figure 3-19: Comparison of ultimate concrete strain for 4 in. diameter cylinder specimens ($f_c^{'}$ = 3500 psi)

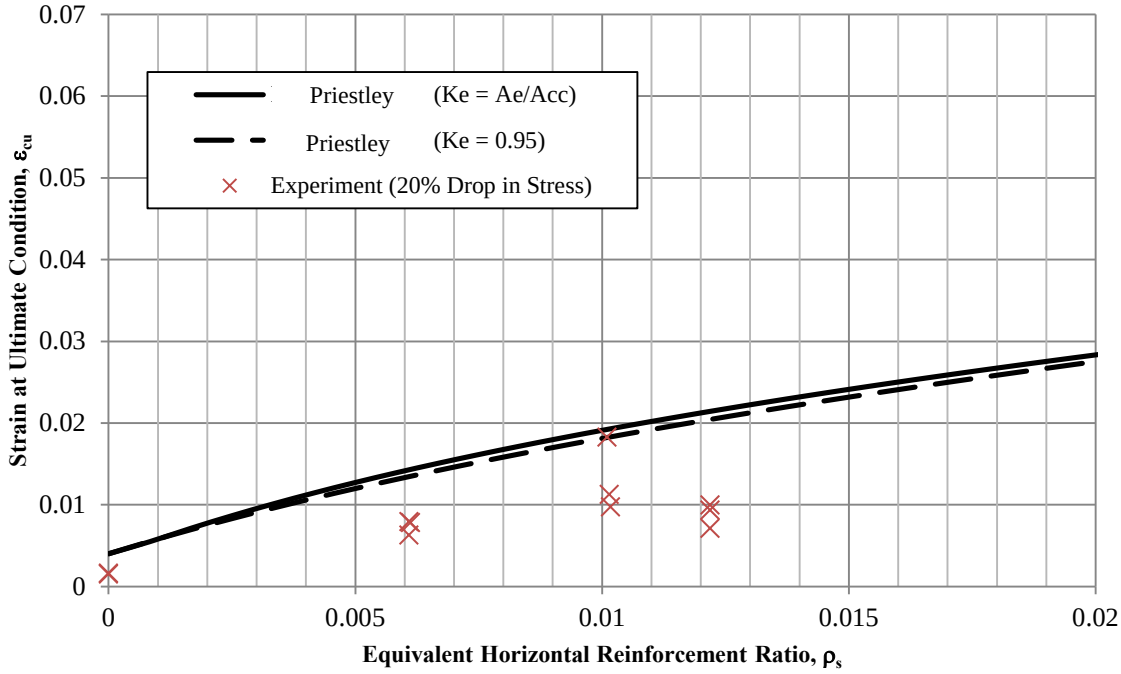

Figure 3-20: Comparison of ultimate concrete strain for 4 in. diameter cylinder specimens ($f_c^{'}$ = 5400 psi)

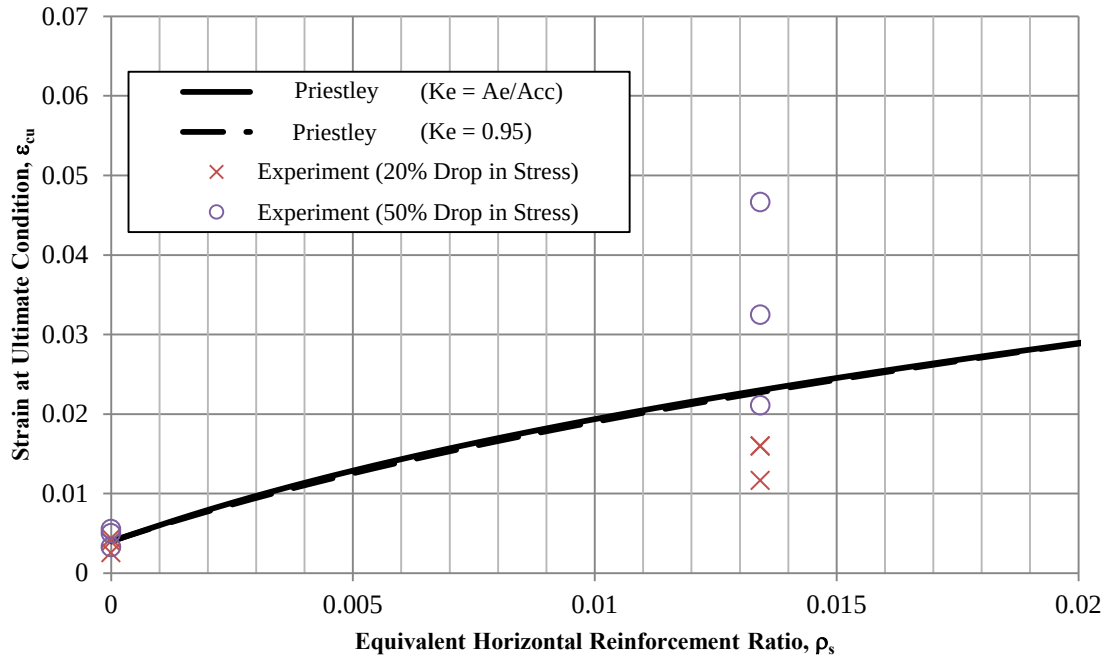

Figure 3-21: Comparison of ultimate concrete strain for 6 in. diameter cylinder specimens ($f_c^{'}$ = 5000 psi)

Similar to the concrete compressive strength and concrete strain at the peak compressive strength, the ultimate concrete strain was influenced by the diameter of the cylinder tested. The influence of size can be seen when comparing Figure 3-21 with Figure 3-18 through Figure 3-20. Figure 3-21 depicts that the ultimate concrete strain based on the 20% drop in peak strength was only 30% lower than the constitutive model compared to the 50% drop in the 4 in. diameter cylinders. Additionally, the theoretical curves within the figures indicate a difference in expected behavior based on the approach for the effectiveness coefficient. The trend in these figures was opposite of the previous trends as the ratio of the effectively confined area to core area was higher than the typical effectiveness coefficient, but got closer together as the diameter of the test specimen increased.

The presence of longitudinal bar in the concrete specimens again had an influence on the strain at the ultimate condition as seen in Figure 3-19. The increased strain capacity of the concrete section increases the overall ductility that would be gained out of a typical bridge column design suggesting the need to account for longitudinal reinforcement in an equation for establishing the amount of confinement reinforcement. The *SDC* (Caltrans 2008) states that the ultimate strain capacity should be established based on the constitutive model selected, but since

this was a common model suggested for use, the strain capacity may need to be further evaluated based on the expected demand of the bridge column design.

Although the experimental and analytical data allows for the ability to draw conclusions for different limits, the computation of the ultimate strain is highly complex as it depends on multiple variables. These variables include, but are not limited to: (1) amount of cross-section under compression; (2) role of longitudinal reinforcement in axial and transverse directions; (3) conservatism of the equation, and (4) size of unit tested. Tackling of this problem requires additional testing on columns with the focus being on the understanding of the confined concrete region. Testing can be used to identify the conservatism within a proposed equation as the data presented within this report indicates that there may be a larger discrepancy in the Priestley et al. (1996) approach since the ultimate concrete strain appeared to coincide with a 50% drop in peak confined stress. Furthermore, this equation is supposed to provide a conservative estimate for the ultimate concrete strain with a reserve capacity of as much as 50%. Testing would also help to identify how much the presence of longitudinal steel contributes to both the axial and transverse behavior to ensure the best possible approach. In addition to the information stated above, the incorporation of curvature demand into a future equation for defining the appropriate amount of confinement reinforcement may be appropriate to improve the efficiency of the design process, while accounting for the expected demand level of a design-level earthquake to meet the performance based criteria of the owning agency.

3.3 Impact of ρ_s on Design

The next step in the project was to conduct a series of analytical analyses that establish the curvature ductility capacity of multiple bridge columns based on the horizontal volumetric confinement equations previously discussed within this report. The critical review was conducted through a series of analytical moment curvature and pushover analyses with the confined concrete properties being established based on the amount of horizontal steel required by a given approach. The equations selected for further comparison establish a baseline value for examining whether demand exceeds capacity within Chapter 4 of this report. Furthermore, the analytical comparisons highlight the variation within the curvature ductility capacity and the need to include certain variables (e.g., longitudinal reinforcement ratio and axial load ratio) into any future equation. The equations selected for comparison were based on the current design of

bridge columns according to the federal highway requirements of *AASHTO* (2012 and 2010) as well as the *ATC-32* (1996) recommendations. The *AASHTO* (2012) equations, Eq. (2-16) and Eq. (2-17), were deemed appropriate for comparison as they are part of the federal highway guidelines and were recommended as for use as part of the 2003 version of the *Caltrans Bridge Design Specifications.* The *ATC-32* (1996) equation, Eq. (2-2), was deemed adequate based on the fact that this equation was developed as part of a program designed to improve the seismic design of California bridges. Furthermore, Eq. (2-2) takes into account a number of variables [e.g., axial load ratio and longitudinal steel reinforcement ratio] that are not included in the equations suggested by *AASHTO* (2012 and 2010).

The first step in the review was to perform a series of moment curvature analyses for a circular column in *OpenSEES* (2010). A circular column was selected for the analysis as Chapter 2 of the report indicated that the amount of steel required by a circular column could be increased by an appropriate amount specified by the governing agency to attain a satisfactory equation for the volumetric ratio of steel in a system that uses tie or welded hoop reinforcement in the cross-section. Figure 3-22 depicts that the analytical model for the moment-curvature analyses consisted of a zero length fiber element with the bottom node fully fixed and the upper node fixed against a shearing displacement. Boundary conditions established in this manner allow for the application of an axial load and moment while preventing sliding which causes an unstable model.

Concrete material behavior was determined based off of the concrete07 uniaxial material model defined in the program by the Iowa State University Research team with properties established using the suggestions of Mander et al. (1988). The section was specified to have an unconfined concrete compressive strength of 4000 psi and no tension capacity. The concrete fibers were discretized using a circular patch in which the extreme fiber of a given region maintained a nominal size of 1 in. x 1 in. to ensure adequate ductile capacity. Fiber size and sufficient ductility was determined appropriate based on a comparison of *OpenSEES* (2012) results with a similar section run in *XTRACT* (TRC Solutions and Chadwell 2007) and *VSAT* (Levings 2009) as shown in Figure 3-23.

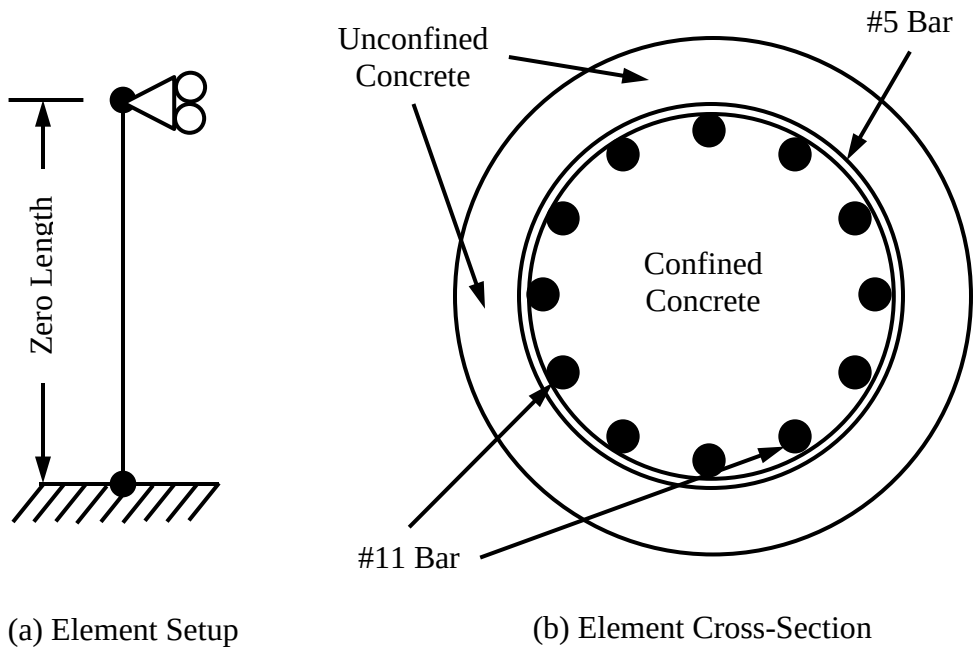

Figure 3-22: Moment-curvature analysis details in OpenSees (2010)

Material behavior of the steel was specified to follow the steel02 uniaxial material model defined in the OpenSEES framework. The longitudinal reinforcing steel was specified to have yield strength of 66 ksi with the strain hardening accounted for by using a secondary slope with a magnitude of 2% of the initial modulus of elasticity. The steel fibers were placed individually throughout the section with the assumption that the longitudinal reinforcing bars would have properties associated with a #11 bar. Additionally, the longitudinal bar size was reduced as needed to maintain a minimum of 8 bars longitudinally within the cross-section. The minimum number of bars was critical to ensure that the curvature ductility capacity was adequately determined in *OpenSEES* (2012), Figure 2-24. This arose as *OpenSEES* (2012) uses the exact location of the steel reinforcing bar in its computation, unlike *VSAT* (Levings 2009) which smears the steel around the section, and a large variation in the moment-curvature results can occur when a small number of bars are present in the final cross-section details. The confining spiral was specified to have the properties associated with a #5 bar and yield strength of 60 ksi. If the longitudinal bar size was reduced to a #9 bar or lower, the confining spiral was adjusted to have properties associated with a #4 bar and yield strength of 60 ksi.

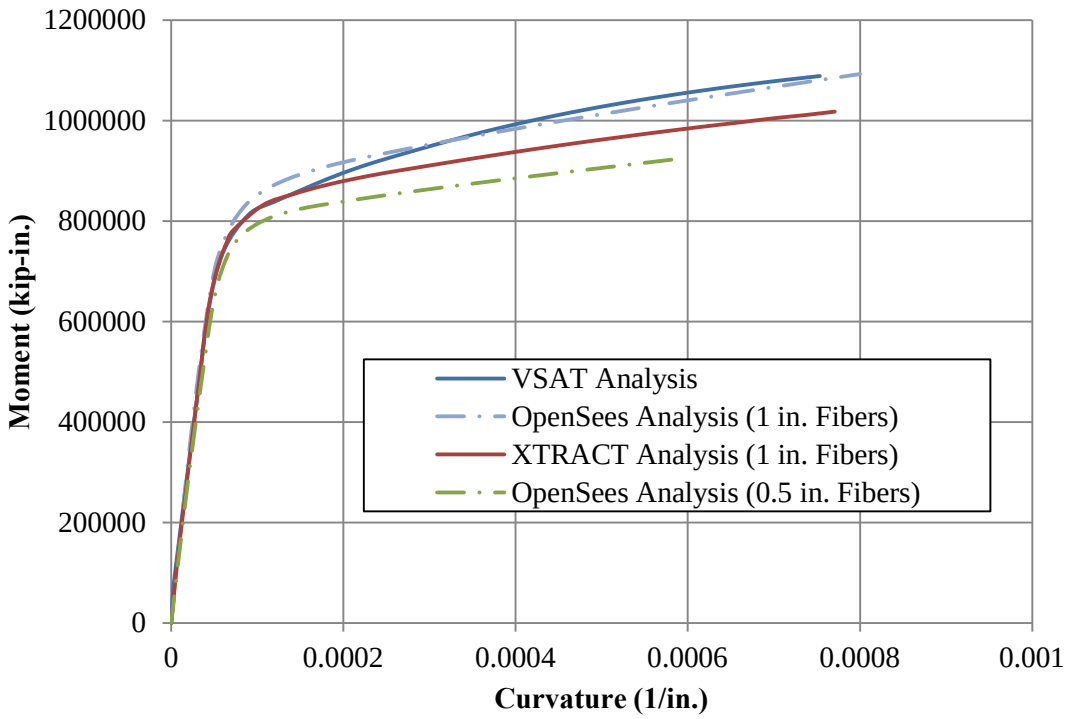

Figure 3-23: Comparison of OpenSEES moment-curvature results to XTRACT and VSAT for a 96 in. diameter column

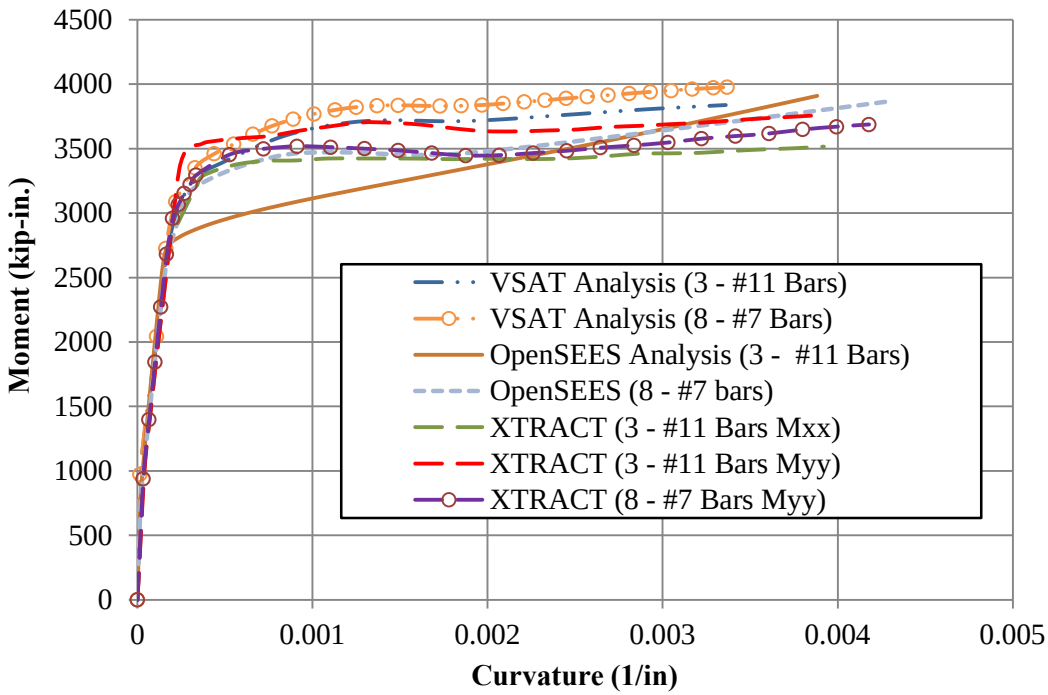

Figure 3-24 : Comparison of moment-curvature analyses based on number of bars in a 24 in. diameter collumn

3.3.1 Section Curvature Capacity

The curvature capacity of the sections were examined by comparing the curvature ductility, μ_ϕ, a unitless term that describes the ratio between the ultimate curvature of the concrete section and the yield curvature of the section. The ultimate curvature was selected to occur at the smaller of the ultimate concrete strain, as specified by Priestley et al. (1996), or an ultimate steel strain of 0.07 for the reasons discussed in Silva and Sritharan (2011). The value of 0.07 strain is close to the value suggested by the SDC (2010) of 0.06 for a #11 bar. The yield curvature was idealized from the moment-curvature curve by extending the elastic slope through the first yield point to the moment at which a concrete strain of 0.004 or steel strain of 0.015 was first attained. The resulting data was then plotted and examined for trends.

The Priestley et al. (1996) equation results are provided in Figure 3-25 and demonstrate that this approach generally provides a consistent level of confinement reinforcement with the axial load ratio typically having the largest influence. In the overall data set, it can be seen that the lower the longitudinal reinforcement ratio and the lower the axial load ratio, the higher the curvature ductility is going to be. In general, each set of axial load data asymptotically approaches a singular curvature value as the data approaches high amounts of longitudinal reinforcement.

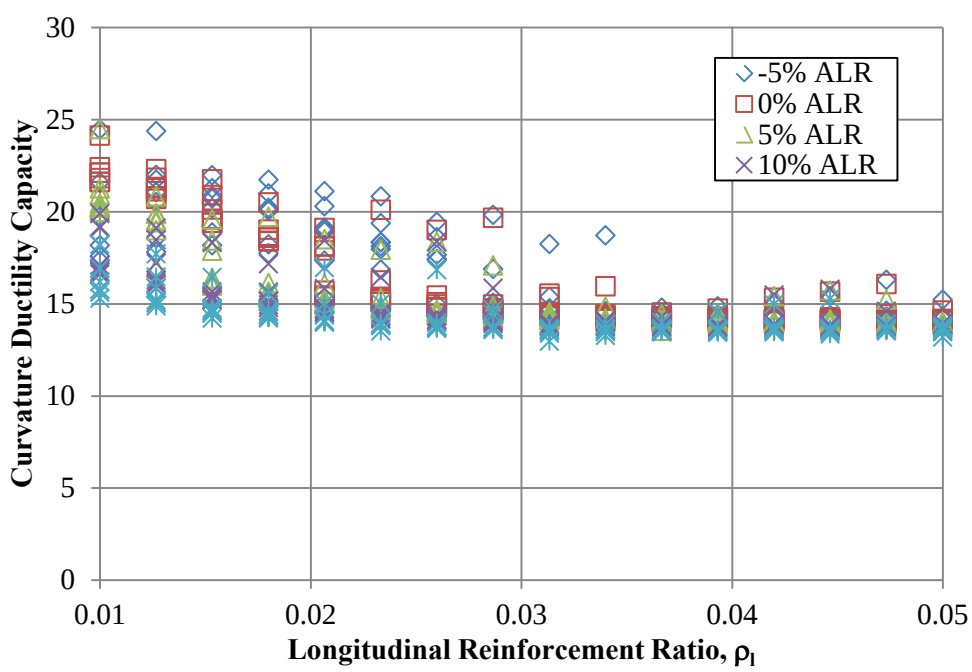

Figure 3-25: Curvature ductility of circular cross-sections assuming confinement according to Eq. (2-2) [ATC-32 1996]

The trends in the data set are more prevalent by removing a set of data, Figure 3-26, corresponding to a column diameter of 48 in. In this data set, the influence of axial load ratio is more readily seen at low amounts of longitudinal reinforcement where the curvature ductility varies between values of 15 and 22.

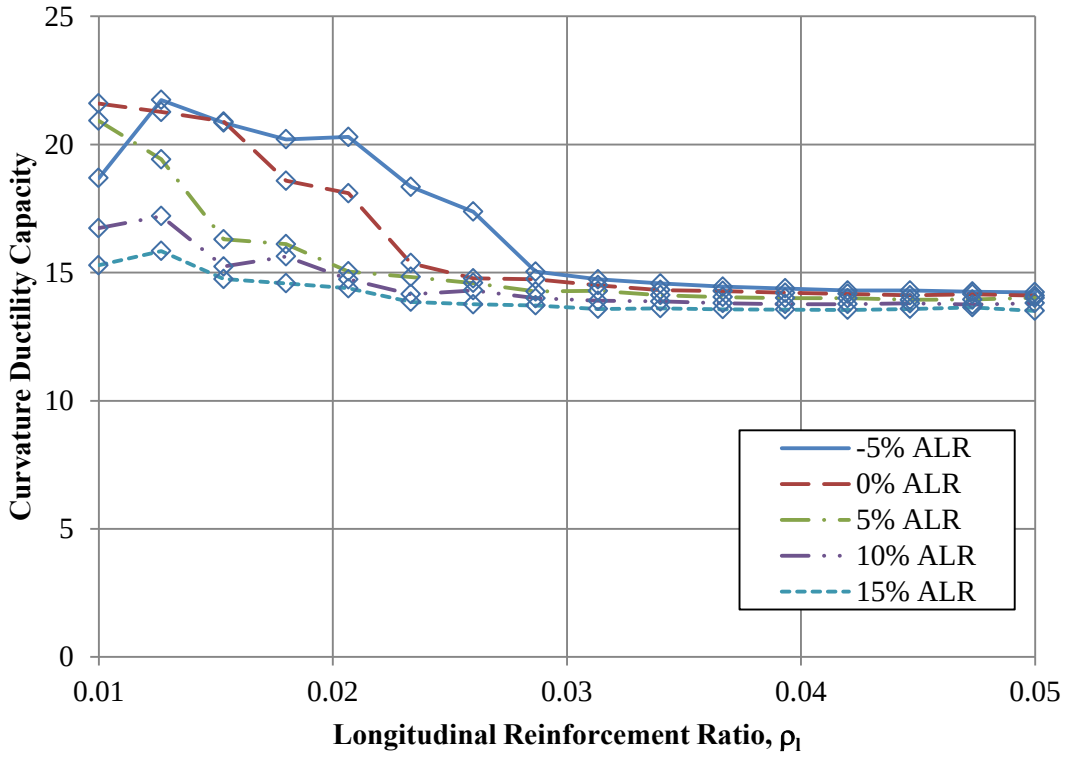

Figure 3-26: Data for a 48 in. column using Eq. (2-2) [ATC-32 1996] for confinement reinforcement

The second set of results provided in Figure 3-27 came from the use of Eq. (2-16) which was established based on the assurance of adequate flexural curvature capacity. In this data set, it can be seen that an asymptotic trend was once again prevalent as the amount of steel reinforcement in the cross-section was increased. Furthermore, the data indicates that the axial load ratio and the amount of longitudinal steel in a cross-section should be considered in the computation of confinement reinforcement. This appears as the curvature ductility capacity will vary between 10 and 25 dependent on the longitudinal reinforcement level, axial load ratio and column diameter. However, in any design, it would be ideal to maintain a minimum curvature ductility capacity no matter the level of longitudinal reinforcement or axial load ratio.

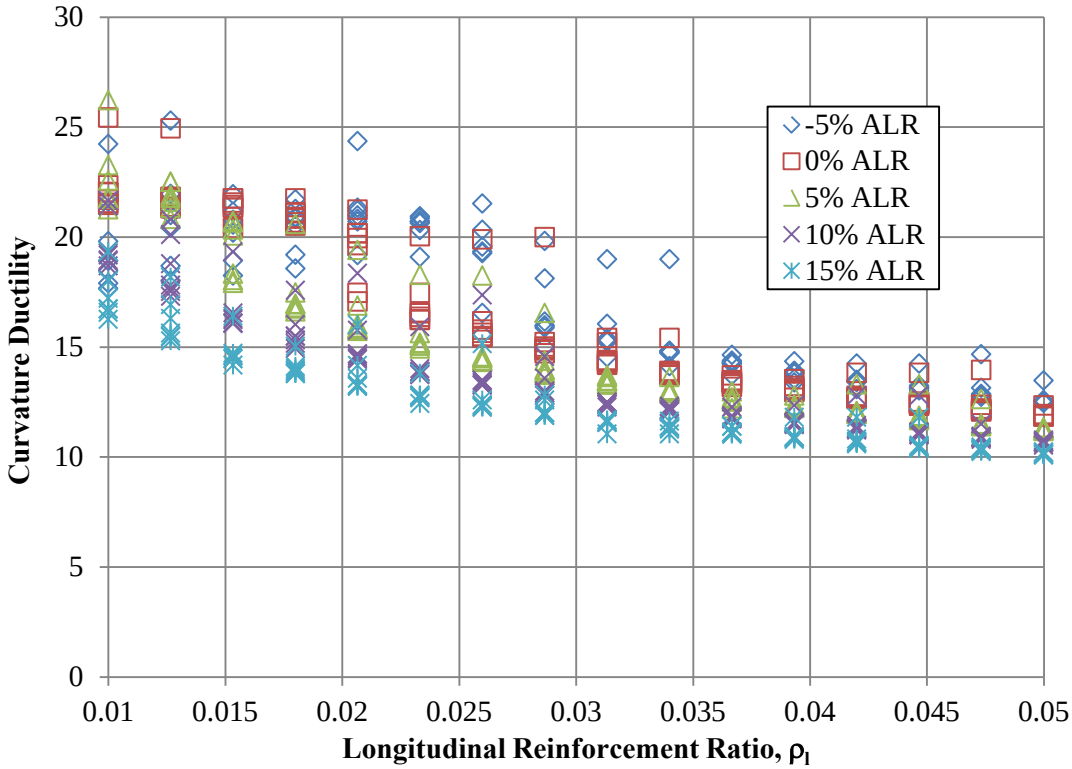

Figure 3-27: Curvature ductility of circular cross-sections assuming confinement according to Eq. (2-16) [AASHTO 2012]

The results of the curvature ductility comparison for circular columns based on the use of Eq. (2-17) for the definition of confinement from AASHTO (2012) are provided in Figure 3-29. This approach was designed to maintain axial capacity of the section after the spalling of cover concrete. The curvature ductility capacity using this approach ranges from 5 to 25 with a variation in data coming from multiple sources. Similar to the data shown in Figure 3-26 and Figure 3-28, it can be seen that the axial load ratio influences the curvature ductility capacity, but it diminishes at very high axial load ratios when the column diameter was greater than 3 ft. The asymptotic trend appears in the data set when an individual column diameter was removed from the overall data similar to Figure 3-27. In the circular sections with a diameter of 3 ft or less, the data has an overall decreasing trend, but does not asymptotically approach a single curvature ductility at high axial load ratios. Part of the variation at the small diameters may be contributed to the number of bars in the given cross-section. However, this indicates an influence of column diameter on the amount of confinement and should therefore be included in a future design equation.

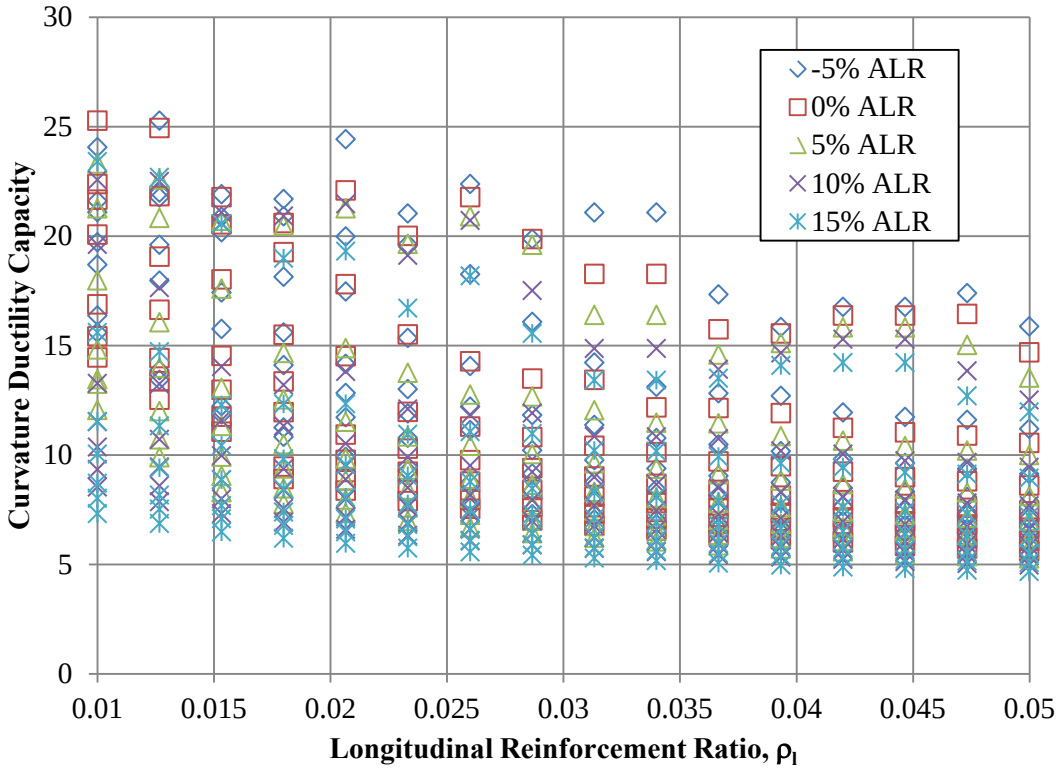

Figure 3-28: Curvature ductility of circular cross-sections assuming confinement according to Eq. (2-17) [Caltrans 2003, AASHTO 2012 and ACI 2008 Minimum]

3.3.2 OpenSEES vs Equation Based Displacement Ductility

The pushover analyses were the next step in performing a critical review of the confinement equations. For this portion of the review, Eq. (2-2) as established by ATC-32 (1996) defined the amount of horizontal reinforcement surrounding the confined concrete core. This particular equation was selected based on the number of variables covered in the equation as well as the consistency of the curvature ductility with an increase of longitudinal reinforcement and axial load ratio. The other approaches discussed in Section 3.3.1 are expected to provide a lower level of displacement ductility based on the curvature ductility capacity indicated in Figure 3-27 and Figure 3-28. The pushover analyses were completed using two different methods: (1) using OpenSEES (2012) based on a fiber based analytical approach, and (2) using equations presented in Priestley et al. (1996) with adjustments made for strain hardening and strain penetration as dictated later in this report as Eq. (3-2). In the pushover analyses, a 4 ft diameter column with a 5% axial load ratio and 2% longitudinal reinforcement ratio using #11 bars longitudinally was used for comparison purposes. Additionally, the column aspect ratio (i.e., the ratio between the height of the column and the column diameter) was varied from 3 to 10 based on current bridge

design practice. Although Caltrans ensures that the column aspect ratio exceeds a value of 4, the low aspect ratio was still examined in order to investigate dynamic impacts and further provide trends within the data sets. The OpenSEES analyses consisted of 37 displacement based fiberized beam column elements along the length of the column with a zero length element based on the uniaxial material Bond_SP01 and the recommendations of Zhao and Sritharan (2007) at the bottom to capture the effects of strain penetration into the foundation.

The reinforcement and concrete details were consistent with the moment-curvature analysis with the exception being that the concrete material model was specified as Concrete03 because of stability concerns with the dynamic analysis to be performed as part of the critical review for demand presented in Chapter 4. The material properties used in the Concrete03 material model were still established according to the recommendations of Priestley et al. (1996) which was based on the work of Mander et al. (1988). The variation in the uniaxial material models should not significantly alter the overall pushover analysis as the main difference in the two material models was the cyclic behavior. A single verification of the difference in the two concrete models is provided in Figure 3-29 where the computer model displacement of a given column was compared with a double integration based on the moment-curvature analysis and the displacement at the ultimate condition, established based on the ultimate curvature of the concrete section, varied by less than 10%. Although a single instance is shown, the results were consistent over the multiple column aspect ratios examined as part of the pushover analyses that were examining the displacement ductility of the system.

As part of the analytical study, the first step was to idealize the moment-curvature results attained for the column section described using the procedures discussed in Section 3.3.1. The resulting idealization is provided in Table 3-3 with a comparison to the full data set shown in Figure 3-30.

Table 3-3: Idealized moment-curvature results for a 48 in. diameter column section

Limit State	Moment (kip-in)	Curvature (1/in)
Yield	51320.47	0.000111
Ultimate	60226.28	0.001663

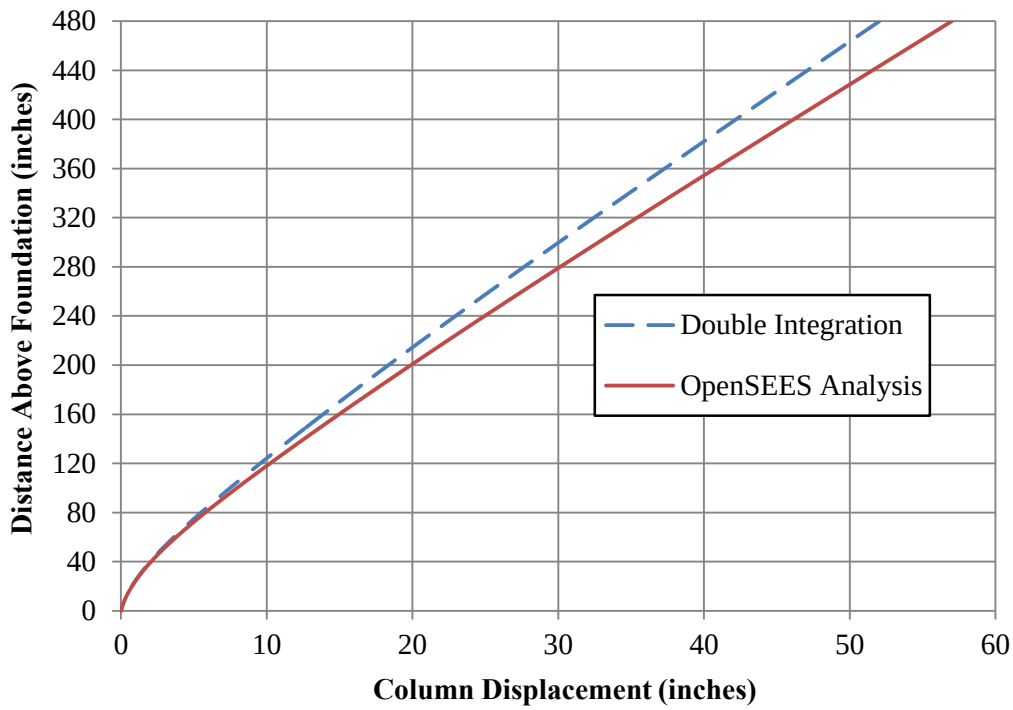

Figure 3-29 : Double integration versus pushover analysis at the ultimate condition for a 48 in. diameter column with an aspect ratio of 10

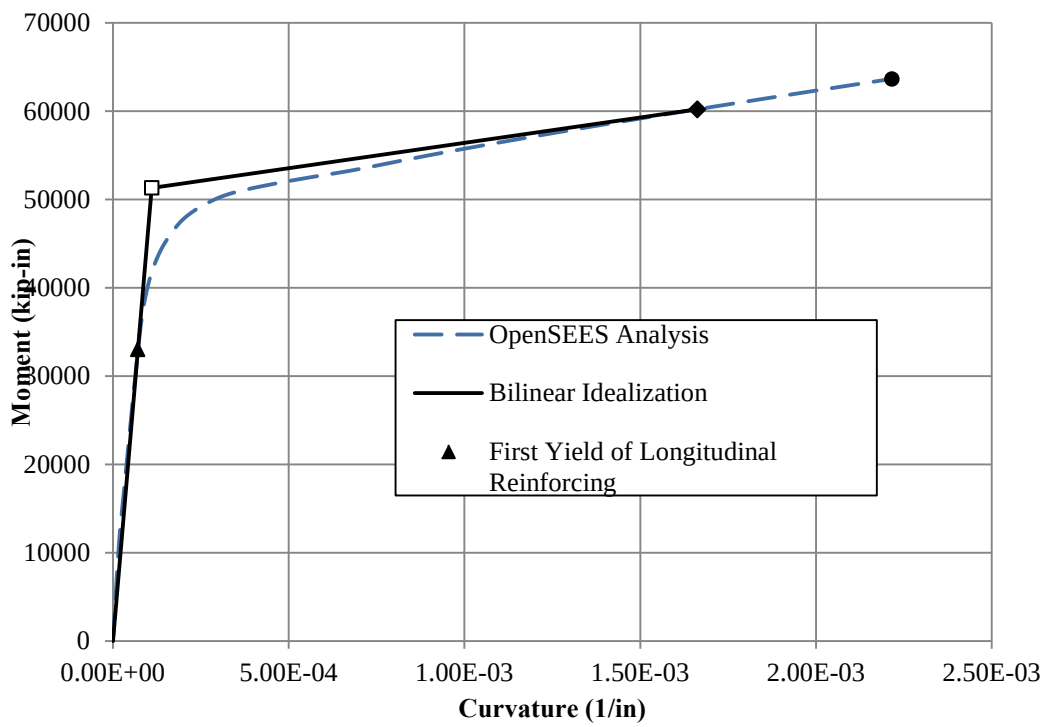

Figure 3-30: Moment-curvature comparison of idealized with full nonlinear analysis

After establishing the idealized moment-curvature response, the equation based method specified in Priestley et al. (1996) with adjustments made for strain hardening and strain penetration, Eq. (3-2), was used to define the displacements associated with any point along the moment-curvature response. The respective force components at a given level of curvature were determined by dividing the moment capacity with the free height of the column since double curvature was not examined as part of this project. This particular equation can be applied to specific limit states of the analysis in Figure 3-30 should a bilinear response be desired instead of the entire curve of the force-displacement response.

$$\Delta = \frac{1}{3}\phi_e l_c^2 + \frac{2}{3} l_{sp}\phi_e l_c + \phi_p l_p l_c \qquad \text{Eq. (3-2)}$$

where, Δ = displacement at any level of curvature;

ϕ_e = elastic curvature = $\left(M/M_y^{'}\right)\phi_y^{'}$ for $M > M_y^{'}$;

ϕ_p = plastic curvature = $\phi - \phi_e$;

l_c = column clear height from point of contra flexure;

l_p = analytical plastic hinge length;

= $0.08l_c + 0.15f_y d_{bl} \geq 0.3f_y d_{bl}$;

= $\alpha l_c + \beta f_y d_{bl} \geq (2\beta) f_y d_{bl}$

l_{sp} = analytical length accounting for strain penetration = $0.15f_y d_{bl}$;

f_y = yield strength of longitudinal reinforcement; and

d_{bl} = diameter of longitudinal reinforcing bar.

After attaining the force and displacement values associated with the hand calculation, the results were compared with the finite element models ran using OpenSEES (2012). Results of the comparison between the analytical computer model and equation based method are provided in Figure 3-31 for two of the trial runs. In this comparison, the idealized bilinear response of the finite element method was established at the yield point based on the strain levels previously discussed for the moment-curvature analysis. However, the ultimate condition was established based on the ultimate curvature of the section as stated in Table 3-3. At the ultimate limit state, the strain levels in the steel and concrete fiber elements were not consistent with the moment-curvature analyses. This is believed to be a function of the nonlinearity at the ultimate limit state, the strain penetration element and the overall spread of plasticity near the column base.

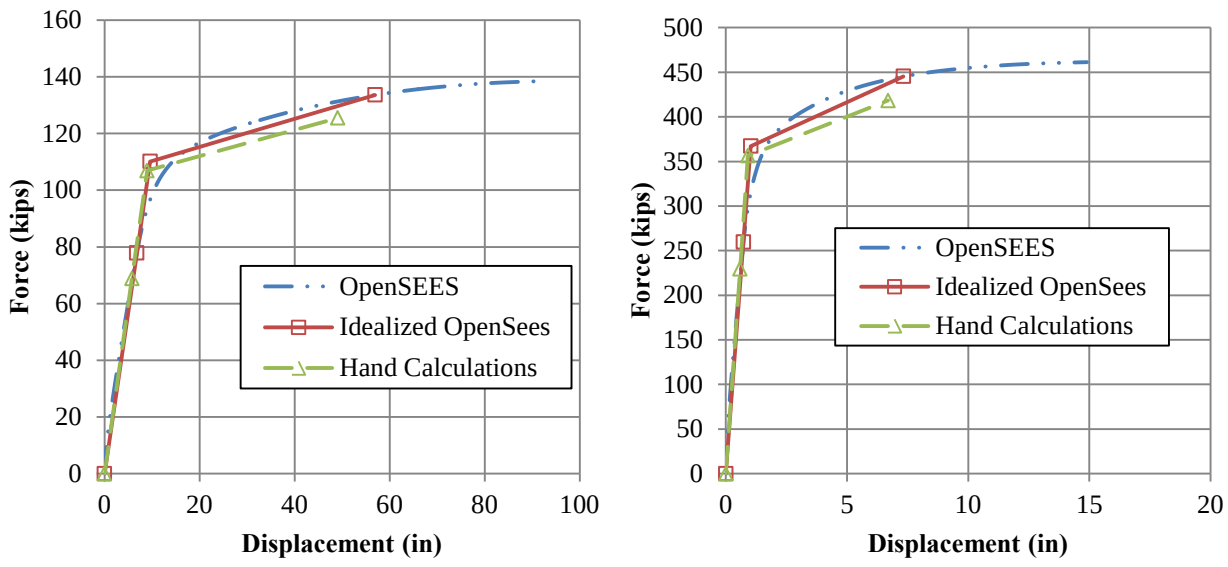

(a) Aspect Ratio of 10 (b) Aspect Ratio of 3

Figure 3-31: Comparison of equation based and OpenSees pushover computations for a 48 in. diameter column with an aspect ratio of 3 and 10

The graphical comparison indicates that the finite element method typically resulted in a higher level of displacement than the hand calculation technique although the ultimate curvature established the end of the pushover analysis. This was found to be mostly associated with the coefficients of 0.08 (alpha) and 0.15 (beta) assumed as part of the analytical plastic hinge length within Eq. (3-2). To better identify a realistic value of these coefficients, a series of additional analyses were undertaken, Figure 3-32. Figure 3-32 suggests that an assumption of 0.08 may be conservative for the coefficient in the analytical plastic hinge length computation depending on the cross-section examined. Furthermore, the alpha coefficient varies with axial load ratio, concrete compressive strength, longitudinal reinforcement ratio, the amount of transverse confinement reinforcement and possibly other parameters not investigated within this study. Using the same analyses that established the alpha coefficient, the beta value was found to be reasonably close to the assumed value of 0.15 at a value of 0.145. Based on these series of analyses, implementation of an alpha coefficient of 0.10 and a beta coefficient of 0.145 to the equation based methodology was undertaken when comparing the computer and hand simulations. These changes are depicted in Figure 3-33, where the modified hand calculations are shown to more closely represent the computer simulation. This suggests that the current equation methodologies are sufficient.

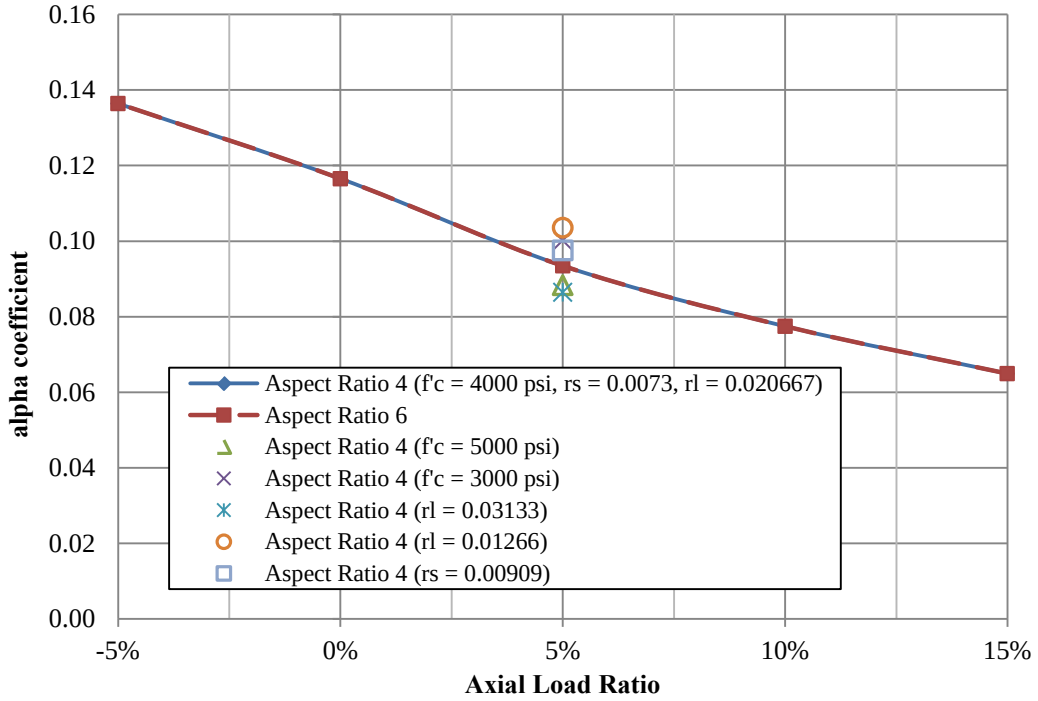

Figure 3-32: Influence of design parameters on the alpha coefficient for determining the analytical plastic hinge length used in Eq. (3-2) for a 48 in. diameter column

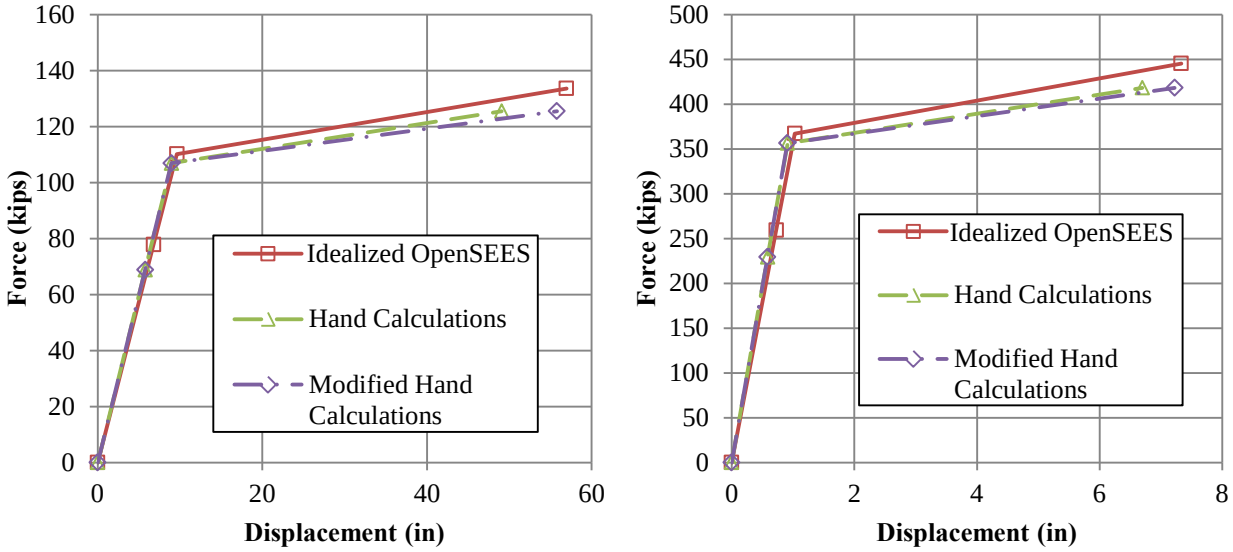

(a) Aspect Ratio of 10

(b) Aspect Ratio of 3

Figure 3-33: Comparison of idealized force-displacement based response with modified coefficients for a 48 in. diameter column with an aspect ratio of 3 and 10

The results of pushover analyses are provided in Table 3-4 where the displacements computed using the two different methods are provided as well as a percent difference in relation to the computer model. Modifications to the coefficients did not significantly alter the yield displacement as the alpha coefficient of 0.10 does not apply to the equation at the yield limit state, where the analytical plastic hinge length is not applicable when a bilinear idealization is assumed.

Table 3-4: Pushover comparison for a 48 in. diameter column using OpenSEES and the modified coefficients in Eq. (3-2)

	Yield Displacement			Ultimate Displacement		
Aspect Ratio	Equation	OpenSEES	Difference	Equation	OpenSEES	Difference
3	0.91	1.03	-11.6%	6.70	7.33	-8.59%
4	1.56	1.73	-9.83%	10.46	11.64	-10.1%
5	2.37	2.60	-8.85%	14.98	16.88	-11.3%
6	3.35	3.65	-8.22%	20.27	23.06	-12.1%
7	4.50	4.88	-7.79%	26.33	30.11	-12.6%
8	5.83	6.28	-7.17%	33.14	38.12	-13.1%
9	7.32	7.87	-6.99%	40.73	47.05	-13.4%
10	8.98	9.62	-6.65%	49.07	56.95	-13.8%

Besides a straight comparison of the displacement values, the displacement ductilities of the two different methods were compared as illustrated in Figure 3-34, and it was found that the finite model typically produced a higher level of displacement ductility. However, both curves exhibit a decreasing trend in displacement ductility as the column aspect ratio increased from 3 to 10. At a column aspect ratio of 10, the difference in the displacement ductility was a value of 0.5 and this was the maximum difference seen at any of the aspect ratios. This difference is a relatively minimal difference between the two different approaches. It should be noted that the curvature ductility in the two methods were different because of the procedures used to establish the displacement values in the idealized bilinear response. The curvature ductility for the equation based methodology was 15 compared to 13.8 for the pushover analysis for all aspect ratios as the same column section was used. Thus, in the critical review of Chapter 4 a curvature ductility capacity of 13.8 was used as a baseline for determining whether demand exceeded capacity to maintain consistency between the static and dynamic computer based simulations.

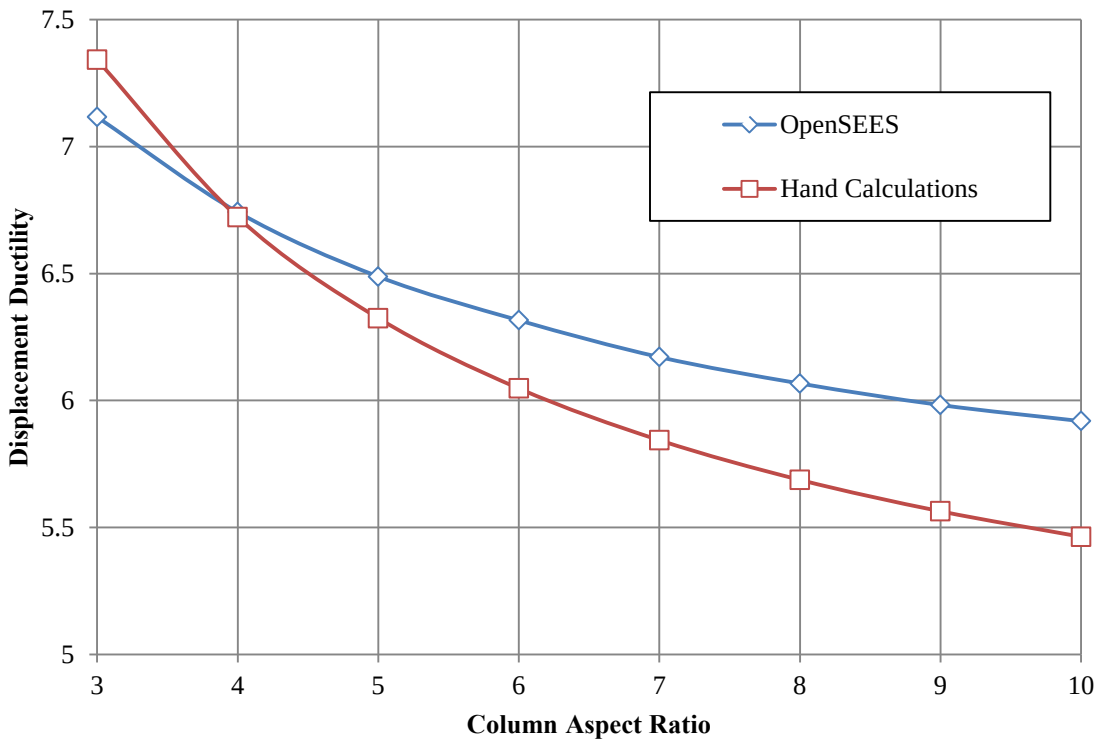

Figure 3-34: Comparison of displacement ductility using a 48 in. diameter column and two approaches one equation based and one computer based

3.4 Summary

This chapter of the report investigated in further detail the impact of different confining equations on the behavior of concrete through a direct comparison of the equations, materials testing and an investigation into the impact on curvature and displacement ductility. The following conclusions can be drawn from these studies:

1. There is no general consensus as to what is the correct approach for determining an adequate amount of confinement. The data demonstrates this as the confinement requirements of some equations were more than double that of others. Furthermore, these equations establish section behavior without the taking into account the demand that the structural system may experience during an earthquake representing a design level or greater event.
2. A non-implicit approach may be used to establish the appropriate amount of confinement based on the curvature demand of the section. As found from the analyses, the curvature capacity of a section, which determines displacement capacity, is highly dependent on axial load ratio, longitudinal reinforcement ratio and to some

extent the ratio of the gross concrete area to the core concrete area and/or the column diameter depending on the equation being examined within this study. However, if a set performance is desired, it may be appropriate to reflect this demand in the confinement equation.

3. Current testing of small scale specimens demonstrated that the ultimate concrete strain suggested by Mander et al. (1988) and numerically established in Priestley et al. (1996) occurs once a 50% drop in the confined concrete stress has taken place. The 50% drop in peak stress could adversely affect the desired response of the system as the concrete may no longer be able to maintain both the axial and lateral load demand in the nonlinear response.
4. The seismic design of a column could be made more efficient with improvements to the horizontal confinement equation. Incorporating the curvature demand into the horizontal confinement equation would indirectly define the ultimate concrete strain according to Eq. (3-1). Therefore, a reduction in time and number of iterations required to get the desired response for a large earthquake design would take place.
5. Comparison of computer and equation based approaches suggests that our current equation based model adequately agrees with computer based models. The equation based model, however, was found to be conservative based on the establishment of plasticity and strain penetration effects in the column. This was noted in Figure 3-33 where the alpha coefficient was shown to vary with concrete compressive strength, longitudinal reinforcement ratio, horizontal reinforcement ratio, and axial load ratio. Furthermore, the assumption of 0.08 was shown to be an average value as the coefficient varied from 0.136 to 0.065 as axial load ratio increased from -5% to 15%.
6. Member displacement ductility was investigated as part of the critical review using Eq. (2-2) as specified by ATC-32 (1996) to define the behavior of the confined concrete. The displacement ductility of the system was found to decrease in a curvilinear fashion from 7.1 at an aspect ratio of 3 to 5.9 at an aspect ratio of 10. These values are normally considered sufficient in seismic design situations where the local member ductility must exceed a displacement ductility of 3 (Caltrans 2010). However, a displacement ductility of 3 for all cases may not be appropriate. Rather, the displacement ductility should be determined based on variables such as the design level

earthquake, the aspect ratio of the system, the period of the system and the importance of a dynamic analysis. This is further emphasized in Chapter 4 where a series of dynamic analyses are undertaken to examine the effectiveness of the ATC-32 (1996) equation subjected to real ground motion records.

CHAPTER 4: OPENSEES DYNAMIC ANALYSES

The information presented in Chapter 2 of this report indicated that the intent of the requirements within the SDC (2010) are such that the designer should perform an inelastic pushover analysis on the global system to ensure the desired displacement ductility is met both globally and locally for each member. Each member is specified to have at least a ductility of three with a preference of at least four or higher. The data presented in Chapter 3 indicates that Eq. (2-2) established by ATC-32 (1996) would meet this condition while helping the designer to better understand the lateral behavior; however, pushover analyses are not typically used in conjunction with some sort of dynamic analysis with earthquake motions to estimate the demand on critical regions of a structure. In Chapter 3, an examination of the curvature and displacement ductility capacities was examined without reference to a demand. Thus, the next step in the review of available confinement equations was to examine the demand that a structural bridge column may experience, while examining the ability of the pushover analysis to capture the effects of actual earthquake loading.

For this portion examining demand, the column analyzed during the pushover analysis was subjected to a series of ground motions using OpenSEES (2012). The mass of the column system was defined such that natural periods based on the secant stiffness to the idealized yield would be 0.5 seconds, 1.0 seconds, 1.5 seconds and 2.0 seconds with a 3% of critical damping. The 3% of critical damping was assumed based on the lower limit recommendations of Chopra (2007) for reinforced concrete. A Rayleigh damping model based on the tangent stiffness only established the necessary damping matrix in OpenSEES (2012) to complete the dynamic analyses. Table 4-1 provides the properties needed to complete the dynamic analyses within the computer simulations including mass, stiffness and the coefficient (β) applied to the stiffness matrix for defining damping.

At the beginning of the dynamic analysis simulations, a gravity load equivalent to a 5% axial load ratio was applied to the column. This task was performed based on the assumption that a bridge column would have an initial loading due to dead loads and other effects that must be applied prior to application of the ground acceleration. After initialization, an unscaled earthquake record was applied to the model. The unscaled earthquake records were selected based on real world ground motions that have occurred throughout history within the state of

California. These records further allow the critical review to establish real world demand levels for comparison with the capacity established as part of the pushover analyses in Chapter 3.

Table 4-1: Dynamic properties for computer simulations (units of kips, seconds and inches)

		Period = 0.5 sec		Period = 1.0 sec		Period = 1.5 sec		Period = 2.0 sec	
Aspect Ratio	**Stiffness**	**Mass**	**β**	**Mass**	**β**	**Mass**	**β**	**Mass**	**β**
3	361.4	2.289	0.0031	9.155	0.0061	20.599	0.0092	36.620	0.0123
4	158.8	1.006	0.0031	4.023	0.0062	9.052	0.0094	16.093	0.0125
5	83.9	0.532	0.0032	2.126	0.0063	4.784	0.0095	8.505	0.0127
6	49.9	0.316	0.0032	1.263	0.0064	2.841	0.0096	5.051	0.0128
7	32.1	0.203	0.0032	0.813	0.0065	1.829	0.0097	3.251	0.0129
8	21.9	0.139	0.0033	0.555	0.0065	1.249	0.0098	2.220	0.0130
9	15.6	0.099	0.0033	0.396	0.0066	0.892	0.0099	1.585	0.0132
10	11.6	0.0733	0.0033	0.293	0.0066	0.660	0.0099	1.173	0.0133

4.1 Earthquake Records

The earthquake records chosen for this part of the investigation were based on events that were critical in the design process changes throughout the history of seismic engineering and would also provide a range of peak ground accelerations and duration of strong shaking. The records selected were the Imperial Valley: *El Centro* record of 1940, the Northridge: *Tarzana Cedar Hill Nursery* record of 1994 and the Loma Prieta: *Coralitos – Eureka Canyon Road* record of 1989.

4.1.1 Imperial Valley Earthquake Record

The Imperial Valley: *El Centro* record of 1940 was the first ground motion selected as it was one of the first full records ever attained and helped establish the earthquake loadings in the design codes. This record has been used for many years to perform a time history analysis when doing a seismic design. The time history record used for the analysis is provided in Figure 4-1, which has a peak ground acceleration (PGA) of approximately 0.3g.

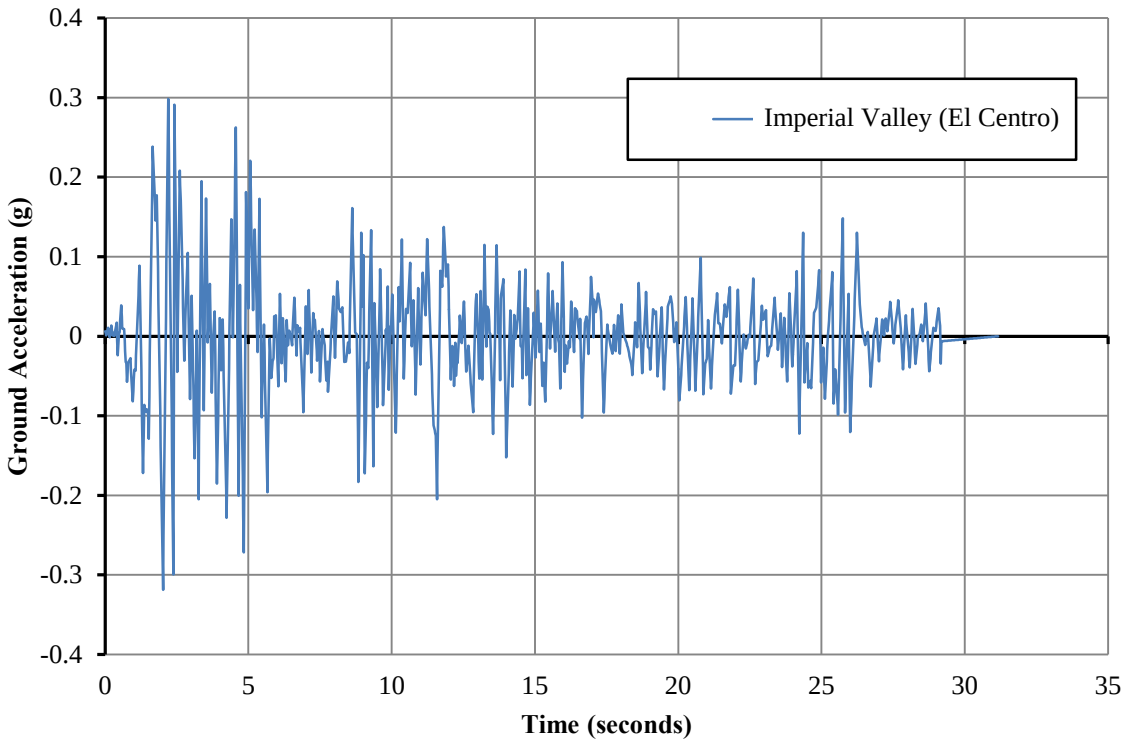

Figure 4-1: Acceleration time history of the 1940 Imperial Valley Earthquake record at the El Centro site for the N-S component

4.1.2 Northridge Earthquake Record

The Northridge earthquake was selected for defining a ground motion record as it significantly altered the design process in North America. This earthquake had one of the highest ever instrumentally recorded ground accelerations that were nearly twice that of gravity while having a moment magnitude of less than 7.0. In addition, this event is known to have produced earthquake records with a velocity pulse. Figure 4-2 provides the time history record used in the analysis.

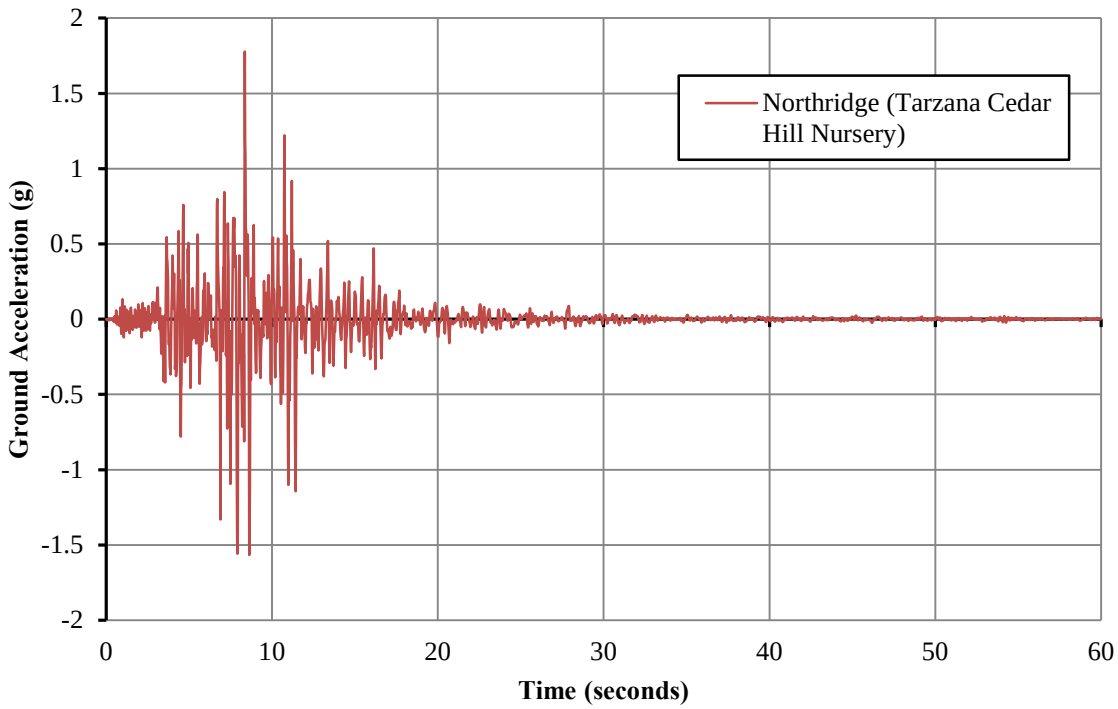

Figure 4-2: Acceleration time history of the 1994 Northridge Earthquake record at the Tarzana Cedar Hill Nursery site

4.1.3 Loma Prieta Earthquake Record

The final earthquake record for this analysis was from the Loma Prieta earthquake of 1989. This particular earthquake record produced a spectral acceleration that generally falls between the selected Imperial Valley and Northridge Earthquake records. The time history record is provided in Figure 4-3.

To better understand the differences in the three selected records for the dynamic analysis as well as standard spectral curves from the SDC (2010), a comparison of the spectral accelerations based on a damping of 5% of critical is provided in Figure 4-4. This figure reinforces that the spectral acceleration of the three records provide different intensities of shaking and produce strong spectral accelerations especially in the period range up to 1.0 seconds. The standard response spectrum curves of the SDC (2010) indicate that the design curves for a Type D soil with a design level and maximum considered earthquake are roughly the intensity of the Loma Prieta earthquake of (1989) and are exceeded at low periods by the selected Northridge record

indicating the possibility of considering the expected curvature and/or the displacement ductility in a future design equation for transverse confinement.

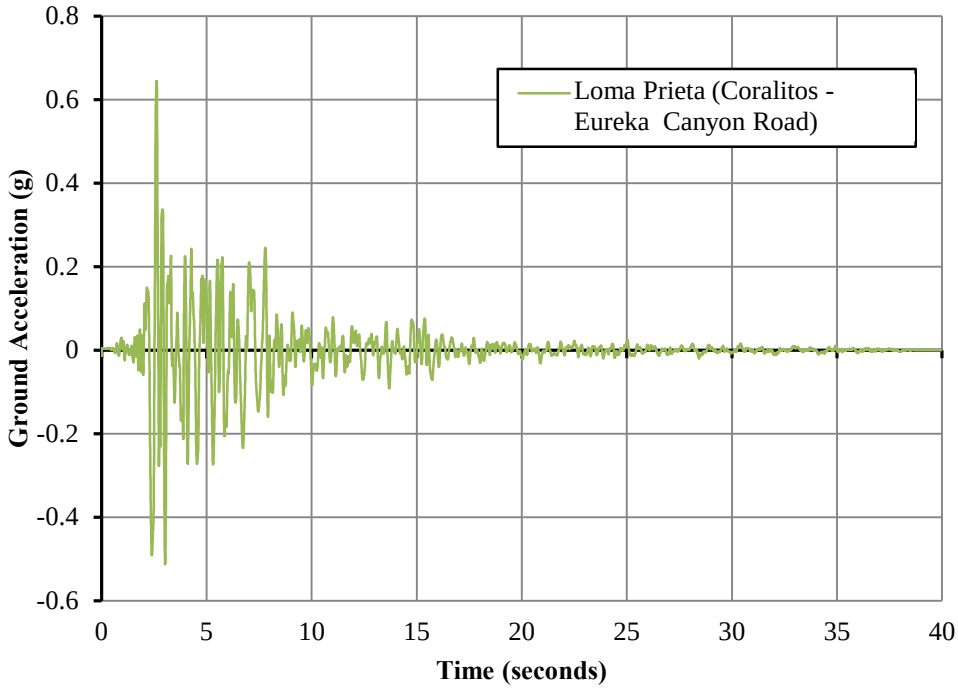

Figure 4-3: Acceleration time history of the 1989 Loma Prieta Earthquake record at the Coralitos – Eureka Canyon Road site

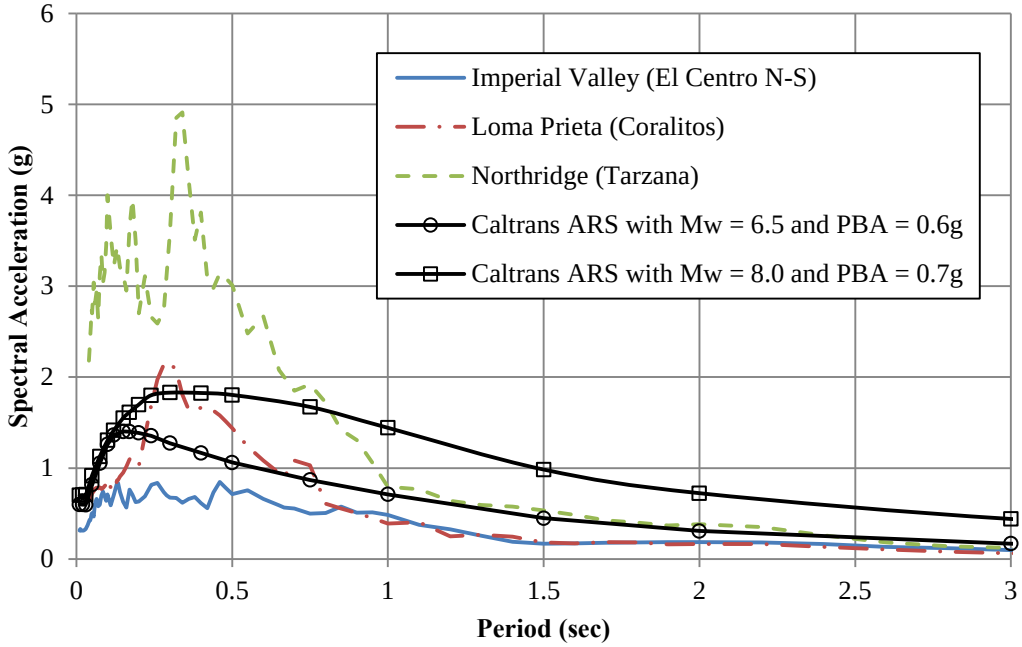

Figure 4-4: Comparison of 5% damped spectral accelerations for selected earthquake ground motion records with the SDC (2010) ARS curves

4.2 Typical Dynamic Analysis Results

For each aspect ratio and associated structural period, a number of results were attained and used to establish the displacement and curvature ductility demands associated with the three ground motion records applied as part of this critical review. The first portion of the data examined was the force displacement response of the single degree of freedom column. Figure 4-5 provides three force-displacement curves in order to provide a general overview of the different behaviors of the system when subjected to the specified earthquake ground motions. The three records were for columns with aspect ratios of 3, 4 and 5 and a natural period of 1.5 seconds.

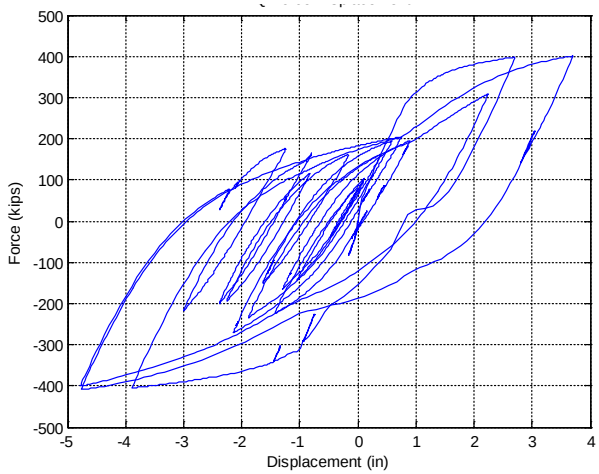

(a) Imperial Valley Earthquake Aspect of 3

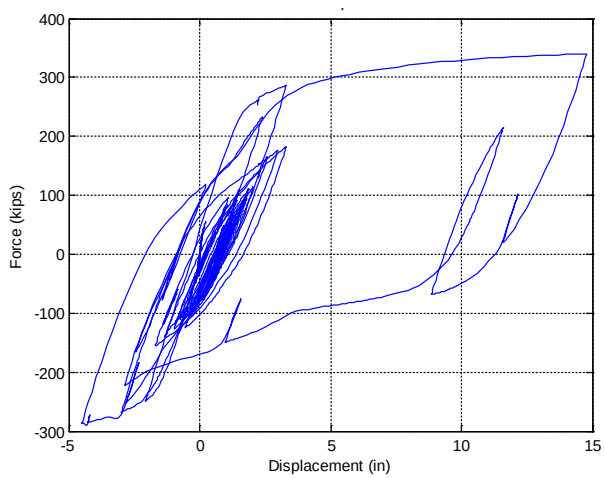

(b) Northridge Earthquake Aspect of 4

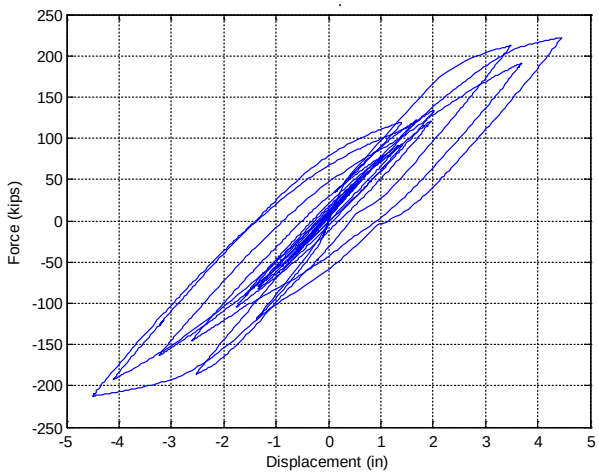

(c) Loma Prieta Earthquake Aspect of 5

Figure 4-5: Typical nonlinear force – displacement response of a SDOF column with a natural period of 1.5 seconds subjected to selected earthquake ground motion records

These three curves help to highlight the variation in the nonlinear response of the single degree of freedom column system at a similar natural period used within this series of analyses. This further reinforces the selection of the ground motion records as the overall responses varied significantly, especially with the selected Northridge earthquake record. In these particular analyses, the data commonly shows, in systems experiencing significant inelastic deformation, a singular large hysteretic loop that corresponds to the high level of acceleration at approximately 8 to 10 seconds, Figure 4-6, and a number of smaller hysteretic loops that dampen the effects of the applied earthquake ground motion. Figure 4-6 presents the time history displacement response for a column with an aspect ratio of 3 and a natural period of 1.5 seconds. The force and deformation associated with the singular hysteretic loop for this column caused the displacement ductility demand to reach 10.9 which exceeds the displacement ductility capacity of 7.3. Furthermore, this deformation caused the curvature ductility demand to reach 17.3, thus exceeding the curvature ductility capacity of 13.8. This indicates a need for improving the current confinement equations for ensuring an adequate seismic response.

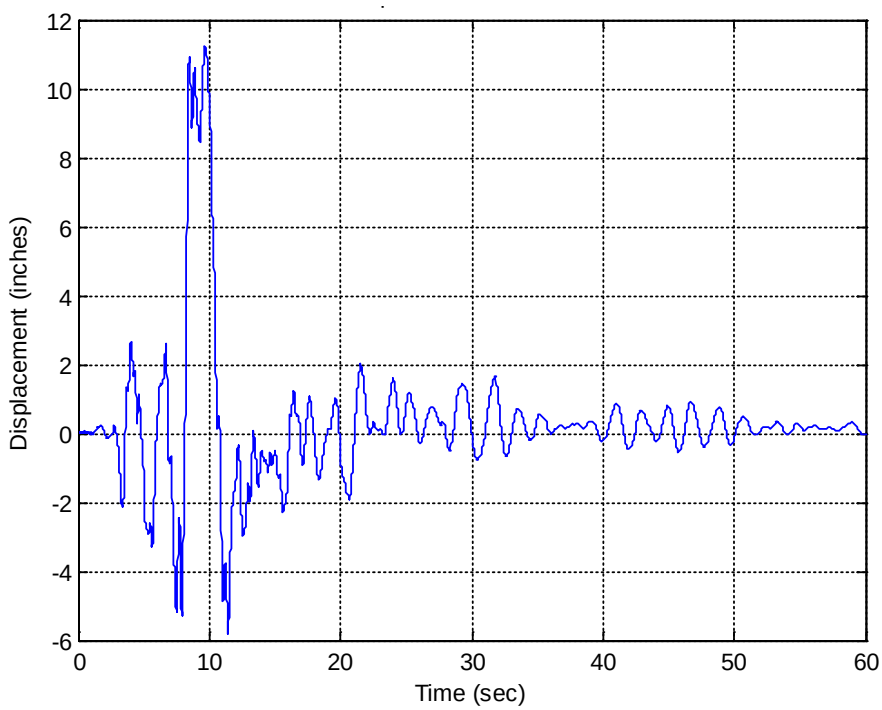

Figure 4-6: Displacement time history for the force-displacement response of a SDOF column with a 1.5 sec period subjected the selected Northridge Earthquake Record

Although varying levels of nonlinear behavior occurred during the application of the ground motions, a number of simulations experienced elastic behavior. Figure 4-7 provides an

example of the elastic behavior obtained during the Loma Prieta earthquake record for a column aspect ratio of 9 and a natural period of 0.5 seconds. The resulting displacement ductility was 0.38 with a curvature ductility of 0.40. Although this particular selected earthquake resulted in an elastic response, the magnitude and intensity of a different record could produce a nonlinear behavior with exactly the same column, mass and reinforcing details. Additionally, the same event with a higher magnitude could also result in a nonlinear response. However, this result indicates that factors such as aspect ratio and period have an influence on the overall demand expected to occur within the system that should be accounted for in a design equation for confinement to improve efficiency.

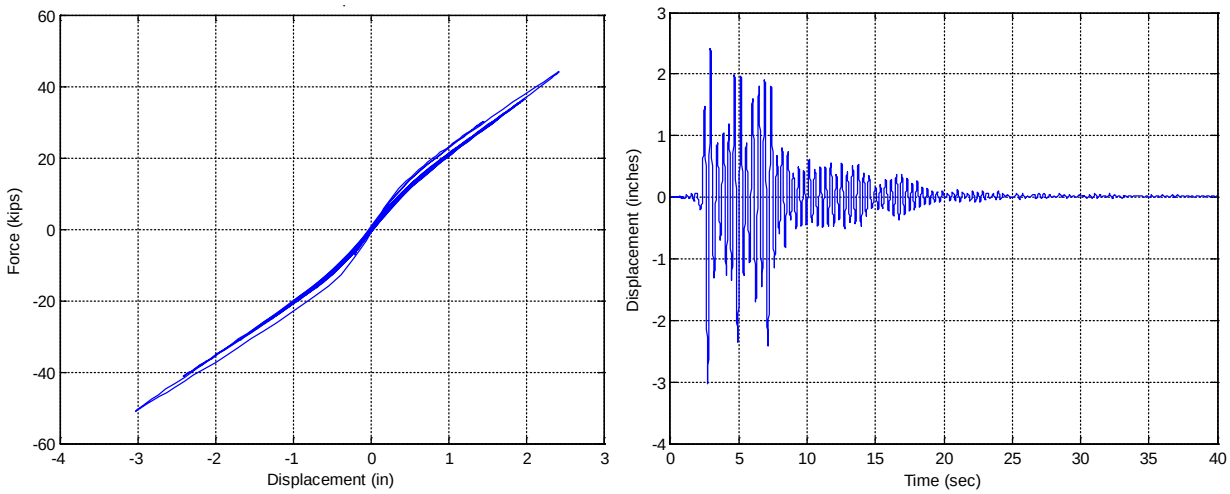

Figure 4-7: Results for a column with an aspect ratio of 9 and a natural period of 0.5 seconds when subjected to the selected Loma Prieta Earthquake record

4.3 Earthquake Demand

Although the individual data sets provide numerous results, data was compiled into a series of larger data sets based on the information provided in Table 4-1 to examine the impact of period, aspect ratio and earthquake record on the overall demand experienced by the single degree of freedom system when designed with the confinement level established by the ATC-32 (1996) approach stated in Eq. (2-2). Furthermore, the results provide preliminary evidence as to the demand level for which an individual column should be designed under seismic loading to ensure an adequate lateral response when subjected to a ground excitation.

4.3.1 Displacement Ductility

The examination of the dynamic portion of the analysis consisted of taking the results and identifying the ultimate displacement of the system for each earthquake and period analyzed per aspect ratio. Once identified, the ultimate displacement for demand was divided by the known yield displacement of the column from the pushover analyses performed in OpenSEES (2012). A comparison of the demand and capacity displacement ductility levels was made for each earthquake record as provided in Figure 4-8 through Figure 4-10.

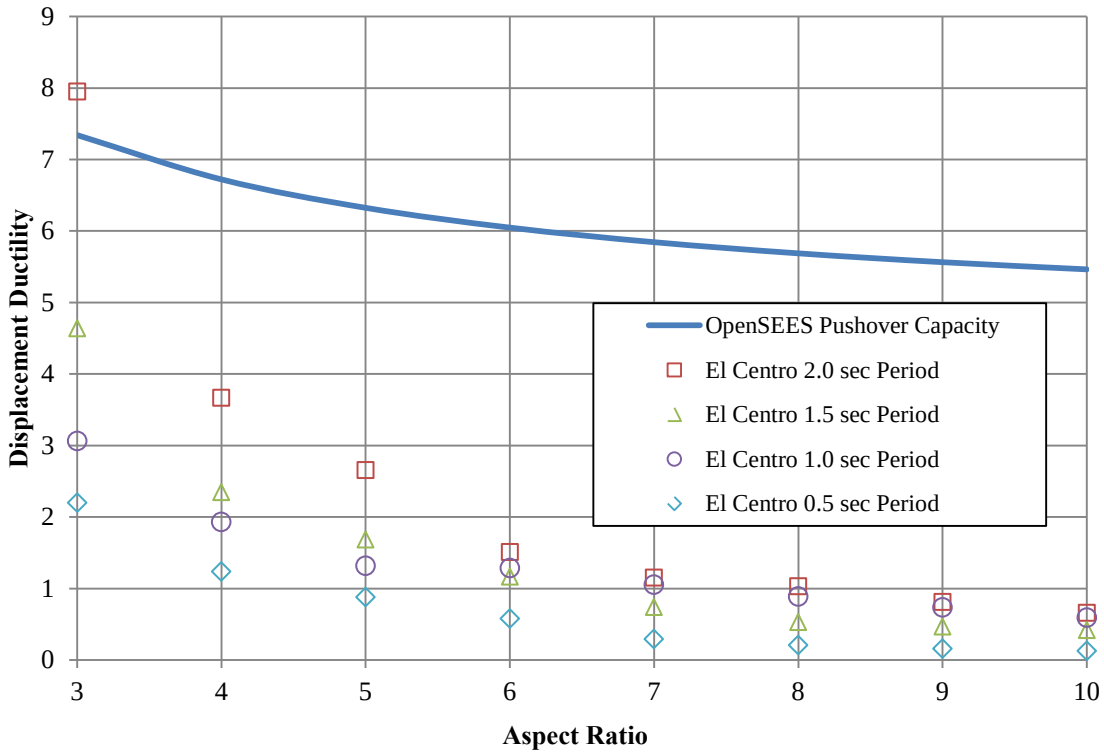

Figure 4-8: Comparison of displacement ductility capacity and demand obtained from dynamic analyses of bridge columns subjected to the Imperial Valley Earthquake record

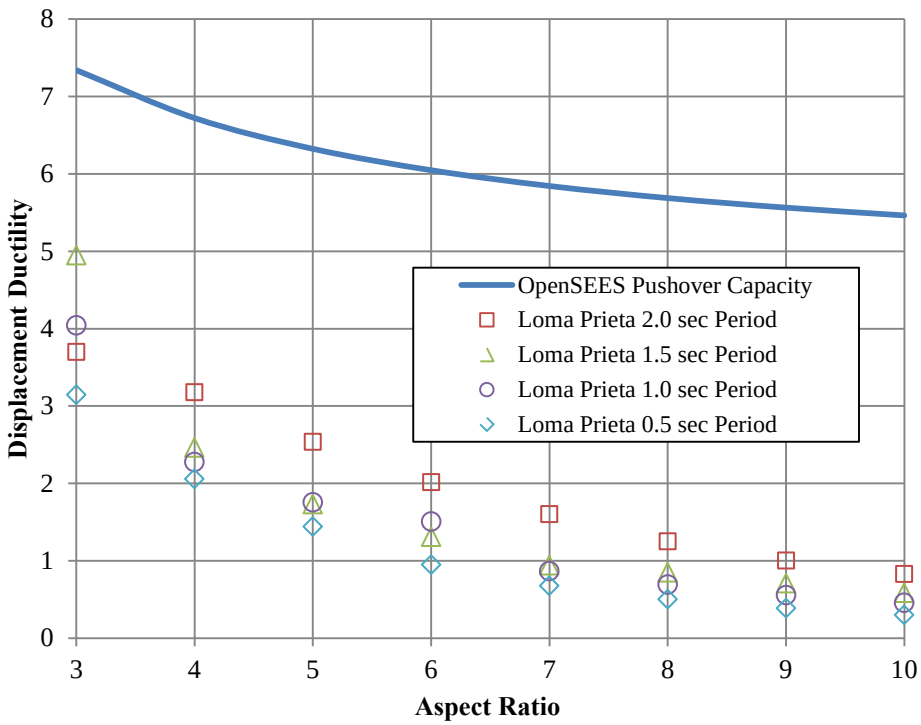

Figure 4-9: Comparison of the displacement ductility capacity and demand obtained from dynamic analyses of bridge columns subjected to the Loma Prieta Earthquake record

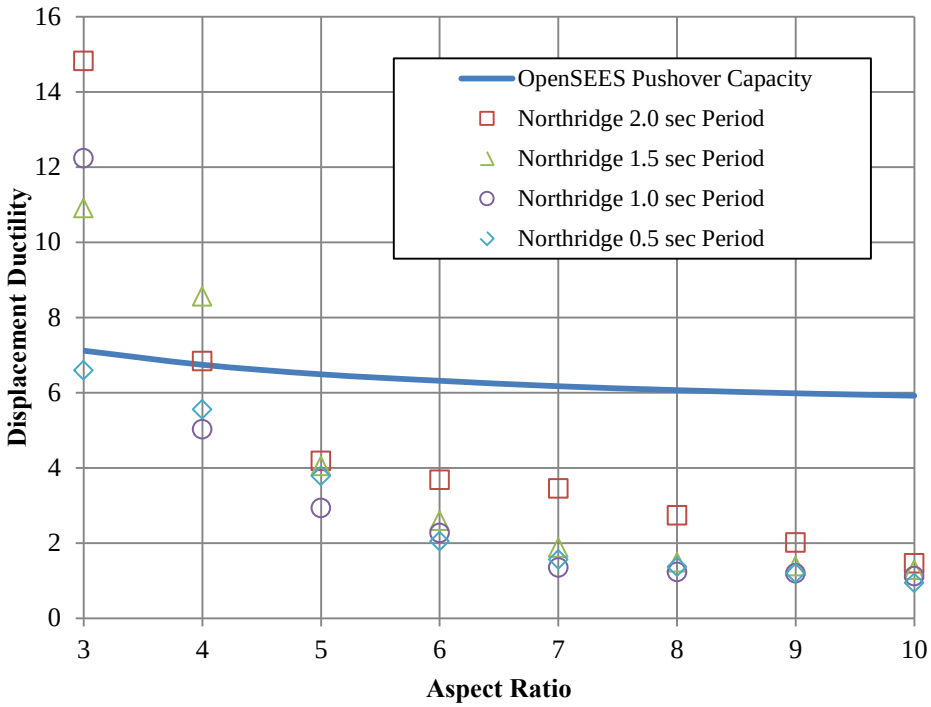

Figure 4-10: Comparison of the displacement ductility capacity and demand obtained from dynamic analyses of bridge columns subjected to the Northridge Earthquake record

Figures 4-8 through 4-10 demonstrate that as the aspect ratio of the column increases, the displacement ductility demand decreases to the point of minimal to no yielding of the column system following a curvilinear trend. Additionally, as the natural period of the system increases an increase in the displacement ductility demand typically occurred. Although the capacity of the system, according to the pushover analysis, exceeded the constant requirements and intent of the SDC (2010) by having a displacement ductility greater than five, Figure 4-8 and Figure 4-10 demonstrated that the displacement ductility demand exceeded the capacity estimated using pushover analyses in OpenSEES at aspect ratios of 4 or less (i.e., the ratio of the column height to the diameter of the column was less than or equal to 4). Although included as part of the analysis, aspect ratios as low as three are not used in a typical Caltrans design because of the high shear and ductility requirements associated with such a system. However, the aspect ratio of four in this analysis is commonly used in designs throughout practice, but the data indicated that the capacity of the system could be exceeded under a design-level or greater earthquake. The fact that the capacity was exceeded indicates the possible need for the inclusion of a dynamic analysis in addition to the pushover approach. Furthermore, the constant specified value for displacement ductility at low aspect ratios may not be appropriate. These trends within the data are demonstrating the need to include some measure of expected earthquake demand in the future development of an approach for defining the amount of transverse reinforcement needed within a cross-section.

4.3.2 Curvature Ductility

The results of the dynamic analyses were extended to examine the curvature ductility demand for comparison purposes with the section curvature capacity information presented in Chapter 3. Figure 4-11 through Figure 4-13 provide the results of the analyses and indicate results similar to the displacement ductility demands. That is to say that as the aspect ratio increased, the curvature ductility capacity decreased. Furthermore, the demand exceeded the capacity based on a pushover analysis in OpenSEES (2012) at low aspect ratios. Although the demand did not exceed capacity in all the selected earthquakes, Figure 4-12, it is possible that a higher magnitude or higher intensity event could cause the same structural system to exceed the capacity. This is seen in the data of Figure 4-12 and Figure 4-13 where the columns with a 2.0

second period experienced significantly higher levels of inelastic deformation than the other natural periods examined for a given earthquake record.

In Figure 4-11 and Figure 4-13, the curvature ductility demand was found to reach a maximum between 16.5 and 18.8. Although not a priority in the Caltrans design methodology, these values exceed the curvature ductility capacity of 13.8 as established by a pushover analysis in OpenSEES by 20% to 36%. When comparing this back to Figure 3-25 for a column cross-section of 48 in. diameter and a 2% longitudinal reinforcement ratio a curvature ductility capacity of 15 was still exceeded by 12% to 25%. This suggests that our current equations for establishment of confinement reinforcement should take into account the expected demand to take place in the overall design.

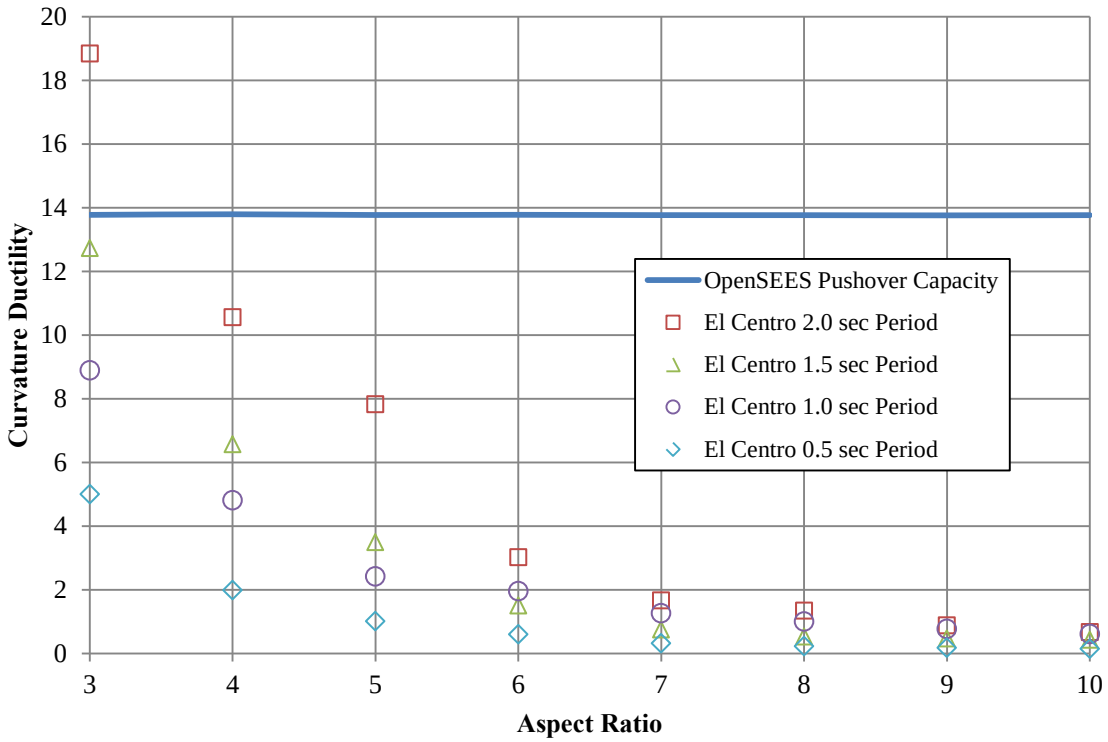

Figure 4-11: Comparison of the curvature ductility capacity and demand obtained from dynamic analyses of bridge columns subjected to the Imperial Valley Earthquake record

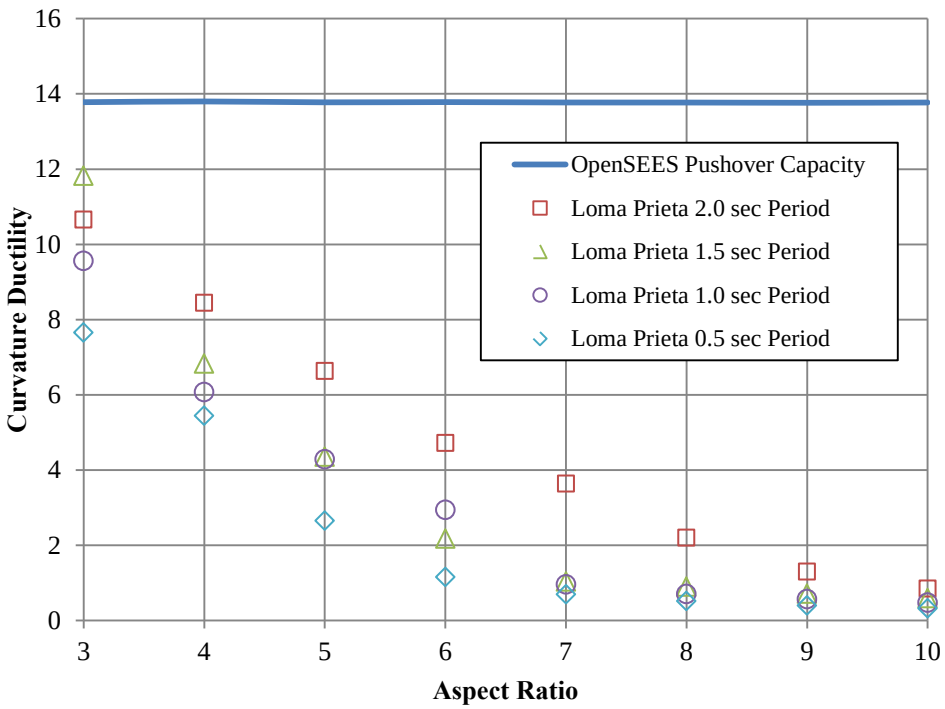

Figure 4-12: Comparison of the curvature ductility capacity and demand obtained from dynamic analyses of bridge columns subjected to the Loma Prieta Earthquake record

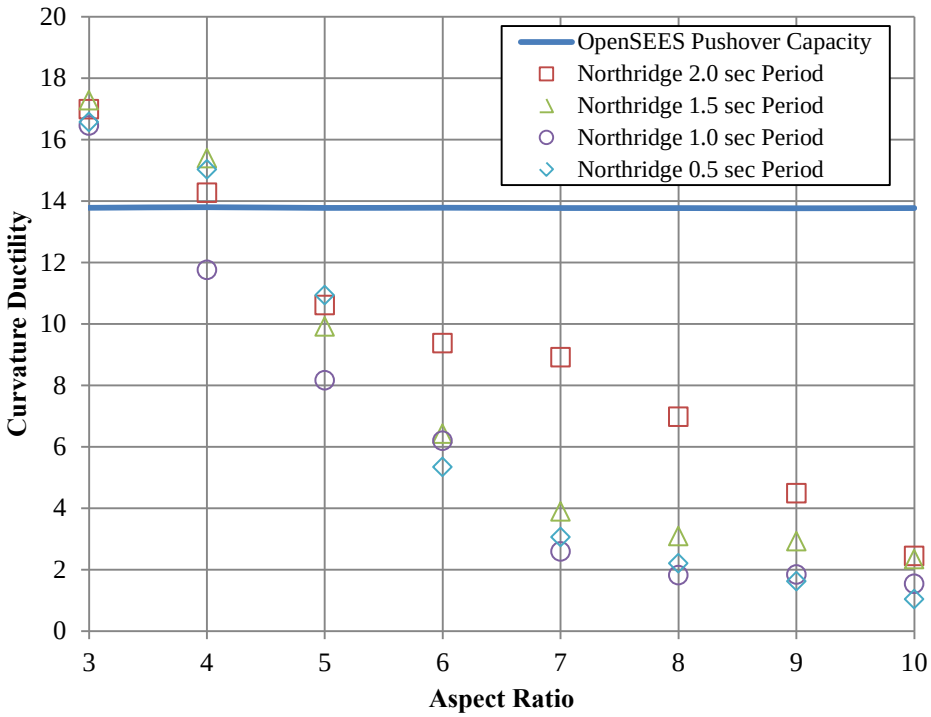

Figure 4-13: Comparison of the curvature ductility capacity and demand obtained from dynamic analyses of bridge columns subjected to the Northridge Earthquake record

4.4 Needed Improvements

This chapter examined a series of dynamic analyses on a single degree of freedom column subjected to three earthquake ground motion records that were selected to capture a range of peak ground accelerations, spectral amplitudes and changes within the knowledge base used for seismic design. The results indicated that the displacement and curvature ductility generally decreased with increasing aspect ratio. However, at low aspect ratios the demand was found to exceed the capacity based on pushover analyses conducted in OpenSEES (2012) as presented in Chapter 3. These results indicate that the way in which reinforced concrete sections are designed must be changed to ensure the safety and sustainability of our infrastructure.

Changing the design methodology for reinforced concrete sections subjected to seismic loading requires looking at three main areas: (1) current equation based requirements to the establishment of the transverse reinforcement; (2) the approach used in determining the adequacy of the design, and; (3) the establishment of the earthquake associated with the design and maximum considered earthquake level. The first task associated with the improvements to the design of transverse confinement reinforcement is the development of a new equation for inclusion into design guidelines that takes into account the curvature ductility demand of the earthquakes considered as part of the performance-based design methodology. NZS 3101 (1995) suggested a design value of 20 in ductile regions at the bottom story of a building and a value of 10 in limited ductility regions. The data within this study indicated that the desired curvature ductility is a function of aspect ratio, period of the structure as well as the earthquake record being examined for the design-level and maximum considered seismic events. The final developed equation should also give due consideration to the axial load ratio, the amount of longitudinal reinforcement in the section, the ratio of the gross area to the core area of the cross-section and the strength of the materials being used. The strength of the materials should also include a deeper investigation into the current knowledge base for the behavior of confined concrete including the establishment of the ultimate strain and the behavior of the system under varying temperatures.

The second task is the establishment of an adequate procedure that captures the overall lateral response and behavior of the system. Caltrans currently adopts the process of designing the appropriate amount of transverse confinement reinforcement by conducting a pushover analysis to ensure that the design of system and its components meet the performance

requirements based on displacement ductility. A further design requirement set forth by Caltrans is that the aspect ratio of a bridge column must be larger than 4 and ideally greater than or equal to 5. If the results do not produce the desired outcome, the design is adjusted until the performance is met. This process, however, does not satisfy all the design requirements as the information presented within this study has indicated that the dynamic effects may result in the capacity of the system being exceeded although meeting the ductility performance requirements at all stages.

The third component of the improvements to the design process arises in the form of the event being considered. This study has shown that an event such as the selected Northridge record can result in a demand that is higher than that is assumed in design. This particular record was already higher than the typical ARS spectral curves noted in the SDC (2010). Although this is the case, none of the events in this document represent a significant event, such as the recent events in Japan and Chile. Accounting for the differences in such large events may possibly be accomplished through the definition of a curvature ductility for the design-level earthquake and using a multiplication factor (e.g., 1.5) to increase the ductility level needed for a maximum considered level earthquake. Pushover, dynamic and section analyses may then be used in conjunction to verify that the curvature ductility capacity exceeds the desired demand at the design-level and greater events.

CHAPTER 5: CONCLUSIONS AND RECOMMENDATIONS

5.1 Conclusions

In the prior chapters, an investigation into the current approaches used for the confinement of concrete columns in seismic situations was undertaken. This included a detailed literature review into equations throughout the United States, New Zealand and Japan. In addition to the literature review, a series of analyses were undertaken to compare column ductility between equation based approaches and computer models through fiber based analyses in OpenSEES (2012). Using the computer models, a series of three unscaled earthquake time histories from historic earthquakes in California were used to examine the ductility and curvature demands on bridge columns and how this compares to current requirements in high seismic regions. Based on the information presented in the previous chapters, the following conclusions were drawn:

1. Existing equations require different amounts of confinement reinforcement in the critical plastic hinge regions. The equations provide different amounts of reinforcement by a factor of 2 – 3 times the smallest value.
2. The equation as established by ATC-32 (1996) for Caltrans and presented in Priestley et al. (1996) falls in the upper range of the confinement reinforcement requirements provided by the different approaches. Although this is the case, the target curvature demand appears to be unclear in the literature. To combat this problem, the establishment of a target curvature demand as a function of column geometry, axial load ratio, longitudinal reinforcement, column aspect ratio is suggested to formulate a more dependable ρ_s requirement.
3. Current understanding of the behavior of confined concrete was found to be lacking in terms of the ultimate strain capacity. This behavior, however, is complicated by the fact that the ultimate strain is influenced by multiple factors including: (1) the area of cross-section under compression; (2) role of longitudinal reinforcement in axial and transverse directions; (3) conservatism integrated into the commonly used equation in Priestley et al. (1996), and (4) size of the column tested during establishment of the ultimate strain.
4. To further examine the impact of the confinement equations, a ρ_s was established using the ATC-32 approach which takes into account material properties and some initial

section designs. In using this approach a series of additional conclusions were drawn and are as follows:

a. Current confinement equations were providing sufficient amounts of reinforcement to meet the intended design procedure of SDC (2010) for a minimum displacement ductility of 3, and the preferred displacement ductility level of 5. However, the demand on the analyzed system was found to exceed capacity at column aspect ratios between 3 and 4. It is noted, however, that Caltrans typically provides designs such that a column aspect ratio be greater than or equal to 4.
b. Aspect ratios greater than 4 for the specific column analyzed could experience a demand greater than the capacity under a larger magnitude or more intense earthquake event. This indicates the need to integrate a demand level displacement or curvature ductility level in the design of transverse confinement reinforcement.
c. The 0.08 coefficient used in the plastic hinge length formulation for Eq. (3-2) changes depending on the concrete compressive strength, longitudinal reinforcement ratio, horizontal reinforcement ratio and other factors not examined as part of this study.
d. The transverse confinement reinforcement was found to influence the displacement ductility such that a decreasing curvilinear trend developed as a function of earthquake demand, column aspect ratio and natural period of the structure being analyzed.
e. Based on the dynamic analyses, it was found that a constant value of displacement ductility may not be appropriate for all column designs and should take into account the events being considered in the design process.

5.2 Recommendations

Based on the conclusions found in this investigation a series of general recommendations are provided for the improvement of the current design process of reinforced concrete bridge columns in high seismic regions. This information is provided below including specific recommendations for Caltrans design practice:

1. A new transvers confinement equation should be developed that takes into account the amount of longitudinal reinforcement, the column aspect ratio, the axial load ratio, column geometry, material properties of the column and the demand of the design-level and maximum considered earthquake events. Since a column design is completed with a pushover analysis, all parameters associated with column properties and the axial load ratio are adequately addressed in SDC. However, the target demand for the column displacement or curvature should be updated based on the findings in this report.
2. The equation should better relate to the desired ultimate concrete strain within the confined region. Additionally, experimental testing should be performed on columns of multiple sizes with varying levels of reinforcement with the goal of better defining the confined concrete behavior of the system. This recommendation highlights a weakness in confinement models developed to date, which are based on testing completed on solid concrete members subjected to uniaxial compression under displacement control. This is an idealized condition compared to the stress distribution within a compression block in a plastic hinge region of bridge column.
3. Target curvature and displacement ductility should be established for design based on the expected demand for the structural system being designed. In SDC, the target displacement is assumed. However, this should be updated based on the findings in this report including the fact that some earthquakes can cause significantly higher displacement demand than assumed in design.
4. After development of the new equation, a series of analytical and experimental techniques should be used to validate the new approach including the dependence of displacement ductility demand as a function of aspect ratio, magnitude of the seismic event, intensity of the seismic event and the period of the structural system. This recommendation will ensure that a premature column failure would not develop as a result of the actual demand exceeding that assumed or due to the influence of path load path dependent effects.
5. Consideration should be given to the current seismic events used in the definition of the spectral acceleration values for the typical design. This is the case as the typical ARS curves should give consideration to larger events such as those recently experienced in Japan and Chile.

6. The final component should be a deeper investigation into the effects of the use of a pushover versus dynamic analysis when verifying the performance requirements for the (1) fully operational; (2) operational; (3) life safety, and; (4) near collapse limit states that may be used in a design process.

5.3 Road Map

In consideration of the above recommendations and the investigation completed in this study from comparisons of different confinement equations to evaluating dynamic responses of columns designed with specific quantities of confinement reinforcement, this section presents a road map for possible improvements to SDC. The confinement requirement in SDC is unique in that it does not provide a prescriptive confinement equation. Instead, the designer is expected to provide adequate reinforcement such that the columns in single column bents can reach a target displacement ductility between 3 and 4 while the columns in multi-column bent can reach a target displacement ductility between 3 and 5. In this process, nonlinear concrete models such as that recommended by Mander et al. (1988) is used and the plastic displacement is calculated based on a theoretical plastic hinge length.

While the SDC approach is comparable if not better than those provided by other confinement requirements, several steps can be taken to improve the confinement requirements of SDC. These requirements are to: 1) ensure adequate safety of bridge columns designed for seismic loads; 2) provide uniform reliability for columns designed according to SDC; and 3) prevent confinement failure beyond what has been perceived from cyclic testing of columns. Steps that can be taken to improve the SDC requirements are summarized below:

1. A prescriptive confinement equation is not used in SDC. However, it may be useful to include such an equation to obtain a preliminary quantity while member level analysis could be used to finalize the quantity of the confinement reinforcement. This equation could be kept simple, but should integrate a target curvature ductility demand in the range of 15 to 20 in this effort.
2. SDC requires a constant ductility capacity for all columns in a specific category (e.g., single column bent). Making this requirement a function of column aspect ratio with a lower aspect ratio requiring ductility above that suggested in SDC will be appropriate.

3. Requiring higher ductility for columns in multi-column bents over those in single column bents need to be reversed in order to ensure comparable level of damage for all columns in a seismic region. This is because the cap beam flexibility reduces the system and member ductility in multi-column bents.
4. It should be realized that available experimental data that have led to the confinement equations were generated using concrete specimens subjected to constant axial stress and does not represent the confinement zone in column plastic hinges. SDC does not specify a confinement concrete model, but endorses that developed by Mander et al. (1988). It is shown that the reliability of the ultimate compression strain may be questioned and should be evaluated. Integrating a reliable equation to quantify the ultimate compression strain with due consideration to clearly defined acceptable damage to the extreme compression region would be appropriate.
5. Experimental column ductility capacity verification has been typically done under cyclic loading whereas it is shown that the columns may experience much higher ductility demand under an earthquake dynamic loading. Experimentally evaluating column behavior subjected to earthquake-dependent load paths and updating the SDC design requirement accordingly will be appropriate. This will prevent unexpected damage to columns as witnessed in large earthquakes occurred overseas in recent years.
6. In evaluating force-displacement response of bridge columns, SDC uses a theoretical plastic hinge length. It is shown such an approach is inadequate and that the theoretical plastic hinge length depends on the axial load and aspect ratios. This concern can be minimized by requiring integration of curvature along the column height to obtain the column lateral displacement.

CHAPTER 6: REFERENCES

American Association of State and Highway Transportation Officials (AASHTO). 2012. *LRFD Bridge Design Specifications, customary U.S. units 6th Edition.* Washington D.C.: AASHTO.

AASHTO. 2010. *Guide Specifications for LRFD Seismic Bridge Design 1st Edition with 2010 Interim Revisions.* Washington D.C.: AASHTO.

American Concrete Institute (ACI). 2008. *Building Code Requirements for Structural Concrete (ACI 318-08) and Commentary (ACI 318R-08).* Farmington Hills, MI: ACI.

Applied Technology Council (ATC). 1996. *Improved Seismic Design Criteria for California Bridges: Provisional Recommendations.* Redwood City, CA: Applied Technology Council.

Bayrak, O., and Sheikh, S. 2004. "Seismic Performance of High Strength Concrete Columns Confined with High Strength Steel." *Proceedings of the 13th World Conference on Earthquake Engineering.* Vancouver, B.C., Canada: IAEE

California Department of Transportation (Caltrans). 2003. *Bridge Design Specifications.* Sacramento, CA: Caltrans.

Caltrans. 2010. *Seismic Design Criteria Version 1.6.* Sacramento, CA: Caltrans.

Canadian Standards Association. 1994. *Code for Design of Concrete Structures for Buildings (CAN3-A23.3-M94).* Rexdale, Ontario, Canada: Canadian Standards Association.

Chopra, A. K. 2007. *Dynamics of Structures 3rd Edition.* Upper Saddle River, NJ: Pearson, Prentice Hall.

FEMA-273. 1997. *National Earthquakes Hazard Reduction Program (NEHRP) Guidelines for the Seismic Rehabilitation of Buildings (ATC-33 project).* Washington, D.C.: FEMA.

FEMA-274. 1997. *NEHRP Commentary on the Guidelines for the Seismic Rehabilitation of Buildings (ATC-33 project).* Washington, D.C.: FEMA.

Japan Society of Civil Engineers. 2010. *Standard Specifications for Concrete Structures 2007 – "Design"* (JGC No. 15). Japan: Japan Society of Civil Engineers.

Kawashima, K., Kosa, K., Takahashi, Y., Akiyama, M., Nishioka, T., Watanabe, G., Koga, H., and Matsuzaki, H. 2011. "Damage of Bridges during 2011 Great East Japan Earthquake." *Proceeding of 43rd Joint Meeting, US-Japan Panel on Wind and Seismic Effects*. Tsukuba, Japan: UJNR.

Leet, K. M., Uang, C., and Gilbert, A. M. 2011. *Fundamentals of Structural Analysis 4th Edition.* New York, NY: McGraw-Hill Companies, Inc.

Levings, J. C. 2009. “Development of a versatile section analysis tool for use in seismic design.” *Master’s Thesis.* Ames, Iowa: Iowa State University.

Mander, J., Priestley, M. J. N., and Park, R. 1988. “Theoretical Stress-Strain Model for Confined Concrete”. *Journal of Structural Engineering* 114(8): 1804-1826. USA: American Society of Civil Engineers.

Mander, J., Priestley, M. J. N., and Park, R. 1988. “Observed Stress-Strain Behavior of Confined Concrete”. *Journal of Structural Engineering* 114(8): 1827-1849. USA: American Society of Civil Engineers.

Missouri Department of Transportation (MODOT). Accessed Online: May 2012. *Engineering Policy Guide.* Missouri, USA: MODOT. Accessed at: epg.modot.org.

National Oceanic and Atmospheric Administration (NOAA) / National Geophysical Data Center (NGDC). Accessed Online: May 2013. “Failed Bridge Support Picture by M. Celebi, U.S. Geological Survey.” Accessed at: http://ngdc.noaa.gov/hazardimages/picture/show/459 as part of the Image Database.

North Carolina Department of Transportation (NCDOT). Accessed Online: May 2012. North Carolina, USA: NCDOT. Accessed at www.ncdot.gov.

Open System for Earthquake Engineering Simulation (OpenSees). 2012. *OpenSees Version 2.3.2*. http://opensees.berkeley.edu/

Park, R. 1996. “The Revised New Zealand Concrete Design Standard.” *Proceedings of the Eleventh World Conference on Earthquake Engineering – Acapulco, Mexico.* Mexico: Elsevier Science Ltd.

Priestley, M. J. N., Seible, F., and Calvi, G. M. 1996. *Seismic Design and Retrofit of Bridges*. New York: John Wiley & Sons, Inc.

Priestley, M. J. N. 2000. “Performance-Based Seismic Design”. *Proceedings of the 12th World Conference on Earthquake Engineering, Auckland, New Zealand.*

Priestley, M. J. N., Calvi, G. M., and Kowalsky, M. J. 2007. *Displacement-Based Seismic Design of Structures*. Pavia, Italy: IUSS Press.

Shelman, A., Levings, J., and Sritharan, S. 2010. *Seismic Design of Deep Bridge Pier Foundations in Seasonally Frozen Ground: Final Report # UAF08-0033.* Fairbanks, Alaska: Alaska University Transportation Center.

Silva, P., and Sritharan, S. 2011. "Seismic Performance of a Concrete Bridge Bent Consisting of Three Steel Shell Columns." *Earthquake Spectra* 27(1): 107-132. USA: Earthquake Engineering Research Institute.

South Carolina Department of Transportation (SCDOT). 2008. *Seismic Design Specifications for Highway Bridges Version 2.0.* Columbia, SC: SCDOT.

Sritharan, S., Priestley, M. J. N., and Seible, F. 2011. "Seismic Design and Experimental Verification of Concrete Multiple Column Bridge Bents." *ACI Structural Journal* 98(3): 335-346. USA: American Concrete Institute.

Standards New Zealand. 1995. *The Design of Concrete Structures (NZS 3101:1995)*. Wellington, New Zealand: Standards New Zealand.

Standards New Zealand. 2008. *Concrete Structures Standard: Part 1 – The Design of Concrete Structures (NZS 3101: 2008)*. Wellington, New Zealand: Standards New Zealand.

Tanabe, T. 1999. *Comparative Performances of Seismic Design Codes for Concrete Structures.* New York, USA: Elsevier.

Transit New Zealand. 2005. *Bridge Manual Second Edition with July 2005 Amendments.* Wellington, New Zealand: Transit New Zealand.

TRC Solutions, and Chadwell, C. 2007. *XTRACT v. 3.0.8.* http://www.imbsen.com/xtract.htm

United States Geological Service (USGS). Accessed Online: May 2012. *Earthquake Hazards Program.* Washington D.C., USA: USGS. Accessed at: earthquake.usgs.gov.

Vandegrift, D., and Schindler, A. 2006. *The Effect of Test Cylinder Size on the Compressive Strength of Sulfur Capped Concrete Specimens.* Final Report for the Highway Research Center at Auburn University. Auburn, Alabama: Highway Research Center and Department of Civil Engineering at Auburn University.

Watson, S., Zahn, F. A., and Park, R. 1994. "Confining Reinforcement for Concrete Columns". *Journal of Structural Engineering* 120(6): 1798-1824. USA: American Society of Civil Engineers.